A MASS SPECTROMETRIC STUDY OF THE THERMAL DECOMPOSITION OF AZOETHANE AT LOW PRESSURES

by

WILLIAM DEMPSEY CLARK

APPROVED:

(Adviser for the thesis)

A THESIS

Presented to the Department of Chemistry
and the Graduate School of the University of Oregon
in partial fulfillment
of the requirements for the degree of
Doctor of Philosophy

June 1958

APPROVED:

[redacted]

(Adviser for the thesis)

PREFACE

The work described herein was undertaken in order to accomplish two goals. The first was the construction of a mass spectrometer and associated equipment for use in continually monitoring the kinetics of a chemical reaction in the gas phase. The second was the use of this equipment in the actual study of the kinetics of a thermal decomposition. The first compound studied was azomethane (McCoy, 1955). The present thesis will cover the work on azoethane together with a description of part of the instrumentation.

The work described herein commenced on December 20, 1951 and, with the exception of processing of the data and the writing of this thesis, was brought to a close on December 10, 1956. The first three years were largely consumed with the construction of instrumentation and the checking out and calibration of it. While the last two years were largely spent in experimentation, a considerable portion of this period was also devoted to rebuilding instrumentation which did not perform satisfactorily after experimentation had begun.

While three years was spent in the construction of instrumentation, this thesis will describe only two of the major items. The instrument has been previously described by Engh. (1952). Since that time many changes

have been made and new pieces of equipment have been constructed. Among these are a battery electrometer, a magnet power supply for use in sweeping the mass spectrum magnetically, a thermostat and phase shift thermoregulator, an emission regulator, and almost 100 glass diaphragm leaks in addition to the many changes in the existing circuitry and in the source construction. Because this thesis is intended to report only experimental results, the majority of the additional construction work will not be reported here. The two items discussed here are included because of their uniqueness and because of the desire to have plans, specifications, and circuits of these devices on record as soon as possible. The items not covered here will be reported on later in the literature.

As in all experimental work, the data contained herein is not complete. A considerable amount of work on this subject remains to be done. As the reader progresses through the text he will find suggested avenues for further research. Many of these avenues have been investigated to some extent. However where these investigations became too time consuming it was considered advisable to return to the original chosen path. Preliminary results obtained on some of these tangential investigations were encouraging and where further work, in the opinion of the author, would be fruitful, it is so noted in the text.

The name on the title page suggests that this work was accomplished by one man. This is not true. Many people have aided in the accomplishment of what follows and it is a pleasure to acknowledge at least some of these contributions at this time. The United States Atomic Energy Commission was of great help in supplying needed funds throughout the entire

to actual assistance in the assembling of an electronic component for the instrument. His help, encouragement, and understanding were available on all problems, regardless of size.

The persons described above are to a large extent responsible for any fruits borne of the five years of work covered by this thesis at the University of Oregon. It is with deep humility and profound thanks that I take this opportunity to acknowledge their contribution.

William D. Clark

January 1958

Los Alamos, New Mexico

TABLE OF CONTENTS

LIST OF TABLES

LIST OF FIGURES

LIST OF FIGURES (continued)

CHAPTER I

Introduction

Molecularity and Order

In order to avoid confusion so often encountered in reports concerning chemical kinetics a clear distinction should be made between the order of a reaction and its molecularity.

The order of a reaction is an experimental result. Equation (1) expresses in general the rate of change of concentration of a given chemical species as a function of time.

$$-\frac{dC_x}{dt} = KC_x^n \qquad (1)$$

Here C_x is the concentration of species x, t is time, K is the specific rate constant, n is the order of the reaction and can be either an integer or a fraction. If equation (1) fits the experimental data best when n = 1, then the reaction is said to be first order, n = 2: second order and so on.

In the event the product of several concentrations are necessary to describe the reaction, then

$$-\frac{dC_x}{dt} = K C_1^a C_2^b C_3^c \cdots \qquad (2)$$

and n will be equal to a + b + c ....

Molecularity is obtained from the knowledge of the mechanism by which the reaction proceeds and suggests the number of molecules coming together to form an intermediate complex which decomposes into the products. It does not, however, say anything about the activation process. A collision between two molecules may result in one having excess energy. After a short time this activated molecule will either decompose or transfer its excess energy to another molecule via a collision. When it decomposes the reaction will be unimolecular in that only one molecule was involved in the reaction even though two molecules were involved in the activation process. If, however, the collision resulted in the formation of a complex consisting of the two colliding molecules united with a chemical bond (weak and unstable though it may be) the reaction would be considered to be bimolecular. As long as the reaction is simple, i.e. involves a single step, the order and molecularity will be identical and equal to the number of stable molecules which unite to form the complex.

However, relatively few really simple reactions exist. Most reactions involve two or more steps. Under these conditions the identity is lost and the order results from an empirical rate law which fits experimental data, whereas the molecularity may be deduced only from knowledge or speculation about the mechanism. Thus, in general, a unimolecular reaction does not demand first order kinetics any more than a bimolecular reaction demands second order kinetics.

This research is concerned with a first order, unimolecular, homogeneous reaction in the gas phase.

History of Unimolecular Reactions

For many years no unimolecular homogeneous gas reactions were known and many workers were of the opinion that none existed. In 1919 Trautz and Bhandarkar reported that the thermal decomposition of phosphine was unimolecular and homogeneous above 945°K. Later (Hinshelwood and Topley 1924) it was found to be heterogeneous. Then Daniels and Johnston (1921) reported that the thermal decomposition of N_2O_5 followed first order law and was homogeneous. These results stood for many years until Ogg (1947, 1950) showed that, in spite of being first order the reaction is not unimolecular but has a more complex mechanism. However, since 1921 many gaseous reactions which have been shown to be first order have been reported (Frost and Pearson, Kinetics and Mechanism 1953). Later work on some of these showed them to be chain reactions.

At the time Trautz and Bhandarkar (1919) reported their work, it seemed obvious that a first order law required a unimolecular reaction and a second order law required a bimolecular reaction. If this were true and reactions in the gas phase depended on bimolecular collisions, it followed that first order gas reactions were not possible.

The Radiation Hypothesis

The discovery of first order, unimolecular, homogeneous gas reactions appear to give substance to the Radiation Theory of Activations as suggested by Perrin (Les Atomes 1913)(1919), Trautz (1918), and W. C. McC. Lewis (1918). The statement of the original, simple form of the Radiation Hypothesis is:

In ordinary thermal reactions molecules are put into an active state by the absorption of infra-red radiation emitted by the walls of the containing vessel. The frequency of this radiation may be calculated from the equation

$$\frac{d\ln K}{dt} = \frac{Nh\nu}{RT^2} \qquad (3)$$

where K is the thermal reaction rate constant, N is Avogadro's number, h Planck's constant, and ν the frequency desired. From this it appears that when the reaction was reversed infrared radiation of frequency ν should be emitted.

Almost from the outset the theory ran into trouble. Langmuir (1920) showed that the density of infrared radiation inside a hohlraum was insufficient to account for observed rates. Daniels and Johnston (1921) found that N_2O_5 was transparent at 1.16 micron, the wave length predicted by (3) from the temperature coefficient of the thermal reaction rate. It was also found (Daniels, 1926; Taylor, 1926; Lewis and Mayer, 1927) that by increasing the intensity of the infrared radiation of the calculated wave length, no increase in rate was observed. The coup de grace was given the theory with the experimental fact that reaction rates fall off below a critical pressure (see Fig. 3, p. 38). This fact is entirely inexplicable on the basis of the radiation hypothesis but is a definite prediction of the collision theory of activation.

The radiation theory has since been shown to be without merit and is presented here only because of its historical interest. It is an excellent example of a beautiful theory meeting some ugly facts.

The Collision Theory of Activation

Although the collision theory of activation was extant for years before the discovery of first order unimolecular reactions, it was not understood how a collision process could produce them, hence the detour considering the radiation hypotheses. When the radiation theory was found to be without merit, the collision theory was re-explored. In 1922, Lindemann and independently, Christiansen suggested that activation by collision was compatible with first order kinetics if there were a time interval between collisions that was short compared to the mean life time of an activated molecule. If this were true, an equilibrium concentration of activated molecules, that was directly proportional to the concentration of the reactant, could be maintained. The consequences of Lindemann's suggestion can be shown by the following example. This treatment has become known as the Hinshelwood-Lindemann theory of unimolecular reactions, (HL theory). Consider a chemical reaction with the following stoichiometry.

$$A \xrightarrow{K} B + C \tag{4}$$

Associated with this reaction would be the mechanism

$$A + M \xrightarrow{k_1} A^* + M \tag{5}$$

and the reverse reaction,

$$A^* + M \xrightarrow{k_2} A + M \tag{6}$$

also

$$A^* \xrightarrow{k_3} B + C \tag{7}$$

In equation (5) and (6) M can be a molecule of either A, or one of the products, or an added inert gas. Equation (5) gives the activation reaction whereas (6) and (7) give the two methods by which deactivation can occur. In the following derivation A, A*, M, B, and C denote concentrations in some convenient units (i.e. moles/liter).

From equation (7) it follows that

$$\frac{dB}{dt} = k_3 A^* \tag{8}$$

and since

$$\frac{dB}{dt} = -\frac{dA}{dt} \tag{9}$$

then

$$-\frac{dA}{dt} = k_3 A^* . \tag{10}$$

Now considering equation (5), (6), (7) as describing the entire reaction, we consider the relationship for dA^*/dt and obtain

$$\frac{dA^*}{dt} = k_1 AM - k_2 A^* M - k_3 A^* . \tag{11}$$

Applying the Lindemann suggestion of a time delay and the resultant steady-state concentration of A* which is very small compared to other substances present, we may write as an approximation,

$$\frac{dA^*}{dt} = 0 . \tag{12}$$

Then equation (11) becomes

$$A^* = \frac{k_1 MA}{k_2 M + k_3} \tag{13}$$

Substitution of (13) into (10) yields

$$-\frac{dA}{dt} = \frac{k_3 k_1 MA}{k_2 M + k_3} \tag{14}$$

Now at low pressures $k_3 >> k_2 M$ and (14) becomes

$$-\frac{dA}{dt} = k_1 MA \tag{15}$$

which is a second order law. However at high pressures $k_2 M >> k_3$ and (14) becomes

$$-\frac{dA}{dt} = \frac{k_1 k_3}{k_2} A \tag{16}$$

which is a first order law.

So we see that one prediction of the HL theory is that unimolecular gas reactions should become second order at low pressures. The results of this research verifies this prediction as seen in Figure 3 on page 38.

At this point the question is often raised why is this change from first to second order kinetics not observed during any given run. As long as the concentration of M as an activator or deactivator is constant throughout a given run, each run will follow first order kinetics independent of pressure. This is the case when the products just compensate for the loss of reactant.

In general the HL theory does much to explain unimolecular gas reactions. However, it does not give results which are compatible with experimental data.

From equation (1) we obtain the expression for a first order reaction

$$-\frac{dA}{dt} = K A . \qquad (17)$$

Solving for the specific rate constant, K we obtain

$$K = -\frac{1}{A}\frac{dA}{dt} . \qquad (18)$$

Comparing this with equation (14) we find

$$K = \frac{k_3 k_1 M}{k_2 M + k_3} . \qquad (19)$$

Included in equation (19) is the assumption that M is constant in the time interval used in calculating a first order K from experimental data. Solving equation (19) for $\frac{1}{K}$ gives

$$\frac{1}{K} = \frac{k_2}{k_3 k_1} + \frac{1}{k_1 M} . \qquad (20)$$

Now from equation (16) we define a high pressure rate constant which is independent of pressure

$$K_\infty = \frac{k_1 k_2}{k_2} . \qquad (21)$$

Substituting (21) in (20) gives

$$\frac{1}{K} = \frac{1}{K_\infty} + \frac{1}{k_1 M} \qquad (22)$$

which is the second prediction of the HL theory. That is a plot of

$1/K$ vs $1/M$ should give a straight line whose slope is $1/k_1$ and whose intercept is $1/K_\infty$. This prediction was found to be in error. When experimental data were plotted, using the initial pressure as M, the line showed considerable curvature (see Figure 4, page 39).

Perhaps the most serious defect in the HL theory is the assumption that all activated molecules react at the same rate. It seems reasonable to expect the highly energized molecules to have a shorter lifetime than those with lower energies. This being so k_3 would be a function of the pressure and a plot of $1/K$ vs. $1/M$ no longer yields a straight line.

To account for the curvature in the plot of $1/K$ vs. $1/M$ three theories have been advanced. These are due to Kassel (1928), Rice and Ramsperger (1928), and Slater (1954) and all are based on the Lindemann mechanism. The theories of Kassel, and Rice and Ramsperger are quite similar. In view of this, only the Kassel theory will be considered. The Slater theory and the Kassel yield nearly the same results if the substitution

$$n = 2s - 1 \qquad (23)$$

is made. Here s is the effective number of oscillators in the molecule according to Kassel, and n is the number of oscillators in the Slater theory.

The Slater theory requires only the activation energies in the way of experimental data. However it is limited to rather the small number of molecules for which a full spectroscopic study and vibrational analysis can be made. Slater (1953) has reported a complete

derivation for the case of the cyclopropane molecule. In consideration of the fact that the results of the Slater and Kassel treatments are similar and that the Kassel treatment requires only that experimental data usually obtained in kinetic work together with the evaluation of a difficult integral, only the Kassel treatment will be discussed in this report (see Chapter V).

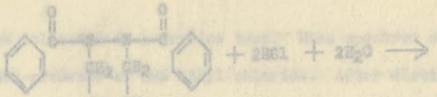

CHAPTER II

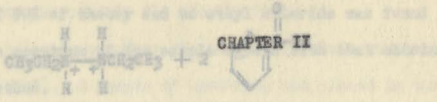

Preparation of Sample

Azoethane is a colorless liquid having a boiling point of 58.0°C (Renaud and Leitch, 1954) and a melting point of less than -80°C. It was prepared from sym-diethylhydrazine by mild oxidation.

The sym-diethylhydrazine was prepared by the method according to Hatt (Organic Syntheses, 1943).

The method proceeds as follows:

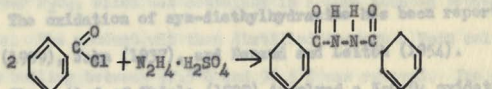

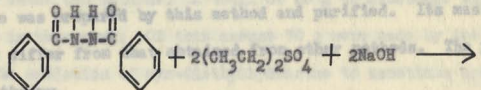

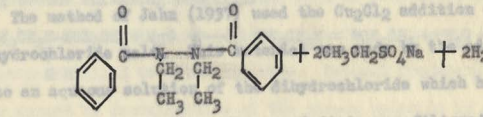

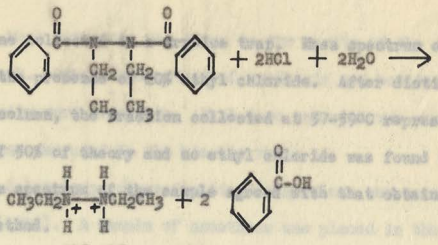

The dihydrochloride salt was recrystallized from an ethyl alcohol and water mixture at least five times. The resulting material was a snow-white mass of needle crystals which on standing in open air slowly developed yellow spots. It was thought that these yellow spots were areas in which oxidation had begun. After further recrystallization the product was kept in an air-tight bottle under an atmosphere of dry nitrogen. No further difficulty was experienced.

The oxidation of sym-diethylhydrazine has been reported by Thiele (1909), Jahn (1937), and Renaud and Leitch (1954).

The method of Thiele (1909) involved a K_2CrO_4 oxidation. The oxidation was quite vigorous and the yields were small (about 10-20%). A sample was prepared by this method and purified. Its mass spectrum did not differ from that obtained from other methods. The yield was 14% of theory.

The method of Jahn (1937) used the Cu_2Cl_2 addition compound of the dihydrochloride salt. This material was made by the addition of $CuCl_2$ to an aqueous solution of the dihydrochloride which had been buffered with sodium acetate. The precipitate was filtered, washed, and dried in vacuo. The dried precipitate was then heated to 200°C and the

azoethane collected in a dry-ice trap. Mass spectrum of the product showed the presence of 20% ethyl chloride. After distillation through a Todd column, the fraction collected at 57-59°C represented a total yield of 50% of theory and no ethyl chloride was found to be present. The mass spectrum of the sample agreed with that obtained from the first method.

The method of Renaud and Leitch (1954) was found to be the most straightforward and gave the highest yields. In this method an aqueous solution of 16.1 g (0.1 M) sym-diethylhydrazine dihydrochloride, 8 g (0.2 M) NaOH, and 45 ml water was added to a flask fitted with a magnetic stirrer, Vigreaux column, a receiver, and containing 29 g (0.135 M) HgO in 45 ml water. Stirring was started and continued for 10 minutes, at which time the stirrer was removed and the flask was gently heated. The material boiling between 50°C and 70°C was collected and dried by passing it over P_2O_5, which was contained in a tube mounted between two dry-ice traps. The product was then distilled through a Todd column and the fraction boiling between 57.5°C and 58.5°C was removed. The yield was 80-90% of theory. The mass spectrum of this product agreed with that from the other two methods. A total of 80 g of azoethane was produced and used in this work. Of this amount 70 g were made by the last method.

The oxidation of sym-diethylhydrazine to azoethane proceeds according to the following equation:

$$CH_3CH_2N\text{-}NCH_2CH_3 + HgO \longrightarrow CH_3CH_2N{=}NCH_2CH_3 + H_2O + Hg$$

(H H)

Much attention was given to the purity of the azoethane used in this work. Other than method of synthesis and boiling point, no criteria for purity were available. Much more material was used in the purity work than was used in the kinetic runs.

A low temperature fractionating column was constructed after LeRoy (1950). A sample of azoethane was placed in the column and cooled to -80°C. A total of six fractions were removed at temperature increments of 15°C and their mass spectra run. In the azoethane obtained from the first and second methods of synthesis, some acetonitrile and n-butane was found. However, the spectra obtained from the six fractions on a sample from the third method did not differ from each other. From these data it was assumed that we had (a) a better product from method three (Renaud and Leitch, 1954) and (b) that the mass spectrum was indeed the true spectrum of azoethane.

In Figure 1, the mass spectrum of azoethane is reproduced exactly as it appeared on the Leeds and Northrup Speedomax Recorder. In this spectrum the magnet current was varied and not the accelerating voltage as is usually the case.

Most of the peaks expected from azoethane appear. The 86 peak is, of course, the parent peak. The 57 peak corresponding to the fragment $CH_3CH_2NN^+$ is a major peak together with the 43 peak ($CH_3CH_2N^+$) and the 28 and 29 peak (N_2^+ and $CH_3CH_2^+$). The high 41 peak could possibly have been due to acetonitrile present as an impurity. However, repeated fractionations failed to alter its size. Several fragments with mass 41 could be formed by decomposition of the parent molecule by electron bombardment. Among these are CH_3CN^+, and $CHNN^+$. Neither of these seems especially probable. Rearrangement or recombination could lead to

FIGURE 1

Mass Spectrum of Azoethane. A Reproduction of an Actual Run.
See Table IV for Details. Spectrum Scanned Magnetically.

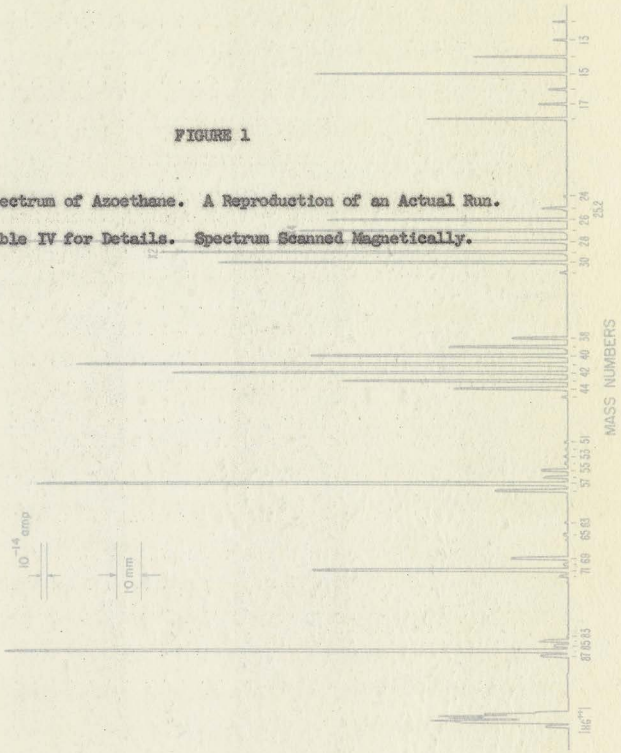

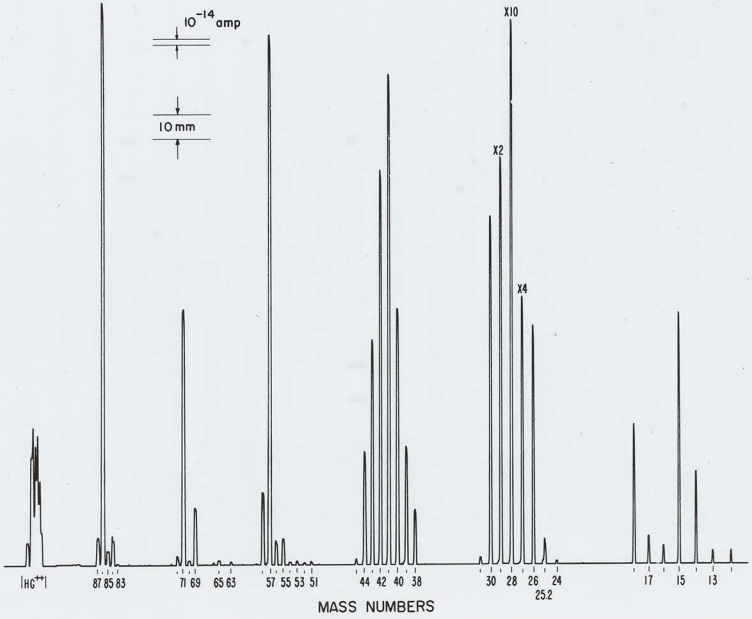
10^{-14} amp
10 mm
X10
X2
X4
|HG++|
87 85 83
71 69
65 63
57 55 53 51
44 42 40 38
30 28 26 24
25.2
17
15
13
MASS NUMBERS

$CH_3CH_2C^+$, but this does not appear probable either. It is not possible to decide which fragment or process is chiefly responsible for the 41 peak and, in fact, all could contribute. If one uses 40 volt ionizing electrons instead of the 70 volts usually used, the mass spectrum of azoethane remains very much the same with the exception of a decrease in the peaks at masses 41, etc. The effect is the same as decreasing the amount of acetonitrile in a mixture and observing the decrease in the mass spectrum of acetonitrile in the spectrum of the mixture. If this effect is real and the interpretation of the facts given above is correct, the possibility of organic synthesis by electronic bombardment appears possible.

The complete mass spectrum is given in Table I and was obtained from the spectrum shown in Figure 1. In order to fit Figure 1 onto a standard page it was necessary to reduce its size photographically. The original tracing was ~1.50 times as large as Figure 1.

It has not been possible to pump down the vacuum system in any mass spectrometer, using a tungsten filament as an electron source, to the point where no peaks are obtained with a detector capable of recording 10^{-15} amps. There is always at least a mass 18 (water), and a mass 28 (carbon monoxide). At these levels of sensitivity a "clean" system will not give a mass 32 peak (oxygen). As a matter of fact, the presence of a mass 32 peak is almost always indicative of a leak in the system. These residual peaks are known as background and the spectra obtained must be corrected for them. This is done by taking a spectrum immediately before running the sample and subtracting the height of the background peaks from those obtained from the sample. This rather simple correction is

TABLE I

Mass Spectrum of Azoethane (see Fig. 1)
(corrected for background)

Mass-Charge ratio (m/e)	Type of Peak	Relative Intensity	Mass-Charge ratio (m/e)	Type of Peak	Relative Intensity
12		.35	45	r,i	.16
13		.35	51		.06
14		2.27	52		.06
15		6.04	53		.10
16	r,i	.38	54		.06
17	r,i	.19	55		.64
18		1.21	56		.54
24		.10	57		13.00
25		.64	58	r,i	1.79
25.2	m	.10	59	i	.03
26		5.72	63		.10
27	r	32.39	65		.13
28		24.08	66		.06
29	b	100.00	69		1.41
30	r,i	8.21	70		.13
31	r,i	.19	71		6.10
38		1.37	72	r,i	.22
39		2.72	83		.03
40		6.16	84		.61
41		11.66	85		.32
42		9.20	86	P	13.80
43		5.01	87	i	.70
44	r	1.50			

Notes on Table I

E_{ACCEL} = 2000 V. Leak B (Dia. = 10 micron)

$E_{BOMB.}$ = 70 V. Pressure = 25.3 micron (C.E.C. micromanometer)

$I_{FIL.}$ = 4.65 Amp AC 3 hr. wait for equilibrium

I_{TRAP} = 15.5 μamp. Magnetic Scan 40 ma (mass 12) to 140 ma (mass 102)

I_{Case} = 44.0 μamp. Scan time (mass 12 to 102) = 23 min.

Sensitivity
(mm/micron on recorder, shunt 20) Sensitivity of L and N recorder (Shunt 20)
Azoethane mass 29 (base peak) 62.1 4×10^{-15} amp/mm (with 10^{12} ohm input
mass 86 (parent peak) 8.58 resistor)
N-Butane mass 43 (base peak) 78.5

Symbols: P - parent peak r - rearrangement peak
b - base peak m - metastable ion peak
i - isotope peak

TABLE II

Background Spectra for Figure I

Mass-Charge ratio (m/e)	Peak Height (mm)	Mass-Charge ratio (m/e)	Peak Height (mm)
15	2.0	40	2.0
16	1.5	41	7.0
17	8.0	42	8.0
18	35.0	43	8.0
26	2.5	44	20.0
27	10.5	56	1.0
28	43.0	57	1.0
29	4.5	71	3.0
30	6.0	86	1.0
39	3.0		

possible because the peak height is a linear function of the pressure over a wide range of pressures. The background spectrum for the sample given in Figure 1 is given in Table II.

It should be pointed out that the data given in Table I are relative peak heights. Because the mass spectrum of any sample is a function of the geometry of the particular instrument and the ionization efficiency of the source and bombarding electron beam, it is exceedingly difficult to obtain absolute mass spectra.

In most instruments the magnet current is held constant and the accelerating voltage is slowly changed to obtain a spectrum. While this instrument had this capability it was not used to any great extent in this work because of "discrimination" or "voltage effect." If any mass is brought to focus at several different settings of magnet currents and accelerating voltages, it is noticed that the peak height will vary, usually becoming small at lower accelerating voltages. The exact relationship between accelerating voltage and peak height is also a function of the geometry of the instrument and the different voltages applied to the source. This effect is known as "discrimination." It cannot be dispensed with but it can be reduced to a constant effect by choosing an accelerating voltage and keeping it constant throughout any work done with the mass spectrometer. A spectrum is then obtained by varying the magnet current. It was in this manner that the spectrum given in Figure 1, page 15 was obtained and in fact in this entire work.

CHAPTER III

Experimental Method

The procedure usually followed during the course of a kinetic run is summarized below. A sample of azoethane was admitted to a sample introduction system. The purpose of this system was to provide a means of sample introduction into the thermal decomposition flask and determining the initial pressure in this flask. In the pressure range 0 to 200 microns, this initial pressure was easily determined through the use of a Consolidated Engineering Corporation micromanometer. However, in the range from 200 microns to 100,000 microns the pressure determination was more difficult. This was accomplished by introducing a sample of azoethane into a pipette of known volume under a known pressure. This pressure was determined through the use of a 0 to 50 millimeter Wallace-Tiernan absolute aneroid manometer. The volume and pressure of this pipette was so chosen that upon expansion into the reaction flask the desired initial pressure would be obtained. In the pressure range 1000 microns to 50,000 microns the Wallace-Tiernan manometer was used directly as a measure of the pressure. In the range 50,000 microns to 100,000 microns a mercury manometer was the pressure measuring device. These

four pressure measuring systems were carefully calibrated and cross-checked to give a true scale of pressure from 1 micron to 100,000 microns. When the pipette and subsequent expansion was used, the ideal gas law was assumed to hold true. This was shown to be true for butane, normal hexane, argon, and azoethane.

With the sample in the reaction flask, the flask was shut off from the sample system and the decomposition run was begun. Because the thermostat was always at the operating temperature at which the run was to be made at the time of the sample introduction, it was necessary to complete the sample introduction and pressure measurement in as short a time as possible. This was made necessary by the fact that decomposition started as soon as the sample gas entered the heated flask, resulting in a pressure increase. Part of the gas would then expand out of the reaction flask if communication between it and the sample system was not stopped as quickly as possible. In an effort to get consistent pressure measurements, the following criterion was used for measuring the initial pressure. Immediately after a sample was allowed to enter the reaction flask, observations were made of the change of pressure with time. As the sample expanded into the reaction flask, the pressure fell toward a lower value. As long as the pressure was falling, communication between the sample system and the reaction flask was maintained. The fall in pressure began to slow up and finally stopped. At this moment the stopcock was shut off between the two systems. Using this technique no difficulty was involved in reproducing any given kinetic run within the experimental accuracy. The time required for the sample introduction varied from 10 to 45 seconds, longer times being required at lower initial pressures when using the 13 liter reaction flask.

FIGURE 2

Above: Peak Rise Times with the Spectrometer Tube at Room Temperature and at 300° C

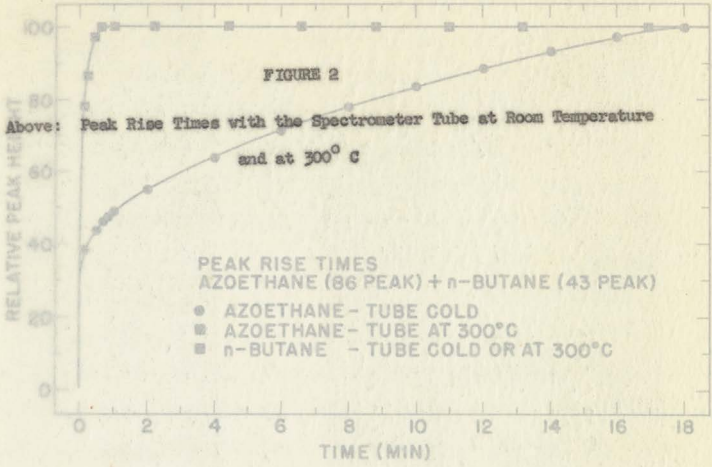

Below: Pump Out Times with the Spectrometer Tube at Room Temperature and at 300° C

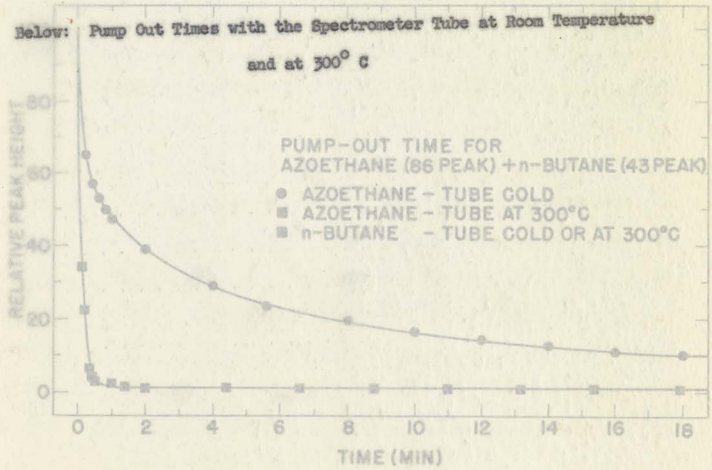

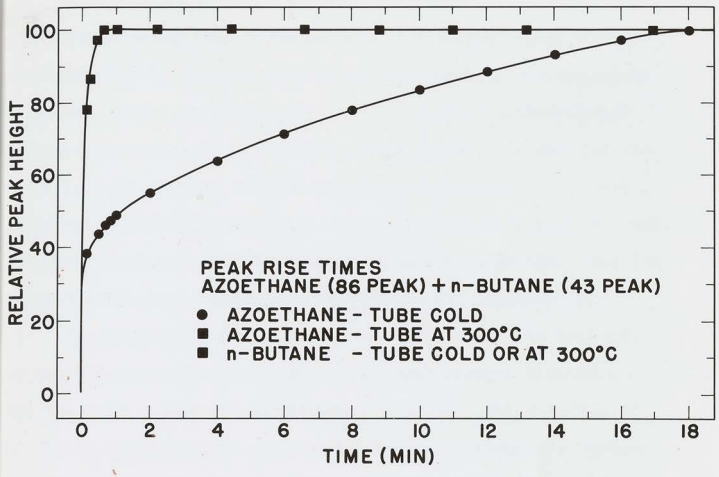
RELATIVE PEAK HEIGHT
100
80
60
40
20
0
0
2
4
6
8
10
12
14
16
18
TIME (MIN)
PEAK RISE TIMES
AZOETHANE (86 PEAK) + n-BUTANE (43 PEAK)
● AZOETHANE - TUBE COLD
■ AZOETHANE - TUBE AT 300°C
■ n-BUTANE - TUBE COLD OR AT 300°C

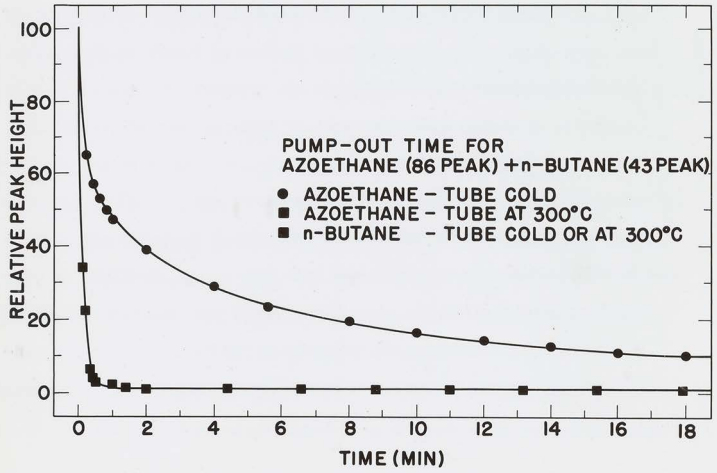
RELATIVE PEAK HEIGHT
100
80
60
40
20
0
0
2
4
6
8
10
12
14
16
18
TIME (MIN)
PUMP-OUT TIME FOR
AZOETHANE (86 PEAK) + n-BUTANE (43 PEAK)
● AZOETHANE - TUBE COLD
■ AZOETHANE - TUBE AT 300°C
■ n-BUTANE - TUBE COLD OR AT 300°C

The molecular leak in the center of the reaction flask was connected directly to the inlet of the mass spectrometer. A small sample of gas was removed from the reaction flask continuously and in most cases the parent peak (mass 86) of azoethane was continuously monitored. In two runs (No. 104 and 123) the entire spectrum of the decomposing system was monitored. Run 104 was made at a temperature of 260.0°C and a pressure of 25,500 microns and was followed for 600 minutes. Run 123 was at 260.0°C, 10.3 microns, and was followed for 1200 minutes.

One great difficulty which presented itself early in this work was the time necessary for the sample to attain adsorption equilibrium with the walls of the mass spectrometer. This time varied from 15 to 30 minutes depending on the initial pressure. A typical case is shown in Figure 2. Immediately after the introduction of the sample, the 86 peak of azoethane rose to about 40% of its final value. Hereafter, the rise was rather slow and consumed 18 minutes before a steady value was reached. In an effort to correct this condition, the entire tube, comprising the mass spectrometer and the pumping lead, was wrapped with nichrome wire heaters imbedded in asbestos. Many curves of the type shown in Figure 2 were run. It was discovered that after the tube was heated to 300°C a further increase in temperature had no significant effect. The effect of heating the tube to 300°C is shown by the second curve in Figure 2. It is seen that the peak rise now reaches 100% of its final value in less than 30 seconds. In an effort to show that this "stickiness" was a function of the particular compound and not of the instrument itself, other compounds were run and peak rise times obtained on them. The second curve on Figure 2 is the peak rise time of n-butane

with the tube either at room temperature or at 300°C. No significant change was discovered in the peak rise time for n-butane when the temperature of the tube was raised from room temperature to 300°C. This was also true of many other hydrocarbon compounds. It was also discovered that alcohols, aldehydes, ketones, and amines behaved much in the same way as azoethane but to varying degrees. The results of this work indicate that the more polar the compound the more "sticky" it becomes, with amines and carboxylic acids being the chief offenders. This same effect was also noted with respect to the pump-out times for some of these compounds. Figure 2 shows two curves obtained with azoethane with the tube hot and cold and with n-butane again with both hot and cold tube. It is seen from these curves that maintaining the temperature of the tube at 300°C improves the pump-out characteristics of azoethane to a considerable degree. In the data that follows, runs 1 through 18 were made with a cold tube. Runs 19 through 151 were made with a hot tube.

The technique used in obtaining the data on the kinetic runs followed one of two methods. In both methods the parent peak (mass 86) was followed as a function of time. In the first method the deflection of a galvanometer in the output circuit of the electrometer was recorded as a function of time. This method became too time consuming because it required continuous attention for long periods. Therefore, the second method was evolved, which consisted of adjusting the mass spectrometer so that the parent peak was being observed. This was then recorded on a Leeds and Northrup Speedomax recorder. After appropriate corrections,

made necessary because of background in the mass spectrometer, the data were taken from the Speedomax recorder charts and plotted. A plot of the logarithm of the peak height versus time was made for each run and the best straight line drawn through the data. In most cases, the data obtained followed a straight line for at least 2 half-lives. In the higher pressure region this was reduced to approximately 1 to 1 1/2 half-lives before deviation from a straight line was observed. Specific rate constants were obtained by multiplying the slopes by 2.303. In the lower pressure runs, it was necessary to apply a leak-out correction to the specific rate constant so obtained.

A great deal of experimental work was necessary in order to determine the value of the leak-out correction as a function of temperature. During the course of this work two different flasks and leaks were used, a 2 liter flask for high pressures and a 13 liter flask for lower pressures. In the range of 3000 microns to 100,000 microns the leak used was so small that no leak-out correction was necessary. The high pressures in this range gave more than sufficient signal in spite of the small leak, so that the peak height could be followed with ease. In the lower ranges, however, in order that a sufficient signal level be obtained, a larger leak was necessary. Of course, the larger leak meant that a larger percentage of material would be lost through leak-out. It was in this range that leak-out corrections were necessary. In the range 80 to 3000 microns the leak-out correction was small. It amounted to, at its greatest, 3% of the observed value of the specific rate constant. However, in the range 1 to 80 microns pressure the leak-out correction became quite large and at the lowest pressure and temperature it amounted to 50% of the observed

rate of decrease of the height of the 86 peak. It was in this range that considerable work was done in order that a value for this correction could be obtained. According to classic kinetic theory, the number of molecules which will leave the reaction vessel through the leak is given by

$$-\frac{dN}{dt} = \frac{AN}{4V}\sqrt{\frac{8RT}{\pi M}} \qquad (24)$$

where N is the total number of molecules contained in volume V, A is the area of the hole, T is the temperature in degrees Kelvin, M is the molecular weight of the molecule, and t is the time. This expression is the number of molecules that will leave volume V through a hole in a thin membrane of area A in time dt. In our case, A, V, and M are constant. This reduces the above expression to

$$-\frac{dN}{dt} = k\sqrt{T}\,N \qquad (25)$$

where k is the constant containing the above parameters. Further, when only one temperature is considered, $\sqrt{T}$ is constant and we have the expression

$$-\frac{dN}{dt} = k'\,N \qquad (26)$$

This is a first order rate law. Normal hexane was chosen for use in the leak-out experiments because its molecular weight is identical to that of azoethane and further the geometrical size of the molecule also approximates that of azoethane. Constant values for k', using normal hexane,

were difficult to obtain in the temperature range 250°C to 310°C. Obtaining these data was made difficult by the long times that were necessary to complete a leak-out run, and the low signals that were observed because of the small leak-out rate. Although the data were exceedingly scattered, a square root law seemed to be possible. An attempt to resolve this difficulty was made by running leak-out correction curves on azoethane itself at a sufficiently low temperature where thermal decomposition would be much slower than the leak-out rate. This turned out to be about 200°C. Values obtained here were smaller than those obtained from an extrapolation of the leak-out rate of normal hexane at the higher temperatures. Because the data obtained with azoethane at the low temperatures was fairly consistent and reproducible, it was decided to use the square root of temperature law and extrapolate the leak-out values for azoethane from 200°C up into the range at which the kinetic runs were made. The resultant values are shown in Table III.

TABLE III

Leak-out Corrections in Pressure Range 0-80 μ

Temperature °C	$k' \times 10^5$
260	0.84
270	0.84
280	0.85
290	0.86
300	0.87
310	0.88

At the given temperature both the leak-out rate and specific rate constant followed a first order law. This enabled us to subtract the leak-out rate constant from the specific rate constant. In this way a corrected specific rate constant was obtained and all values of this constant were corrected in this manner.

During the entire series of runs a record was made of one or both temperatures from either a platinum resistance thermometer or a calibrated chromel-alumel thermocouple. The thermocouple was placed in a well provided in the center of the reaction flask itself. The platinum resistance thermometer was placed in the air stream in one corner of the thermostat. Agreement between the two temperatures measured was never worse than 0.1°C.

Of the total of 151 kinetic runs made, 133 were straight kinetic runs in which the parent peak of azoethane, mass 86, was followed as a function of time; in 2 runs all the peaks were followed as a function of time; 4 runs were made for the purpose of analyzing the products of the decomposition; 8 runs were made with the reaction flask packed with sufficient Pyrex wool to increase the total surface area a factor of 20. Five of these packed flask runs were at 310°C and in the pressure range of 10 to 100 microns, and three were in the same pressure range but at 270°C; 4 runs were made with a mixture of 90% toluene and 10% azoethane. The purpose of these runs and the data gathered will be presented in the section, "Data and Results."

CHAPTER IV

Data and Results

In this chapter the data and the results of the data will be presented. Only minor conclusions will be drawn. The interpretation and consequences of the results will be taken up in Chapter V, "Discussion of Results."

The data collected during the course of 151 kinetic runs are given in Table IV. In order to conserve space, a system of abbreviations was adopted and is given at the end of Table IV in the section "Explanation of Table IV." In Figure 3, page 38, $5 + \log_{10} K$ vs $\log_{10} P_1$ is plotted for the seven temperatures studied. The solid curves were obtained from the Kassel Theory and will be discussed in a later section.

The results of Runs 1, 9, 10, 11, 12, 16, 22, 55, 63, 79, and 143 are included in Table IV, but are not plotted in Figure 3, page 38. Runs 1 through 12 were made with a cold spectrometer tube and were considered unreliable. A careful check of these runs with a hot tube showed only Runs 1, 9, 10, 11, and 12 were incorrect and only these were omitted. The other runs were omitted because of excessive scatter or instrumental difficulties.

TABLE IV

Summary of Kinetic Runs

(See end of table for explanation of the system used here)

Run No.	Initial Pressure in microns(P_i)	K (sec^{-1})	$Log_{10}(P_i)$	$5+log_{10}K$
(THE FOLLOWING RUNS ARE AT A TEMPERATURE OF 250.00°C (523.16°K))				
9 101	1.014 2	1.700 -5	2.0060	0.2305
54 100	1.500 2	1.219 -5	2.1761	0.0860
53 100	2.937 2	1.341 -5	2.4679	0.1274
41 100	2.972 2	1.116 -5	2.4731	0.0477
40 100	2.993 2	1.762 -5	2.4761	0.2460
52 100	5.870 2	1.596 -5	2.7686	0.2030
39 100	6.037 2	2.271 -5	2.7808	0.3562
38 100	1.211 3	2.349 -5	3.0830	0.3709
51 100	1.222 3	1.811 -5	3.0871	0.2579
(THE FOLLOWING RUNS ARE AT A TEMPERATURE OF 260.00°C (533.16°K))				
12 101	2.390 1	3.695 -5	1.3784	0.5676
13 100	2.810 1	1.482 -5	1.4487	0.1709
14 100	2.830 1	1.368 -5	1.4518	0.1361
11 101	5.080 1	3.693 -5	1.7059	0.5674
50 100	7.630 1	2.263 -5	1.8825	0.3547
10 101	9.690 1	3.132 -5	1.9863	0.4958
49 100	1.540 2	2.948 -5	2.1875	0.4695
48 100	3.010 2	3.417 -5	2.4786	0.5337
15 100	3.086 2	3.555 -5	2.4894	0.5508
16 101	6.106 2	3.417 -5	2.7858	0.5337
47 100	6.476 2	4.098 -5	2.8113	0.6126
46 100	1.169 3	4.593 -5	3.0678	0.6621
17 100	1.232 3	4.900 -5	3.0908	0.6902
98 200	3.100 3	5.335 -5	3.4914	0.7271
99 200	6.250 3	6.045 -5	3.7959	0.7814
100 200	1.260 4	6.383 -5	4.1004	0.8050
104 240	2.550 4	6.586 -5	4.4065	0.8186
101 200	4.975 4	7.100 -5	4.6968	0.8513
103 200	1.060 5	7.331 -5	5.0253	0.8652
102 200	1.090 5	7.311 -5	5.0374	0.8640
(THE FOLLOWING RUNS ARE AT A TEMPERATURE OF 270.00°C (543.16°K))				
122 300	9.760 0	1.714 -5	0.9895	0.2340
123 340	1.030 1	1.924 -5	1.0128	0.2842
121 300	2.160 1	3.031 -5	1.3345	0.4816
151 330	2.180 1	2.878 -5	1.3385	0.4591
150 330	4.110 1	3.281 -5	1.6138	0.5160

TABLE IV (Continued)

Run No.	Initial Pressure in microns (P_i)	K (sec^{-1})	$Log_{10}(P_i)$	$5+log_{10}K$
(THE FOLLOWING RUNS ARE AT A TEMPERATURE OF 270.00°C (543.16°K))				
120 300	4.350 1	4.240 -5	1.6385	0.6274
60 100	8.060 1	6.058 -5	1.9063	0.7823
22 101	8.210 1	6.980 -5	1.9143	0.8439
149 330	8.290 1	4.298 -5	1.9186	0.6333
119 300	9.970 1	5.956 -5	1.9987	0.7750
59 100	1.545 2	7.222 -5	2.1889	0.8587
21 100	1.556 2	6.934 -5	2.1920	0.8410
58 100	3.100 2	7.826 -5	2.4914	0.8935
20 100	3.101 2	8.638 -5	2.4915	0.9364
19 100	6.229 2	1.053 -4	2.7944	1.0224
61 100	6.510 2	9.416 -5	2.8136	0.9739
18 100	1.242 3	1.089 -4	3.0940	1.0370
56 100	1.252 3	1.012 -4	3.0976	1.0052
55 101	1.265 3	9.448 -5	3.1021	0.9753
57 100	1.278 3	1.003 -4	3.1065	1.0013
96 200	3.300 3	1.328 -4	3.5185	1.1232
95 200	6.400 3	1.343 -4	3.8062	1.1281
93 200	1.230 4	1.405 -4	4.0899	1.1477
92 200	2.580 4	1.593 -4	4.4116	1.2022
94 200	4.940 4	1.631 -4	4.6937	1.2125
105 250	4.960 4	1.616 -4	4.6955	1.2084
97 200	1.040 5	1.631 -4	5.0170	1.2125
(THE FOLLOWING RUNS ARE AT A TEMPERATURE OF 280.00°C (553.16°K))				
141 300	2.500 0	2.282 -5	0.3979	0.3583
142 300	5.300 0	3.369 -5	0.7243	0.5275
143 301	5.580 0	4.721 -5	0.7466	0.6740
140 300	9.630 0	4.645 -5	0.9836	0.6670
139 300	1.970 1	5.806 -5	1.2945	0.7639
138 300	3.880 1	8.608 -5	1.5888	0.9349
27 100	8.210 1	1.297 -4	1.9143	1.1129
137 300	8.320 1	1.281 -4	1.9201	1.1076
26 100	1.581 2	1.546 -4	2.1989	1.1892
25 100	3.218 2	1.884 -4	2.5076	1.2751
24 100	6.274 2	2.185 -4	2.7976	1.3395
23 100	1.278 3	2.485 -4	3.1064	1.3953
64 200	2.500 3	2.689 -4	3.3979	1.4296
65 200	5.700 3	3.041 -4	3.7559	1.4830
66 200	1.200 4	3.036 -4	4.0792	1.4823
67 200	2.565 4	3.227 -4	4.4091	1.5088
68 200	4.990 4	3.391 -4	4.6981	1.5303
63 201	9.500 4	2.978 -4	4.9777	1.4739
69 200	9.600 4	3.564 -4	4.9823	1.5519

TABLE IV (Continued)

Run No.	Initial Pressure in microns(P_i)	K (sec^{-1})	$Log_{10}(P_i)$	$5+log_{10}K$
(THE FOLLOWING RUNS ARE AT A TEMPERATURE OF 290.00°C (563.16°K))				
130	300	2.380 0	4.627 -5	0.3766	0.6653
129	300	4.390 0	7.433 -5	0.6425	0.8712
128	300	9.880 0	9.930 -5	0.9948	0.9970
127	300	1.950 1	1.476 -4	1.2900	1.1691
126	300	4.010 1	1.833 -4	1.6032	1.2632
124	300	6.360 1	2.442 -4	1.8035	1.3878
125	300	8.060 1	2.846 -4	1.9063	1.4542
32	100	8.290 1	2.776 -4	1.9186	1.4434
31	100	1.659 2	2.951 -4	2.2146	1.4700
30	100	3.255 2	3.942 -4	2.5126	1.5957
29	100	6.512 2	4.625 -4	2.8137	1.6651
28	100	1.292 3	5.074 -4	3.1114	1.7054
89	200	3.100 3	6.479 -4	3.4914	1.8115
85	200	3.650 3	6.219 -4	3.5623	1.7937
86	200	6.900 3	6.310 -4	3.8389	1.8000
87	200	1.280 4	6.761 -4	4.1072	1.8300
88	200	2.540 4	7.154 -4	4.4048	1.8546
90	200	4.940 4	7.553 -4	4.6937	1.8781
91	200	1.065 5	8.121 -4	5.0274	1.9096
(THE FOLLOWING RUNS ARE AT A TEMPERATURE OF 300.00°C (573.16°K))				
134	300	2.310 0	1.210 -4	0.3636	1.0828
135	300	5.490 0	1.878 -4	0.7396	1.2737
136	300	1.090 1	2.239 -4	1.0374	1.3501
133	300	2.040 1	2.968 -4	1.3096	1.4725
132	300	4.160 1	4.158 -4	1.6191	1.6189
79	201	5.000 1	1.576 -3	1.6990	2.1976
131	300	8.030 1	5.371 -4	1.9047	1.7301
37	100	8.630 1	5.470 -4	1.9360	1.7380
36	100	1.670 2	6.778 -4	2.2227	1.8311
35	100	3.270 2	7.795 -4	2.5146	1.8918
34	100	6.575 2	9.104 -4	2.8179	1.9592
33	100	1.317 3	1.081 -3	3.1195	2.0338
82	200	3.100 3	1.345 -3	3.4914	2.1287
81	200	6.500 3	1.415 -3	3.8129	2.1508
80	200	1.220 4	1.400 -3	4.0864	2.1460
84	200	1.260 4	1.416 -3	4.1004	2.1511
77	200	2.540 4	1.556 -3	4.4048	2.1920
106	250	4.960 4	1.510 -3	4.6955	2.1788
78	200	1.040 5	1.844 -3	5.0170	2.2658
83	200	1.100 5	1.828 -3	5.0414	2.2620

TABLE IV (Continued)

Run No.	Initial Pressure in microns(P_i)	K (sec^{-1})	$Log_{10}(P_i)$	$5+log_{10}K$
(THE FOLLOWING RUNS ARE AT A TEMPERATURE OF 310.00°C (583.16°K))				
114 300	1.300 0	1.969 -4	0.1139	1.2943
113 300	2.300 0	2.147 -4	0.3617	1.3318
118 310	3.780 0	6.736 -4	0.5775	1.8284
112 300	5.120 0	3.024 -4	0.7093	1.4806
116 310	7.980 0	1.094 -3	0.9020	2.0391
111 300	9.880 0	3.881 -4	0.9948	1.5889
115 310	9.910 0	1.119 -3	0.9961	2.0488
145 330	1.070 1	6.621 -4	1.0294	1.8209
8 100	1.240 1	5.101 -4	1.0934	1.7077
110 300	2.120 1	5.335 -4	1.3263	1.7271
117 310	2.170 1	1.334 -3	1.3365	2.1252
148 330	2.200 1	5.773 -4	1.3424	1.7614
7 100	2.370 1	6.690 -4	1.3748	1.8254
118 320	3.120 1	6.736 -4	1.4942	1.8284
4 100	3.330 1	7.392 -4	1.5224	1.8688
146 330	3.880 1	8.813 -4	1.5888	1.9451
147 330	4.140 1	8.855 -4	1.6170	1.9472
109 300	4.180 1	7.511 -4	1.6212	1.8757
1 101	5.170 1	2.750 -4	1.7135	1.4393
2 100	5.260 1	9.262 -4	1.7210	1.9667
107 300	8.130 1	1.006 -3	1.9101	2.0026
108 300	8.320 1	1.009 -3	1.9201	2.0039
144 330	8.440 1	1.206 -3	1.9263	2.0814
62 100	8.630 1	1.235 -3	1.9360	2.0918
116 320	9.490 1	1.094 -3	1.9773	2.0391
115 320	1.010 2	1.119 -3	2.0043	2.0488
3 100	1.047 2	1.010 -3	2.0200	2.0043
117 320	1.644 2	1.334 -3	2.2159	2.1252
43 100	1.710 2	1.442 -3	2.2330	2.1590
6 100	1.960 2	1.325 -3	2.2923	2.1222
5 100	3.086 2	1.390 -3	2.4894	2.1430
42 100	3.310 2	1.784 -3	2.5198	2.2514
44 100	7.180 2	1.953 -3	2.8561	2.2907
45 100	1.316 3	2.291 -3	3.1193	2.3600
73 200	2.650 3	2.601 -3	3.4233	2.4151
72 200	6.400 3	3.007 -3	3.8062	2.4781
71 200	1.300 4	2.994 -3	4.1139	2.4763
74 200	2.520 4	3.351 -3	4.4014	2.5252
70 200	2.580 4	3.478 -3	4.4116	2.5413
75 200	4.920 4	3.500 -3	4.6920	2.5441
76 200	9.850 4	3.759 -3	4.993+	2.5751

Explanation of Table IV

In order to conserve space and convey as much information as possible, the following system of notation was used in the above table. The data in columns headed "Initial Pressure" and "K (sec^{-1})," the last number with its sign is the power of ten the number is to be multiplied by, i.e., 1.014 2 reads 1.014×10^{2} or 101.4 and 1.700 -5 reads 1.700×10^{-5}.

The "Run No." is composed of two groups of digits. The first group contains numbers from 1 to 152 and is simply the number of the run. The first digit of the second group indicates the leak used, together with the size of the reaction flask. The following is a list of the leaks used and their characteristics.

TABLE V

Characteristics of Leaks Used

Leak	Observed Hole Diameter (microns)	Length of Hole (microns)	Sensitivity to 43 peak n-butane (mm/μ)
J	1.8	18	0.351
N	14	20	130
5	61	50	1520

The second digit of the second group gives the special purpose of the run in the event there was one. The third digit shows whether the run was acceptable or not.

The following schematic gives the general meaning of the complete Run Number.

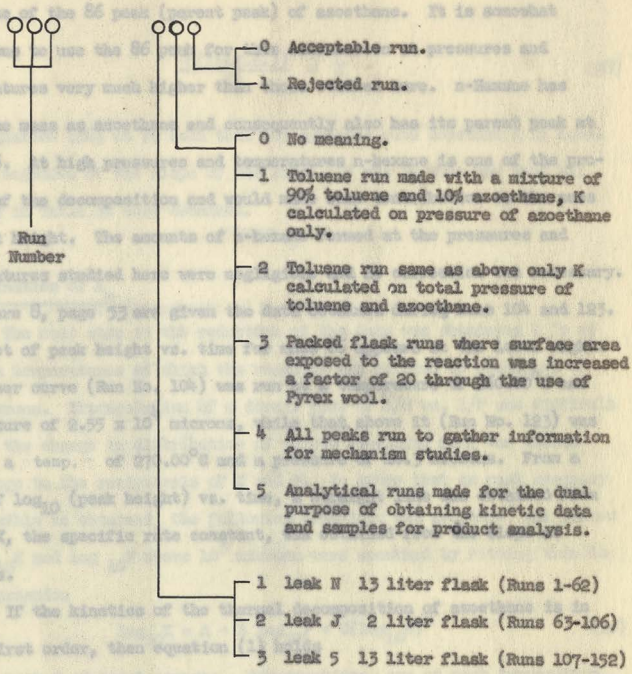

The Specific Rate Constants

The specific rate constants were calculated from the rate of decrease of the 86 peak (parent peak) of azoethane. It is somewhat hazardous to use the 86 peak for this calculation at pressures and temperatures very much higher than those studied here. n-Hexane has the same mass as azoethane and consequently also has its parent peak at mass 86. At high pressures and temperatures n-hexane is one of the products of the decomposition and would make some contribution to the mass 86 peak height. The amounts of n-hexane formed at the pressures and temperatures studied here were negligible and no correction was necessary. In Figure 8, page 53 are given the data obtained during Runs 104 and 123. The plot of peak height vs. time for mass 86 appears at the lower right. The lower curve (Run No. 104) was run at a temperature of 260.00°C and a pressure of 2.55×10^{4} microns, while that above it (Run No. 123) was run at a temp. of 270.00°C and a pressure of 10.3 microns. From a plot of $\log_{10}$ (peak height) vs. time, a straight line was obtained from which K, the specific rate constant, was obtained from the slope as follows.

If the kinetics of the thermal decomposition of azoethane is in fact first order, then equation (1) holds

$$-\frac{dC}{dt} = KC \qquad (1)$$

where C is the concentration. Now the pressure was the concentration unit used and the peak height (P.H.) was directly proportional to the pressure. This allows us to write equation (1) as

$$\frac{-d(P.H.)}{dt} = K(P.H.) \qquad (27)$$

or

$$\frac{-d(\ln(P.H.))}{dt} = K \qquad (28)$$

From equation (28) it is seen that the specific rate constant K is equal to the negative of the slope of the line. It was in this way that all the K's in Table IV were obtained.

Determination of K_∞

The next step in the reduction of the data was obtaining K_∞'s at the six temperatures at which the reaction was carried to pressures of 10^5 microns. Extrapolation of a direct plot of 1/K vs. 1/P was difficult due to the change in distribution of points resulting from the change from logs to the reciprocals of K and P. In order that as much accuracy as possible be obtained, the following technique was adopted. All values of $\log_{10}K$ and $\log_{10}P$ above 10^3 microns were smoothed by fitting them to the expression

$$\log_{10}K = A + B \log_{10}P + C(\log_{10}P)^2 \qquad (29)$$

by the method of least squares. Six equations, one at each temperature, were obtained. From these equations smoothed values for P and K were obtained and their reciprocals plotted giving the curves found in Figure 4. By extrapolation of these curves to infinite pressure (i.e. 1/P = 0) values for K_∞ for the six temperatures were obtained. The reason Figure 4 is included is to convey only two things. These are, the curvature of the

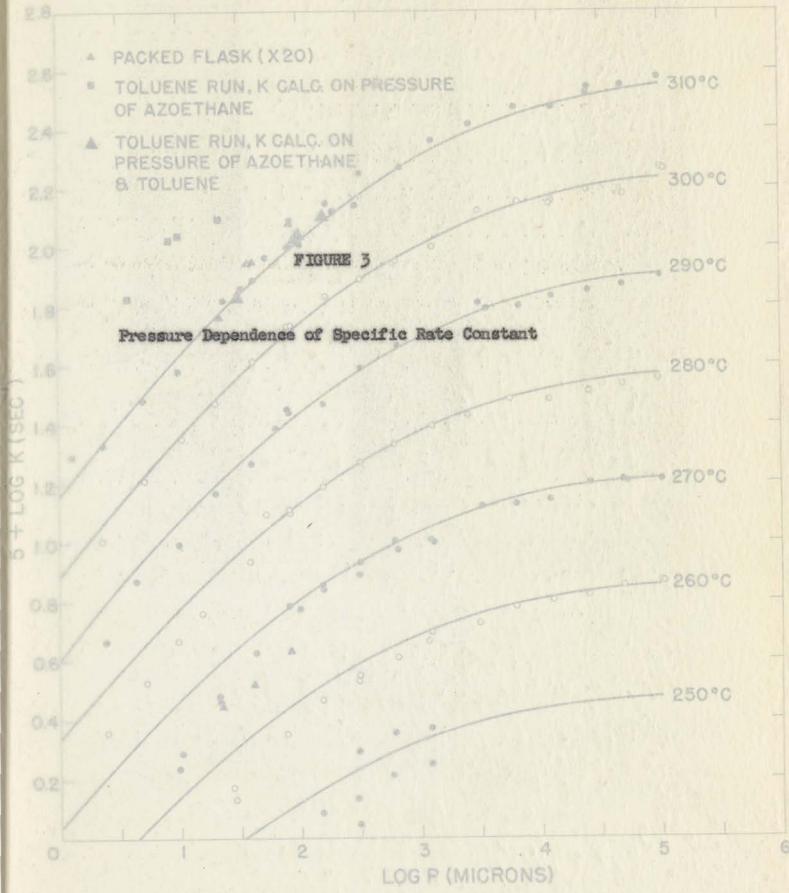

FIGURE 3

Pressure Dependence of Specific Rate Constant

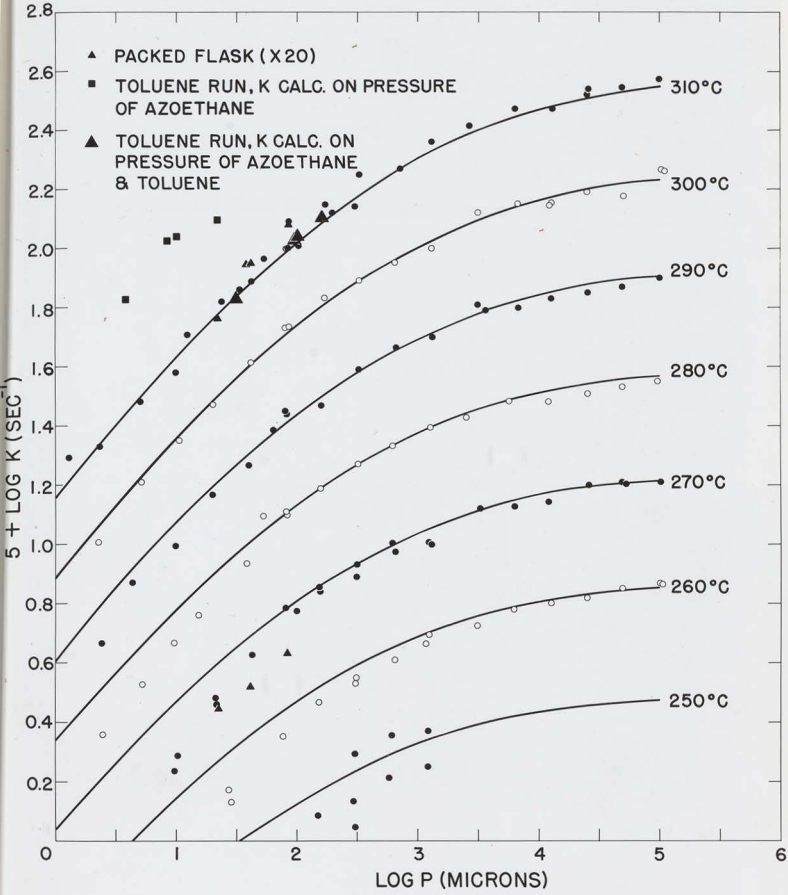
PACKED FLASK (X20)
TOLUENE RUN, K CALC. ON PRESSURE OF AZOETHANE
TOLUENE RUN, K CALC. ON PRESSURE OF AZOETHANE & TOLUENE
310°C
300°C
290°C
280°C
270°C
260°C
250°C
5 + LOG K (SEC⁻¹)
LOG P (MICRONS)
0
1
2
3
4
5
6
0.2
0.4
0.6
0.8
1.0
1.2
1.4
1.6
1.8
2.0
2.2
2.4
2.6
2.8

FIGURE 4

1/K vs. 1/P Plots for the Six Temperatures Used

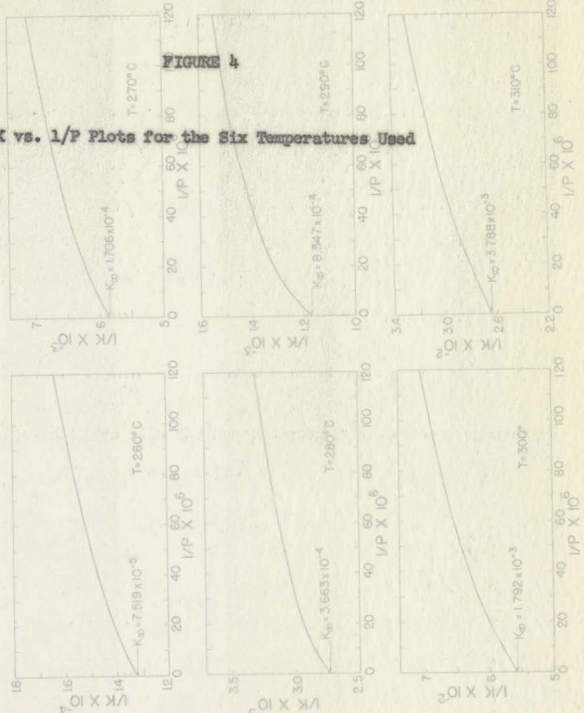

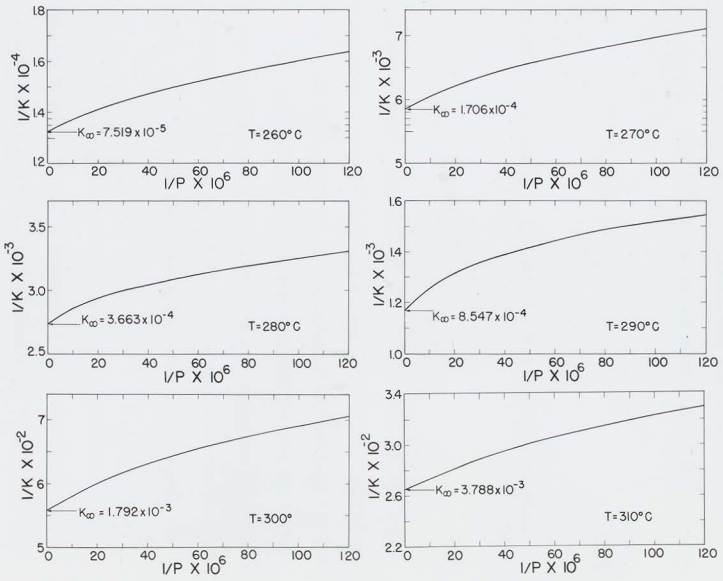
1/K X 10^-4
1.8
1.6
1.4
1.2
K∞ = 7.519 x 10^-5
T = 260° C
0 20 40 60 80 100 120
1/P X 10^6
1/K X 10^-3
7
6
5
K∞ = 1.706 x 10^-4
T = 270° C
0 20 40 60 80 100 120
1/P X 10^6
1/K X 10^-3
3.5
3.0
2.5
K∞ = 3.663 x 10^-4
T = 280° C
0 20 40 60 80 100 120
1/P X 10^6
1/K X 10^-3
1.6
1.4
1.2
1.0
K∞ = 8.547 x 10^-4
T = 290° C
0 20 40 60 80 100 120
1/P X 10^6
1/K X 10^-2
7
6
5
K∞ = 1.792 x 10^-3
T = 300°
0 20 40 60 80 100 120
1/P X 10^6
1/K X 10^-2
3.4
3.0
2.6
2.2
K∞ = 3.788 x 10^-3
T = 310° C
0 20 40 60 80 100 120
1/P X 10^6

1/K vs. 1/P plot and the method by which the different K_∞'s were obtained.

The Activation Energy

Having obtained K_∞ for the six temperatures the activation energy could now be calculated. This is defined by the Arrhenius (1889) equation

$$\frac{d \ln K}{dT} = \frac{E_o}{R_1 T^2} \qquad (30)$$

where E_o is the activation energy. Integration of equation (30) gives

$$K = Ae^{-E_o/R_1 T}. \qquad (31)$$

A plot of $\log_{10} K$ vs. $1/T$ will give $-E_o/2.303\ R_1$ as the slope and $\log_{10} A$ as the intercept. Such a plot is shown in Figure 5 and includes similar plots for several lower pressures. E_o was obtained from the line for infinite pressure. By taking the specific rate constant K= from empirical curves through the experimental points given earlier in Figure 3, page 38, experimental activation energies at different pressures were obtained and are given in Table VI which also gives the frequency factors at the same pressures.

A least squares fit was obtained for the K_∞'s from Figure 4 and the K's from Figure 3, page 38. The equations obtained are given below and are plotted with the experimental data in Figure 5. These equations are:

For infinite pressure (K_∞)

$$\log_{10} K_\infty = 15.7688 - \frac{10,612}{T} \qquad (32)$$

For $P = 10^5$ microns

$$\log_{10} K = 15.7033 - \frac{10,586}{T} \qquad (33)$$

For $P = 10^4$ microns

$$\log_{10} K = 15.4654 - \frac{10,491}{T} \qquad (34)$$

For $P = 10^3$ microns

$$\log_{10} K = 15.0878 - \frac{10,356}{T} \qquad (35)$$

For $P = 10^2$ microns

$$\log_{10} K = 14.6778 - \frac{10,286}{T} \qquad (36)$$

For P = 10 microns

$$\log_{10} K = 15.1551 - \frac{10,799}{T} \qquad (37)$$

For P = 3.16 microns

$$\log_{10} K = 15.6121 - \frac{11,193}{T} \qquad (38)$$

The values for the experimental activation energies and frequency factors given in Table VI were obtained from these least square equations.

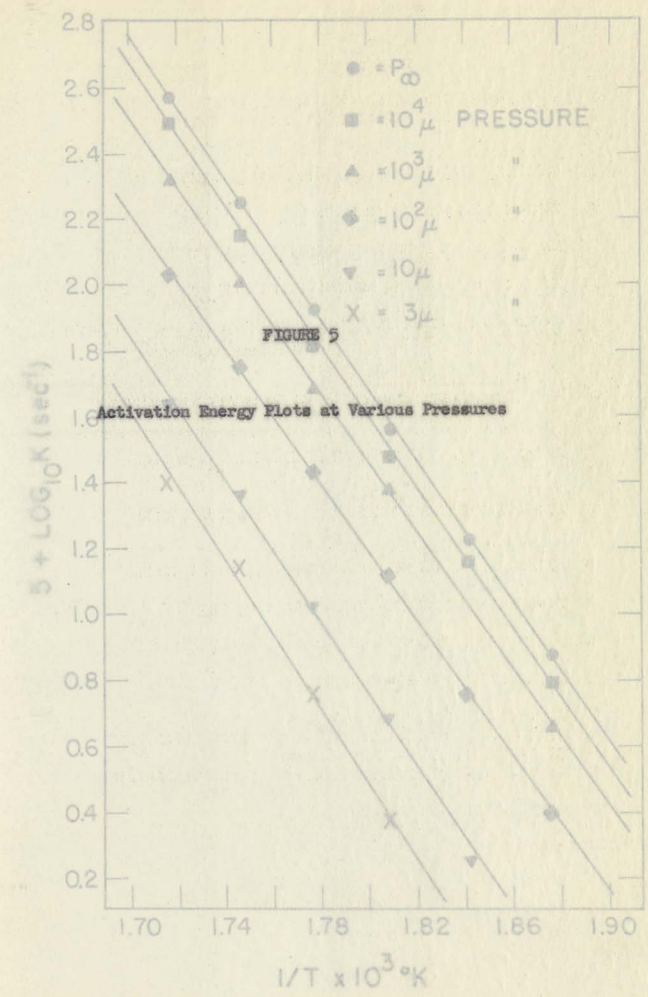

FIGURE 5

Activation Energy Plots at Various Pressures

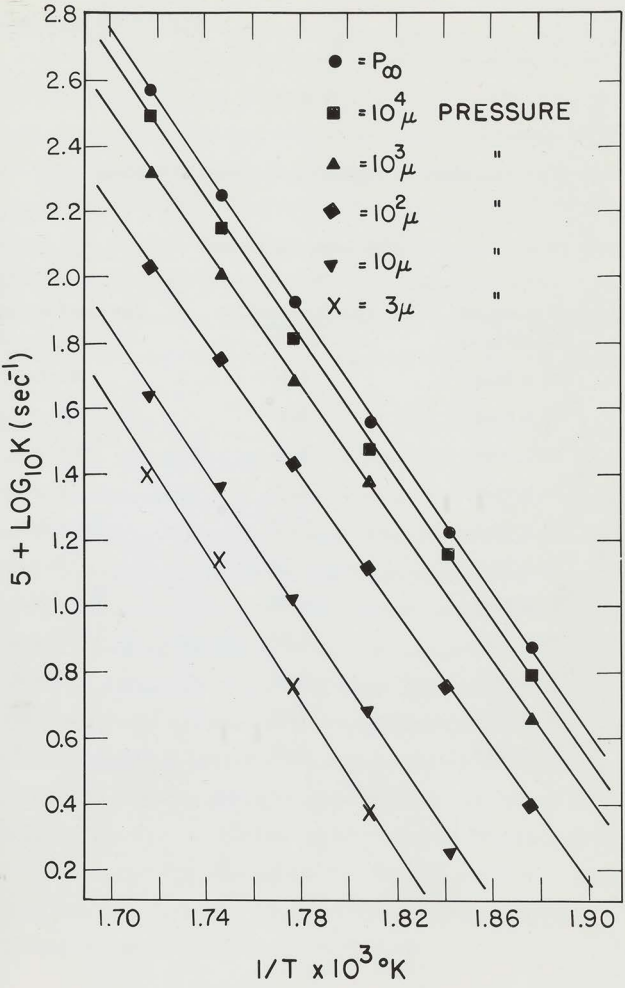
2.8
2.6
2.4
2.2
2.0
1.8
1.6
1.4
1.2
1.0
0.8
0.6
0.4
0.2
5 + LOG10K (sec-1)
1.70
1.74
1.78
1.82
1.86
1.90
1/T x 10^3 °K
● = P∞
■ = 10^4 μ PRESSURE
▲ = 10^3 μ "
◆ = 10^2 μ "
▼ = 10 μ "
X = 3 μ "

TABLE VI

Activation Energy as a Function of Pressure

From Experimental Data

Pressure (microns)	Activation Energy (Kcal.)	Frequency Factor A ($sec.^{-1}$)
infinite	48.5	5.87×10^{15}
1×10^{5}	48.4	5.07×10^{15}
3.16×10^{4}	48.2	4.00×10^{15}
1×10^{4}	48.0	2.92×10^{15}
3.16×10^{3}	47.7	1.97×10^{15}
1×10^{3}	47.4	1.22×10^{15}
3.16×10^{2}	46.9	6.03×10^{14}
1×10^{2}	47.1	4.76×10^{14}
31.6	48.2	8.18×10^{14}
10	49.4	1.43×10^{15}
3.16	51.2	4.09×10^{15}

Packed Flask Experiments

As an experiment to determine if the rate of reaction was independent of the surface area exposed to the decomposing gas, i.e., whether or not the reaction was homogeneous, the reaction flask was packed with Pyrex wool. Using this method the surface area was increased about twenty times (about 20 g. Pyrex wool). Runs 149, 150, 151 at 270.0°C. and Runs 144, 145, 146, 147, and 148 at 310.0°C. were made under these conditions and compared to the data obtained without Pyrex wool. It appears the decomposition is homogeneous in that no change in K could be detected aside from that due to experimental error (see Fig. 3, p.38).

Toluene Experiments

In many thermal decompositions of this type, it has been shown that the reaction proceeds via a chain reaction involving free radicals (Rice and Herzfeld, 1934). The possibility that azoethane proceeded through a free radical chain reaction was checked by the use of toluene as a free radical scavenger. The choice of toluene was dictated by the fact that it does not thermally decompose to any appreciable extent below 700°C. (Blades, et al., 1954). Szwarc (1950) showed that it does act as a methyl scavenger to produce methane and dibenzyl and should thereby inhibit the formation of chains. Runs 115, 116, 117, and 118 at 310.00°C were made with a mixture of 90% toluene and 10% azoethane. When K was calculated, the value found corresponded to the rate constant found with 100% azoethane at the same pressure and temperature (see Fig. 3, p.38). The significance of this result will be considered in Chapter V, "Discussion of Results."

In the toluene runs, the decomposition was allowed to proceed through six-half-lives at which time a mass spectrum was taken of the resulting mixture. The presence of n-propylbenzene and 3-phenylpentane was established without doubt. However, because of the poor resolution in the mass range around mass 182, the presence of 1, 2-diphenylethane could not be stated with certainty even though a peak was observed in the region mass 178-186. It is felt that the presence of n-propylbenzene and 3-phenylpentane is enough to indicate that toluene behaved as expected.

Products of the Reaction

Many runs were made at different pressures and temperatures to investigate what products were obtained from the reaction. In Table IV only two runs are reported. These are Run 105 at 270.00°C and Run 106 at 300.00°C which were both made at pressures of 49,600 microns. The data presented in this section are the results of several special runs (not given in Table IV) made at pressures of 80.0 and 100,000 microns for the sole purpose of product analysis. The analysis of the products was carried out through the use of a gas chromatograph and a mass spectrometer. Because the product mixture at high pressures was so complex, no attempt was made to complete an analysis via the mass spectrometer.

Table VII gives the results obtained by gas chromatography on a product mixture from a decomposition run at a pressure of 100,000 microns and 310.00°C. Table VIII gives the analysis obtained from an average of 15 runs at the same temperature but at a pressure of 80 microns.

TABLE VII

Product Analysis from Gas Chromatography

Average of 5 runs

(All values wt. %)

Initial Pressure = 100,000 microns Temperature = 310.00°C

	wt. %	C	H	N
N_2	27.47	-	-	27.47
C_2H_6	18.87	15.10	3.77	
C_3H_8	3.37	2.76	0.61	
C_3H_6	4.37	3.75	0.63	
isobutane	0.04	0.03	0.01	
n-butane	27.55	22.76	4.79	
butene-1 (?)	2.03	1.74	0.29	
t-butene-2	1.05	0.90	0.15	
c-butene-2	0.58	0.50	0.08	
isopentene	0.90	0.75	0.15	
n-pentane	1.32	1.10	0.22	
C_5 olefins	1.46	1.22	0.24	
3-methylpentane	5.49	4.60	0.90	
n-hexane	1.03	0.86	0.17	
C_6 olefins	0.62	0.52	0.10	
C_7 olefins	2.33	1.96	0.37	
C_8 olefins	1.54	1.30	0.24	
	100.02	59.85	12.72	27.47

Total = 100.0%

TABLE VIII

Product Analysis from Gas Chromatography

Average of 15 runs

(All values wt. %)

Initial Pressure = 80 microns Temperature = 310.00°C

	wt. %	C	H	N
N_2	26.8	-	-	26.8
C_2H_6	4.2	3.4	0.8	
C_2H_4	1.5	1.3	0.2	
C_3H_6	0.6	0.5	0.1	
C_3H_8	2.4	2.0	0.4	
C_4H_{10}	64.8	53.5	11.3	
	100.3	60.7	12.8	26.8

Total = 100.3%

Using the same samples used in obtaining the data for Table VIII, a mass spectrometric analysis was obtained for comparison purposes and is given in Table IX.

The data obtained are summarized in Table X. While the data from mass spectra agree best with theory it is probably fortuitous. From the results of all product analysis done, the conclusion seems to be that the products are not simple. The idea that the reaction proceeds to give n-butane could only be true at low pressures (less than 5 microns). It is evident that as pressures and temperatures increase the products get more complicated.

TABLE IX

Product Analysis from Mass Spectra

Average of 2 runs

(All values wt. %)

Initial Pressure = 80 microns Temperature = 310.00°C

	wt. %	C	H	N
N_2	31.2	-	-	31.2
H_2	0.1	-	0.1	
CH_4	0.2	0.15	0.05	
C_2H_4	3.7	3.17	0.53	
C_2H_6	5.1	4.08	1.02	
C_3H_6	1.8	1.55	0.26	
C_3H_8	2.5	2.05	0.46	
C_4H_8	0.7	0.60	0.10	
n-C_4H_{10}	54.7	45.18	9.52	
	100.0	56.78	12.04	31.2

Total = 100.0%

TABLE X

Summary of Product Analysis

(All values wt. %)

	C	H	N	
Initial Pressure = 80 microns				
Mass Spectra	56.8	12.0	31.2	= 100.0%
Gas Chromatography	60.7	12.8	26.8	= 100.3%
Initial Pressure = 100,000 microns				
Gas Chromatography	59.9	12.7	27.5	= 100.0%
Theory	55.8	11.6	32.6	= 100.0%

Behavior of Several Peaks as a Function of Time

In two of the runs, all masses from mass 12 through mass 105 were recorded. These were Runs Nos. 104 and 123 and were run at pressures of 25,500 and 10.3 microns and temperatures of 260.00°C and 270.00°C respectively. Only those peaks considered most significant were reduced to a relative P.H. scale and plotted as a function of time. These data are given in Figures 6, 7, and 8. In Table XI the P.H.'s for the different peaks are given which were the highest recorded during the run at that mass number. These P.H.'s were equated to 100% and used in Figures 6, 7, and 8. The P.H.'s as given in Table XI are in millimeters as obtained from the recording and were obtained exactly as given in Figure 1, page 15, for azoethane. The scale given in Figure 1, page 15 also applies here. The sensitivity of the mass spectrometer at

TABLE XI

Maximum Peak Heights

Equated to 100% for Use in Figs. 6, 7, 8 (in mm.)

Mass Number	Peak Height at 10.3 μ Run 123 T = 270.00°C.	Peak Height at 2.55×10^{4} μ Run 104, T = 260.00°C.	Suggested Ion
15	286	167	CH_3^+
16	39	123	CH_4^+
17	31	21	NH_3^+ (CH_5^+?)
27	1466	940	HCN^+
28	2430	3340	N_2^+
29	4359	2920	$CH_3CH_2^+$
30	582	466	$CH_3CH_3^+$
39	238	310	
40	240	118	
41	885	625	CH_3CN^+
42	623	314	
43	1807	745	$CH_3CH_2N^+$
44	168	80	$CH_3CH_2CH_3^+$ or CO^+
56	111	276	$C_2O_2^+$ (?)
57	555	364	$CH_3CH_2NN^+$
58	292	104	$CH_3CH_2CH_2CH_3^+$
71	444	104	$CH_3CH_2NHCH_2^+$
86	595	320	$CH_3CH_2NHCH_2CH_3^+$

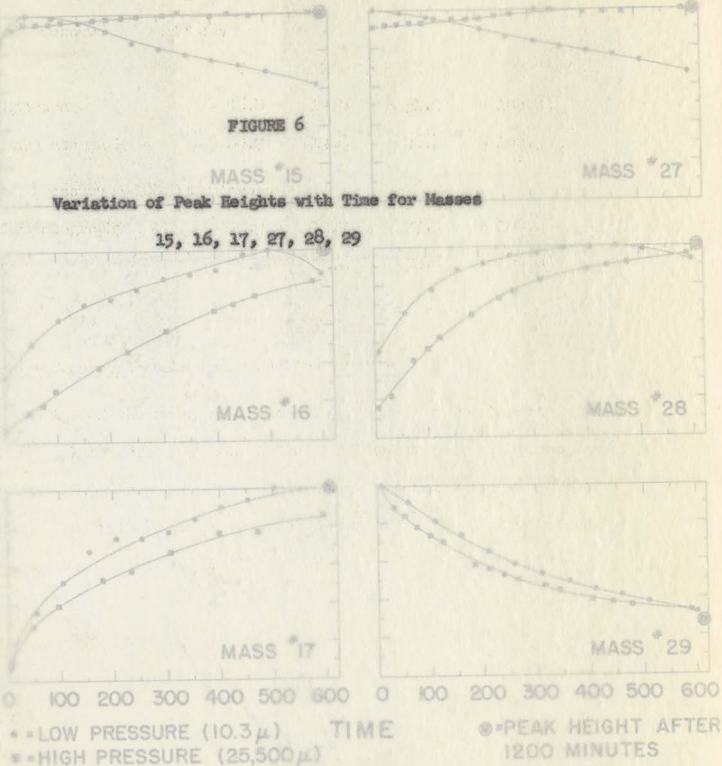

FIGURE 6

Variation of Peak Heights with Time for Masses 15, 16, 17, 27, 28, 29

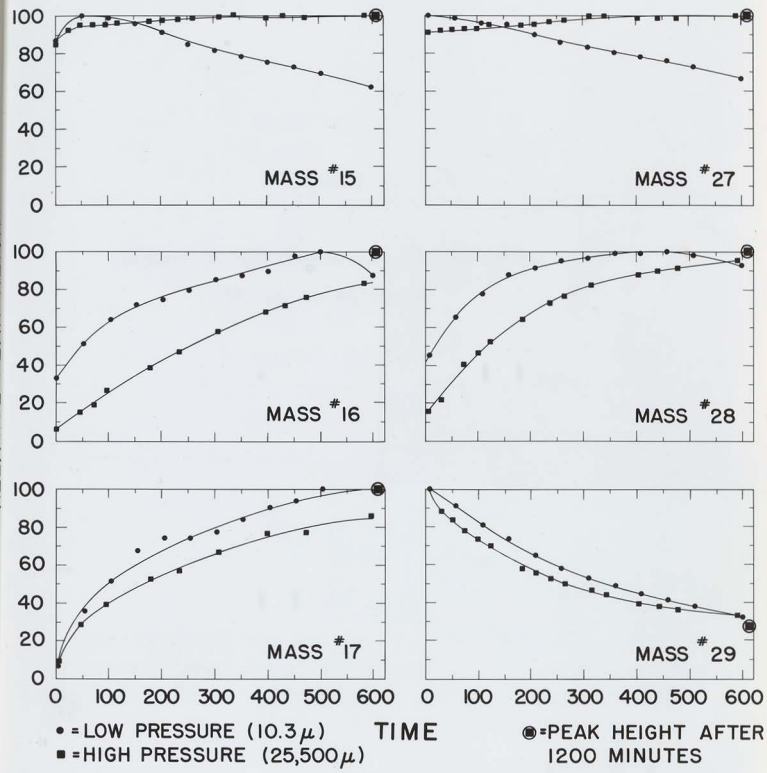
RELATIVE PEAK HEIGHT
100
80
60
40
20
0
MASS #15
MASS #27
MASS #16
MASS #28
MASS #17
MASS #29
0
100
200
300
400
500
600
TIME
• = LOW PRESSURE (10.3 μ)
■ = HIGH PRESSURE (25,500 μ)
◉ = PEAK HEIGHT AFTER 1200 MINUTES

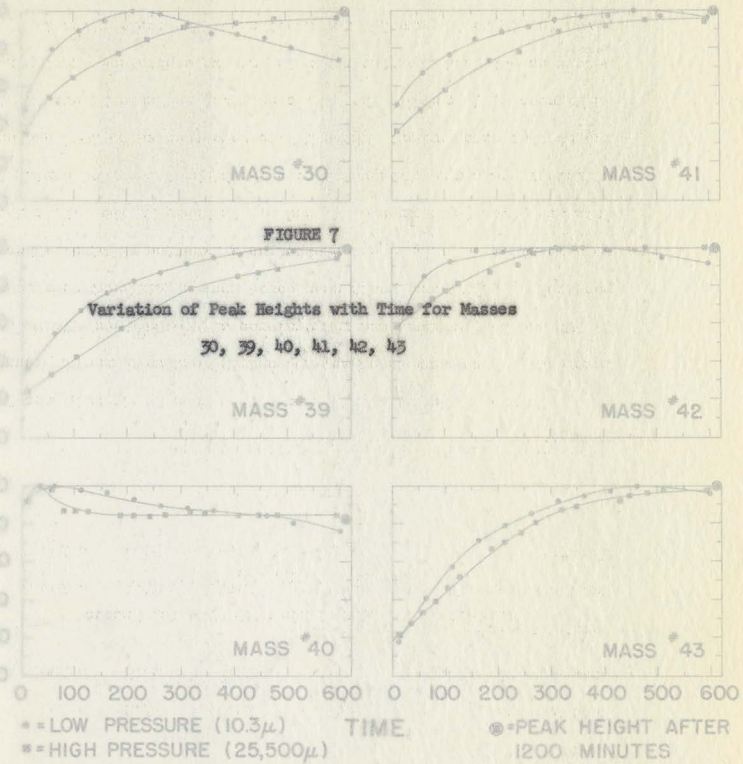

FIGURE 7

Variation of Peak Heights with Time for Masses 30, 39, 40, 41, 42, 43

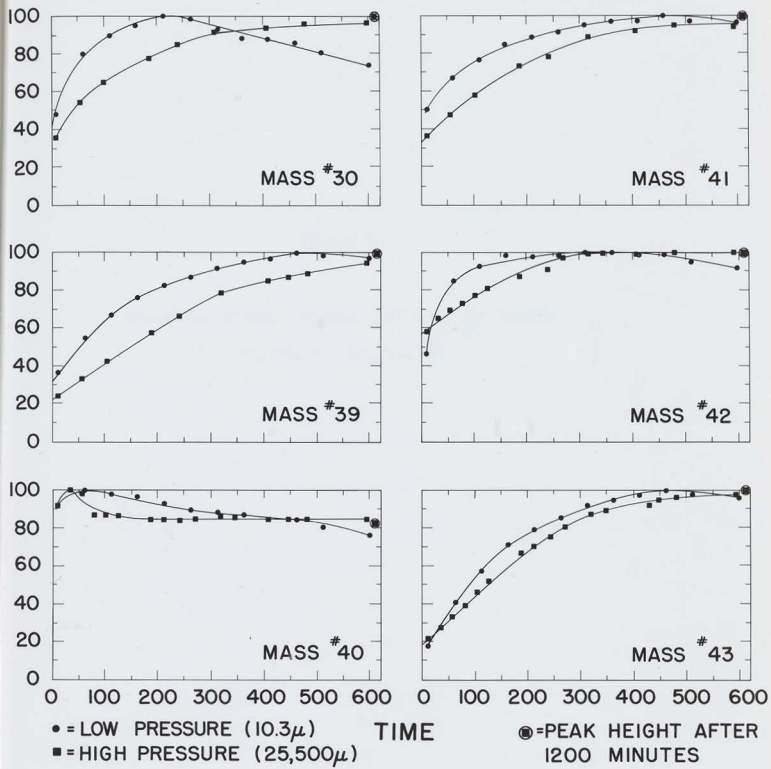
RELATIVE PEAK HEIGHT
100
80
60
40
20
0
MASS #30
MASS #41
MASS #39
MASS #42
MASS #40
MASS #43
0 100 200 300 400 500 600
TIME
• = LOW PRESSURE (10.3μ)
■ = HIGH PRESSURE (25,500μ)
◉ = PEAK HEIGHT AFTER 1200 MINUTES

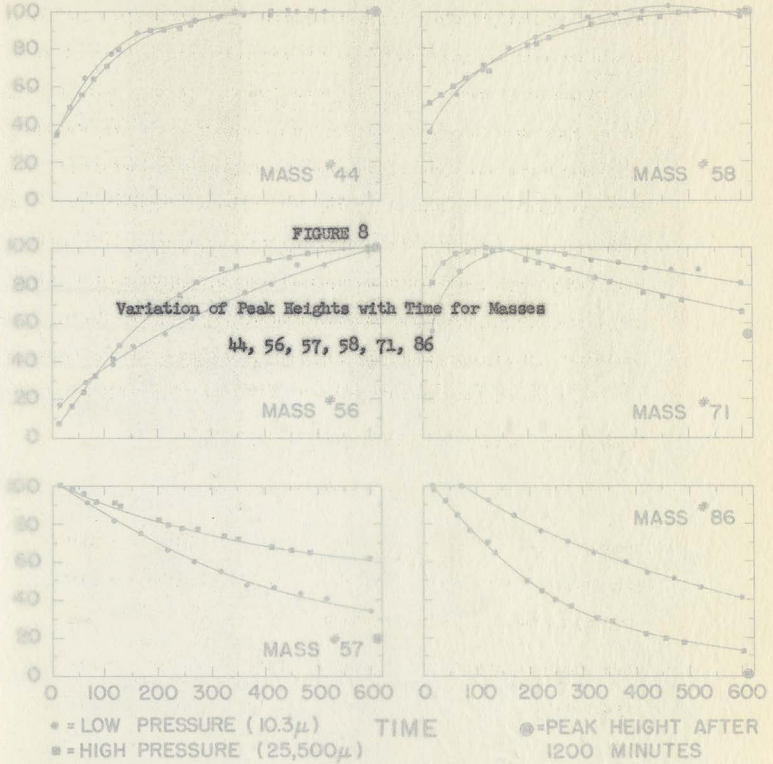

FIGURE 8

Variation of Peak Heights with Time for Masses

44, 56, 57, 58, 71, 86

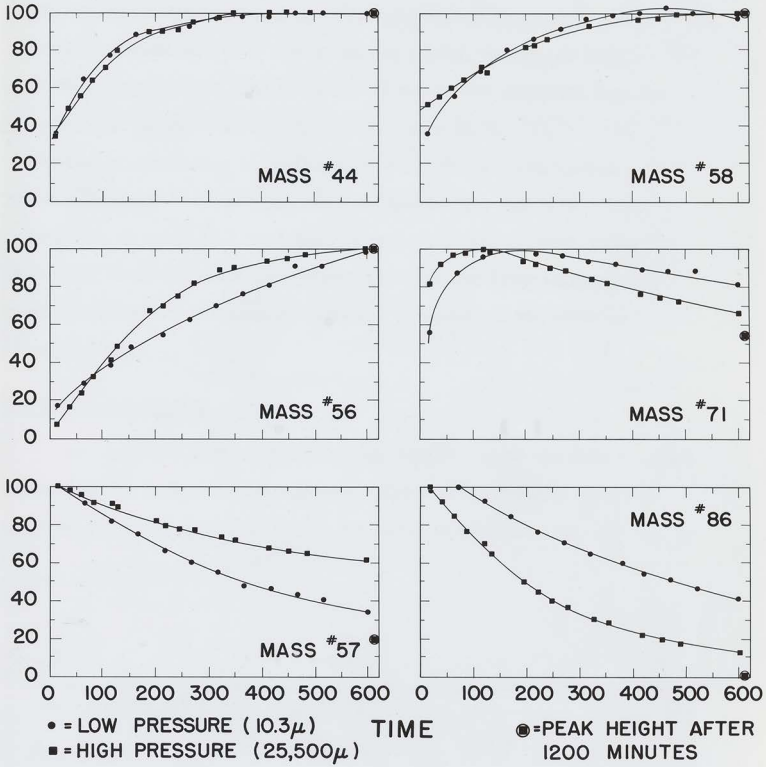
RELATIVE PEAK HEIGHT
100
80
60
40
20
0
MASS #44
MASS #58
MASS #56
MASS #71
MASS #57
MASS #86
0 100 200 300 400 500 600
TIME
● = LOW PRESSURE (10.3μ)
■ = HIGH PRESSURE (25,500μ)
◉ = PEAK HEIGHT AFTER 1200 MINUTES

the different masses may be obtained in units of millimeters deflection of the recorder per micron. In the last column are given the ions which are most likely to be present and that also correspond to the correct mass numbers. Note that at masses 39, 40, and 42, no ions have been suggested and that at masses 17 and 56 the suggested ions are in question. It is worth noting that at masses 31, 45, 73, and 101, the masses corresponding to methylamine, ethylamine, diethylamine, and triethylamine respectively, are not listed. The P.H.'s at these masses were so small (2-5 mm.) that it is safe to assume very little or none of these compounds are present and that the large majority (at least 99.9%) of the nitrogen atoms in azoethane is converted to molecular nitrogen (N_2).

The Kassel Calculation

An important part of this work was the fitting of the data obtained experimentally to the theoretical expression for the specific rate constant as suggested by Kassel (1928) and given in equation (39)

$$\frac{K}{K_\infty} = \frac{1}{\Gamma(s)(R_1T)^s} \int_0^\infty \frac{e^{-x/R_1T}\,dx}{\frac{1}{x^{s-1}} + \frac{K_\infty e^{E_o/R_1T}}{4\sigma^2(x+E_o)^{s-1}N_o}\sqrt{\frac{M}{\pi R_2 T}}} \qquad (39)$$

where

K = specific rate constant

K_∞ = specific rate constant at infinite pressure (see equation (21))

$\Gamma(s)$ = the gamma function of s

s = the effective number of vibrational degrees of freedom in the molecule

R_1 = gas constant in calories/°C mole

R_2 = gas constant in ergs/°C mole

x = $E - E_o$

E = energy in calories

E_o = activation energy in calories

N_o = 9.6612×10^{15} P/T molecules/cm^3

P = pressure in microns

T = temperature in °K

σ = molecular diameter in centimeters

M = molecular weight

The form of the integral is usually simplified by making the following substitutions.

$$D = \frac{1}{\Gamma(s)(R_1T)^s} \qquad (40)$$

$$A = K_\infty e^{+E_o/R_1T} \qquad (41)$$

$$B = 4\sigma^2 \sqrt{\frac{\pi R_2 T}{M}} \qquad (42)$$

which when substituted in equation (39) gives

$$\frac{K}{K_\infty} = D \int_0^\infty \frac{e^{-x/R_1T}}{\frac{1}{x^{s-1}} + \frac{A}{BN_o(x + E_o)^{s-1}}} \qquad (43)$$

The following values for the constants were used in the calculation.

R_1 = 1.98646 calories/°C mole

R_2 = 8.3144×10^7 ergs/°C mole

π = 3.14159

M = 86.14

$\ln x = 2.302585 \log_{10} x$

From the experimental conditions and data were obtained

K_∞ By a plot of 1/K vs. 1/P and extrapolation to infinite pressure. However, values for K_∞ used in this calculation were obtained from equation 32 and were not the experimental values obtained from Figure 4, page 39. These values are for T = 250°C, 3.056×10^{-5}; 260°C, 7.338×10^{-5}; 270°C, 1.706×10^{-4}; 280°C, 3.848×10^{-4}; 290°C, 8.430×10^{-4}; 300°C, 1.797×10^{-3}; 310°C, 3.733×10^{-3}.

E_o By a plot of $\log_{10} K = \log_{10} A - (E_o/2.303\ R_1T)$ from $K = Ae^{-E_o/R_1T}$. When $\log_{10} K_\infty$ is plotted vs. 1/T, a straight line results having a slope of $-(E_o/2.303\ R_1)$ and an intercept of $\log_{10} A$ (Fig. 5, p. 42)

E_o = 48,538 calories and $A = 5.8720 \times 10^{15}$

P and T From the experimental conditions

σ From a consideration of the molecular diameter of n-hexane

s From the best fit to the data

The two most difficult parameters to evaluate are σ and s. The maximum value that s can have is 3n - 6, where n is the number of atoms in the molecule. There is reason to believe that s cannot be greater than (3n-6)/2.

This point will be discussed further in Chapter V. In the case of azoethane $(3n - 6)/2 = 21$. The calculation was started with $s = 21$ and the best fit was obtained with $s = 18$.

However, a value for σ had not yet been obtained. It was observed that n-hexane and azoethane should have about the same structure and considerable information was available from which a molecular diameter could be calculated for n-hexane. The values obtained from the different methods are given in Table XII.

TABLE XII

Molecular Diameter of n-Hexane

Method	Diameter Å
Molecular Refraction	4.6
Molecular Polarization	6.8
van der Waal's "b"	5.2
Viscosity (gas)	5.0
Viscosity (liquid)	5.8

Average = 5.5 Å

Using the average value of 5.5 Å for the molecular diameter of azoethane, the Kassel integral was evaluated for $s = 15$, 16, 17, 18, 19, 20, and 21. At $s = 18$ and $\sigma = 5.5$ Å the solid curves shown in Figure 3, page 38 were obtained and are in excellent agreement with the experimental data. It is possible to obtain approximately the same curves by choosing different values of s and σ. Table XIII gives the values of s and σ that will give almost the same curve.

TABLE XIII

Values for σ and s for Similar Curves

(see Figure 3, page 38)

σ(Å)	s	σ(Å)	s
13.4	15	4.3	19
9.7	16	3.4	20
7.2	17	2.7	21
5.5	18		

From the form of equation (44) it is seen that a change in the value of s cannot be completely offset by a change in the value for σ. However, any of the values given in Table XIII will give a set of curves so similar so as to be indistinguishable from each other on the scale used in Figure 3, page 38.

It seems reasonable to expect the molecular diameter of azoethane to be about 5.5 Å on two counts. First is the similarity between n-hexane and azoethane. Second, McCoy (1956) found 4.7 Å for azomethane and an increase of 0.8 Å for two methyl groups is of the right order.

The actual evaluation of the Kassel integral was done with an IBM 704 electronic digital computer (Willbanks, 1958)which involved programming the calculation of the integral via Simpson's Rule. Because of the wide range of values encountered during the integration, a scaling factor of 10^4 had to be introduced. Equation (44) shows the integral with the scaling factors.

$$K = \frac{K_\infty}{10^4(10^{-4}R_1T)^s\Gamma(s)} \int_0^{6\times10^4} \frac{e^{-x/R_1T}\,dx}{\frac{1}{(10^{-4}x)^{s-1}} + \frac{A}{BN_o 10^{-4}(x+E_o)^{s-1}}} \qquad (44)$$

The considerations which lead to the decision to use Simpson's Rule are: (1) both limits are known, the upper limit being chosen for machine calculation where the integral converges to eight significant figures, (2) the selection and modification of the interval used was simplified, and (3) the coefficients of the individual terms were powers of 2.

Rewriting equation (44) for integration using Simpson's Rule and including the necessary coefficients, we get

$$\log_{10}K = \log_{10}\left[\frac{1}{3}\frac{K_\infty \Delta E}{10^4(10^{-4}R_1T)^s\Gamma(s)} \sum_{E=E_o+\Delta E}^{105} \frac{C_{sr}\,e^{-x/R_1T}}{\frac{1}{(10^{-4}x)^{s-1}} \quad \frac{A}{BN_o(10^{-4}E)^{s-1}}}\right] \qquad (45)$$

where

ΔE = the integration interval

$1/3$ = a Simpson constant

C_{sr} = Simpson's Rule coefficient

The integral was solved for $\log_{10}K$ since it was to be plotted as $\log_{10}P$ vs $\log_{10}K$ and compared to the experimental plots. Equation (45) is the final form used by the IBM 704 for solution.

In Figure 9, plots of the Kassel integrand vs. energy are given. Here I is equal to the Kassel integrand including the scaling factors

shown in equation (45). The curves are calculated for four temperatures and at one pressure.

The curves shown in Figure 10 are again the Kassel integrand vs. energy, but are at five pressures and at constant temperature. The value for ΔE used in these calculations was 250 calories. Subsequent work showed that ΔE could assume values of 1500 calories before any difference would be seen in the sixth place of the value of the integral.

The values obtained from the evaluation of the Kassel integral are given in Table XIV. These values remain constant for all the values of σ and s given in Table XIII.

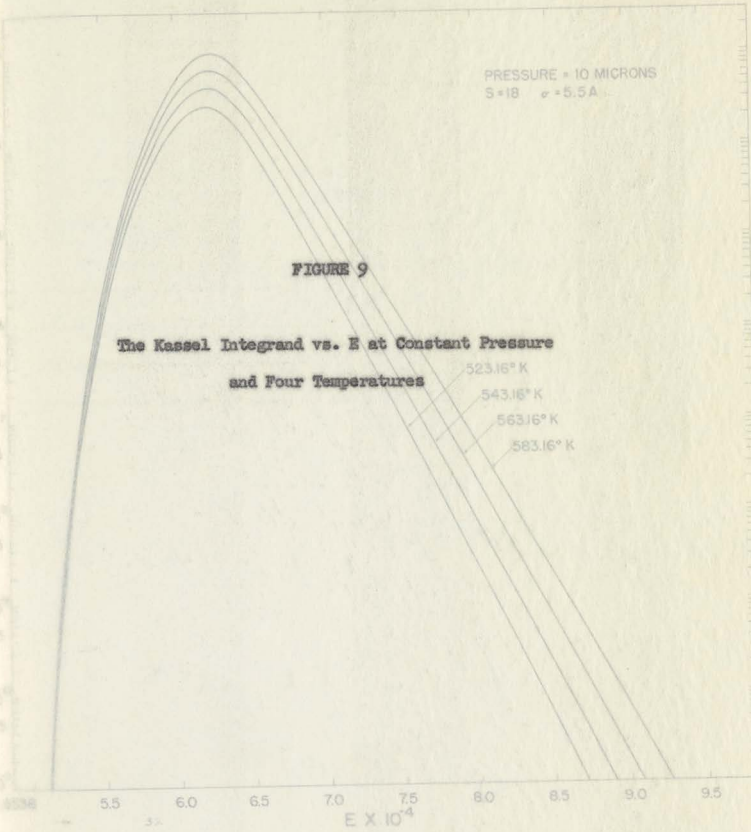

FIGURE 9

The Kassel Integrand vs. E at Constant Pressure and Four Temperatures

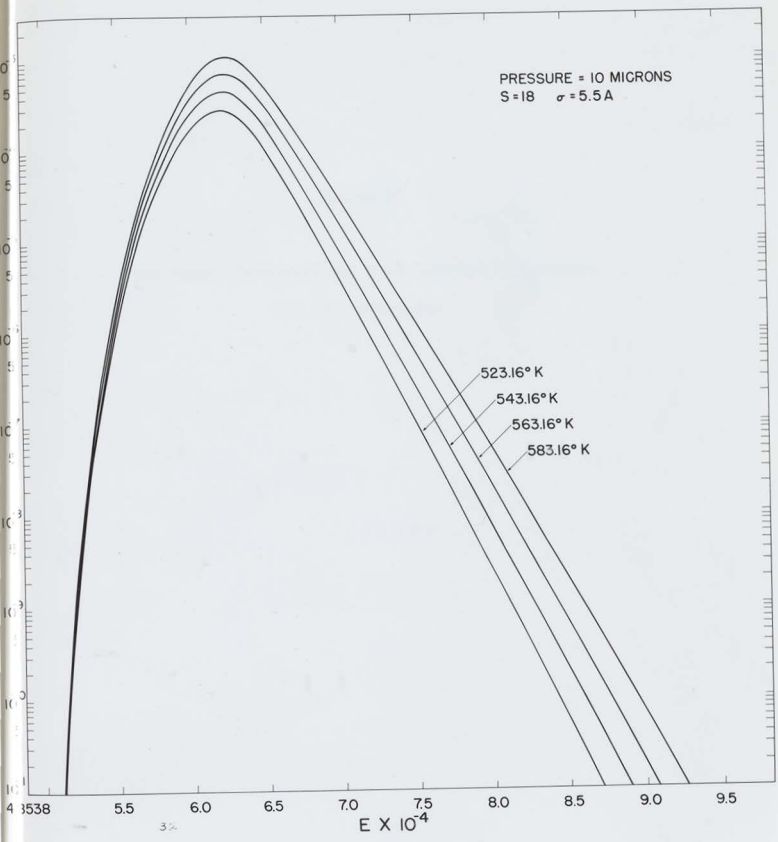
PRESSURE = 10 MICRONS
S = 18 σ = 5.5 A
523.16° K
543.16° K
563.16° K
583.16° K
5.5
6.0
6.5
7.0
7.5
8.0
8.5
9.0
9.5
E X 10^-4

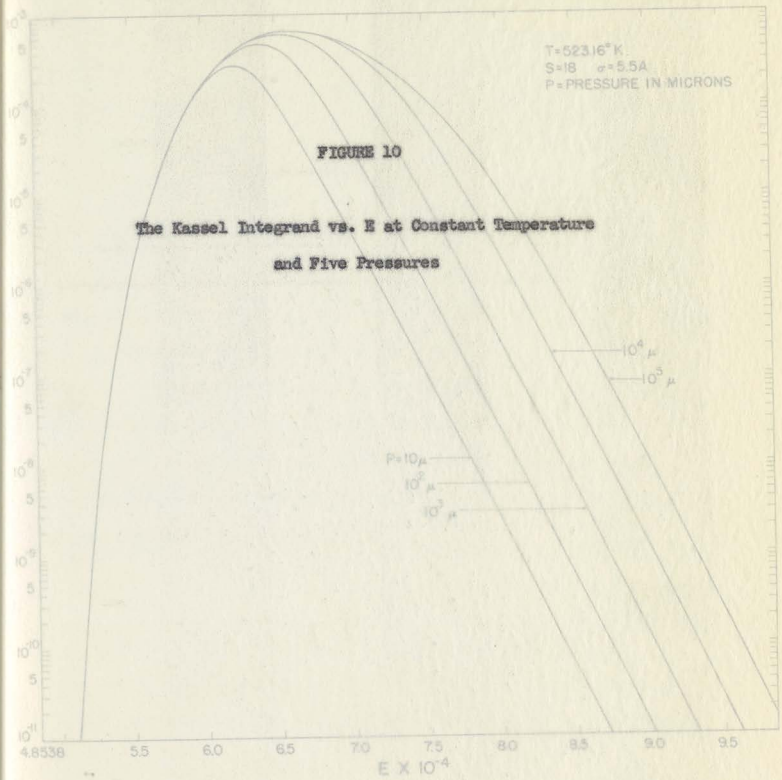

FIGURE 10

The Kassel Integrand vs. E at Constant Temperature and Five Pressures

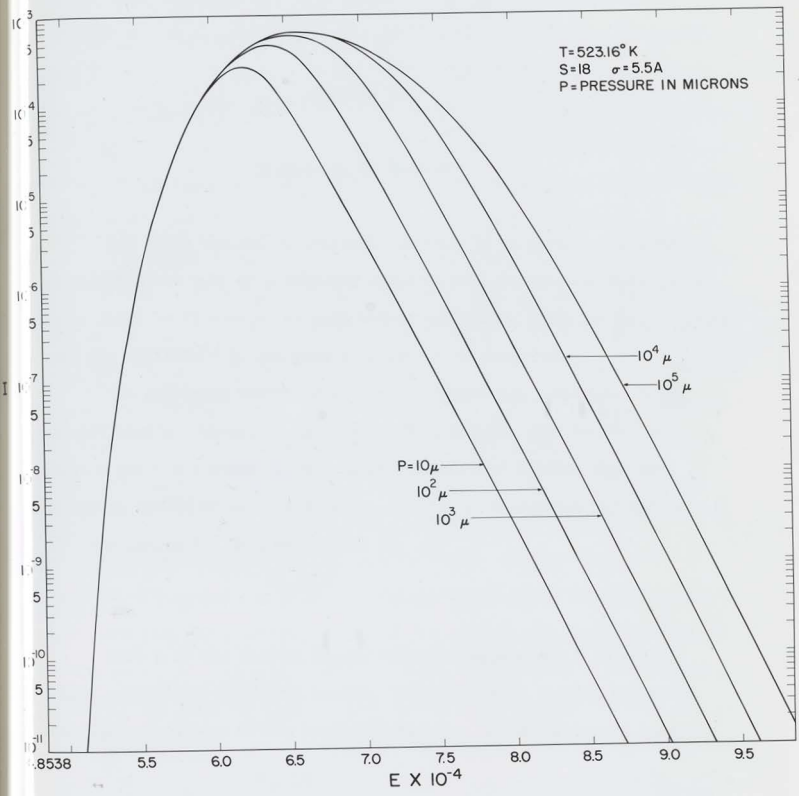
T=523.16° K
S=18 σ=5.5A
P=PRESSURE IN MICRONS
10^4 μ
10^5 μ
P=10μ
10^2 μ
10^3 μ
5.5
6.0
6.5
7.0
7.5
8.0
8.5
9.0
9.5
E X 10^-4

CHAPTER V

Discussion of Results

The first concern of chemical kinetics is to provide a method of calculating the rate of a chemical reaction from fundamental principles. While there is at present no such method available, three general theories that are applicable to gas reactions have been suggested.

The collision theory is by far the oldest and simplest. Using classic kinetic theory, it calculates the collision rate between molecules a and b and assuming only those molecules will react that have energy in excess of some minimum E_o, derives an expression for the specific rate constant. This expression is

$$K = P Z e^{-E_o/R_1T} \qquad (46)$$

Here Z is the kinetic theory collision number and P is the so-called probability or steric factor. This theory is chiefly concerned with the calculation of the frequency factor A of the Arrhenius equation

$$K = A e^{-E_o/R_1T} \qquad (31)$$

where

$$A = P Z \qquad (47)$$

in equation (46). Inability to evaluate the steric factor, P, a priori, has been one of the great drawbacks of the collision theory. It should also be pointed out that E_o in the Arrhenius equation (31) is not quite the same as E_o in the collision theory equation (46) since Z varies with $\sqrt{T}$. The value of P ranges from one to 10^{-8} and can only be obtained from experimental data. The simplicity of the theory is all but destroyed when one attempts to arrive at a value for P by any other means.

The second theory is the absolute reaction rate theory which provides a basis for the theoretical calculation of both the A factor and the activation energy but not with great accuracy. It is usually associated with the name of Eyring and is covered in some detail by Glasstone, Laidler and Eyring (1941). The most important idea the theory introduces is that of the activated complex which is formed by the fusion (for a very short time) of one, two, or three reactant molecules. The number of molecules needed to form the complex determines if the reaction is to be unimolecular, bimolecular, or termolecular. The theory provides a means of calculating the rate of decomposition of the activated complex into products, the potential energy of the complex, and the concentration of the complexes with a given structure and energy content. The application of the absolute reaction rate theory to a specific reaction is often tedious due to the mathematical computations necessary and inaccurate due to the approximations made.

The last of the three general theories is really a special case of the collision theory. This is the case of unimolecular reactions and is the one this report is primarily concerned with. As mentioned earlier,

for many years it was difficult to understand how a unimolecular reaction could exist. After Daniels and Johnston (1921) demonstrated that the N_2O_5 thermal decomposition was first order and attempts to explain this on the basis of the radiation theory failed, it seemed natural that some effort to find a theory to explain this would be made. This was indeed the case, for within ten years several theories had appeared which on close examination proved to be similar. Four theories of unimolecular reactions are due to Hinshelwood (1927), Rice and Ramsperger (1927 and 1928), Kassel (1928), and Slater (1939, 1948 and 1953).

Using the collision theory and with the aid of the Lindemann time-delay suggestion, Hinshelwood evolved a theory of unimolecular reactions that was treated in Chapter I. Also from Chapter I, equation (22), we see that the Hinshelwood-Lindemann theory predicted a straight line from a plot of 1/K vs. 1/M. That this is not the case has been shown by many investigators and also by this work (see Figure 4, page 39).

The theories of Rice and Ramsperger and that of Kassel are nearly identical. In this report we will adopt the notation HL, KL, and SL, for the three theories of Hinshelwood, Kassel, and Slater. The presence of the L indicates all three incorporate the Lindemann time-delay suggestion.

While this report is mainly concerned with the KL theory and comparing experimental data to it, a few words of comparison between the SL and KL theories may serve as background material.

The most satisfactory theory of unimolecular reactions from many points of view is the SL theory. In three excellent papers, Slater (1939, 1948, 1953) explores in some detail his treatment as compared to others and applies it to the case of cyclopropane. It is beyond the scope of this

paper to consider in detail the SL theory and therefore only a brief summary will be given.

The model Slater assumes is a polyatomic molecule whose oscillators are classical and harmonic. He sets up a series of internal coordinates q_1, q_2, ··· and describes the molecular motions in terms of these. Decomposition occurs when any coordinate attains a critical value q_0. As the oscillators are harmonic the potential energy is quadratic in the q's and therefore the internal motion can be resolved into normal modes 1, 2, 3,··· with frequencies ν_1, ν_2, ν_3 ··· which are independent if the motions are truly harmonic. On this point the SL and KL theories differ in that KL assumes the oscillators to be lightly coupled and that energy can flow from one oscillator to another where SL does not. The SL theory clearly states that the variation of any given q is only a function of the time since the last collision. The amplitude factors, α_s, are constants dependent on the particular q being considered and are obtained from inertial and force constants of the molecule. To obtain the α_s's a complete spectroscopic vibrational study of the molecule must be made. This limits the general usefulness of this theory to that relative small number of molecules for which a complete vibrational analysis has been made or can be made.

In general, the SL and KL theories are quite similar. Instead of calculating the probability of one bond acquiring a critical energy E_0, as KL does, SL calculates the frequency with which a given q will attain a critical distance q_0. This frequency is dependent on the vibrational frequencies, energies and phases of the individual oscillators. Using no concealed assumptions or questionable approximations, Slater proceeds with a rigorous treatment that results in an equation relating the specific rate constant, K, and P (pressure) having the form

$$\frac{K}{K_\infty} = \frac{1}{\Gamma(n/2 + 1/2)} \int_0^\infty \frac{X^{\frac{n-1}{2}} e^{-X} dX}{1 + X^{\frac{n-1}{2}} \Theta^{-1}} \qquad (48)$$

where

$$\Theta = \frac{aN}{\nu}\left(\frac{E_o}{R_1 T}\right)^{(n-1)/2} F_n$$

$$X = (E - E_o)/R_1 T$$

$$a = 4\sigma^2\sqrt{\frac{\pi R_2 T}{M}}$$

N is the number of molecules per cc., n is the number of modes of vibration, ν is the mean vibrational frequency of the n modes of vibration. F_n is a function of n and the amplitude factors of the vibrational modes and is equal to $(4\pi)^{(n-1)/2}(n/2 - 1/2)!\,\mu_1\mu_2\cdots\mu_n$ where $\mu_s = |\alpha_s|/\alpha$. α_s is the amplitude factor of a particular mode of vibration and $\alpha^2 = \sum \alpha_s^2$.

A consideration of equation (48) shows it behaves as expected. At high pressures N and therefore Θ tend toward infinity which means the right hand side of equation (48) tends toward unity giving $K = K_\infty$.

The SL theory is the most elegant of the four for it requires only the activation energy from experimental data. It also fills the void left by HL by including the notion that high energy molecules will react faster than those with low energy. The value for n is determined by the theory and not chosen to provide the best fit to the experimental data as is done in the KL theory. The problem of 1/K vs. 1/M plots giving straight lines in the HL theory is also eliminated. SL theory gives 1/K vs. 1/M plots consistent with experimental data.

With all the advantages it has, it would seem odd if no fault could be found. There are only two serious disadvantages: First, the SL model contains only classical oscillators and makes no provision for molecular vibrations being quantized or anharmonic and, second, no account is taken of the fact that the molecules have kinetic energy when they react. The SL treatment is one in which it is assumed the molecule is at rest.

The KL theory while not so rigorously developed as the SL theory is nonetheless quite useful in treating unimolecular reactions. As mentioned earlier, this work is concerned with both the development of an experimental technique and the application of the results to unimolecular kinetics. The data obtained from experimental studies of the kind discussed in this report are directly applicable to the KL theory.

There are a number of similarities between the KL and SL theories. The all-important one is that they both make allowance for the shorter lifetimes of the more energetic molecules. Whereas SL considered a reaction from the point of view of q_0 reaching some critical value, KL simply assumed that an activated molecule would react when some bond in the molecule acquired an energy of E_0 or greater. Further KL showed (Kassel, 1928) that on the basis of this assumption and using the statistical mechanical approach, it is possible to calculate the way the specific reaction rate constant (K) of activated molecules varies with the energy content of the molecule. Using this approach the relationship given by equation (39) was obtained.

$$\frac{K}{K_\infty} = \frac{1}{\Gamma(s)(R_1T)^s} \int_0^\infty \frac{e^{-X/R_1T}\,dX}{\frac{1}{(X)^{s-1}} + \frac{K_\infty e^{+E_o/R_1T}}{4\sigma^2(X+E_o)^{s-1}N_o}\sqrt{\frac{M}{\pi R_2 T}}} \qquad (39)$$

Here the notation is the same as that given earlier. We observe that X in equation (39) is equal to E - E_o and in equation (48) X = E-E_o/R_1T. Writing Θ in terms of its factors and changing X to the form used in (39), equation (48) can be rewritten for comparison as

$$\frac{K}{K_\infty} = \frac{1}{\Gamma(L)(R_1T)^L} \int_0^\infty \frac{e^{-X/R_1T}\,dX}{\frac{1}{(X)^L} + \frac{\nu}{4\sigma^2(E_o)^L N_o F_n}\sqrt{\frac{M}{\pi R_2 T}}} \qquad (49)$$

where L = (n + 1)/2.

According to SL, F_n is about unity and ν has the same units and magnitude of A in $A = K_\infty e^{+E_o/R_1T}$. Also X is small compared to E_o. Therefore, all that is necessary to make the results of the two theories nearly identical numerically as well as formally is the relationship

$$s = \frac{n+1}{2} = L,$$

or

$$n = 2s - 1 \qquad (23)$$

which was pointed out in Chapter I. In giving this result SLater pointed out that not more than half of the available (3N - 6) oscillators (where N is the number of atoms per molecule) will ever be required to fit the KL theory to the experimental data. The results of KL calculations on

azomethane and azoethane showed that for azomethane 12 oscillators ($3N - 6 = 24$) were required and azoethane ($3N - 6 = 42$) required 18 oscillators.

The Activation Energy

The activation energies obtained from experimental data are given in Table VI, page 43 together with the frequency factor. These values were taken from "best fit" lines drawn through the experimental points shown in Figure 3, page 38. It is seen from Table VI that the values for E_o fall to a minimum at a pressure of about 300 microns where they begin to rise again, reaching a value of 51.6 kcal. at about 3 microns. It is interesting to compare this result to that expected from theory. Table XV gives the activation energies obtained from the Kassel curves shown in Figure 3, page 38. The experimental activation energies from Table VI, page 43 are repeated for comparison purposes. Apparently the KL theory predicts a decrease in activation energy with decreasing pressure. This prediction is not fully borne out by the experimental data for azoethane, especially at low pressures. At least part of the difficulty may be due to the leakout correction difficulty at low pressures in that this correction becomes very important in the zero to 100 micron range.

It is of some interest to compare the activation energies the different theories should give at "zero" and "infinite" pressures and those obtained from experiment. Given in Table XVI are the expressions for the activation energy predicted by the different theories.

TABLE XV

Activation Energies from Kassel Curves

Pressure (microns)	Kassel activation energies (kcal.)	Experimental activation energies (kcal.)
Infinite	48.5	48.5
100,000	48.2	48.4
10,000	47.4	48.0
1,000	46.0	47.4
100	44.0	47.1
10	42.6	49.4
3.16	41.8	51.2

TABLE XVI

Activation Energies at Zero and Infinite Pressure from the HL, KL, and SL Theories (N_o being held constant, not P)

Theory	P_∞	P_o
HL	$E = E_o - (s - 1)R_1T$	$E = E_o - (s - 3/2)R_1T$
KL	$E = E_o$	$E = E_o - (s - 3/2)R_1T$
SL	$E = E_o$	$E = E_o - (n - 2)R_1T/2$

Using the value 18 for s and from equation (23), page 9, n = 33, the following values for the activation energy are obtained.

TABLE XVII

Values for Activation Energies

(kcal/mole, T = 553.16°K)

Theory	P_∞	P_o
HL	29.8	30.4
KL	48.5	30.4
SL	48.5	30.3

All three theories agree on the zero pressure activation energy while at infinite pressure the HL theory value is 18.7 kcal low. This is reasonable when it is recalled that HL does not consider the rate of reaction to be affected by the amount of energy in excess of E_o contained in the activated molecule. This omission results in the HL activation energy being essentially independent of pressure.

It is unfortunate that this decrease in activation energy cannot be detected with some degree of accuracy at lower pressures. Aside from the leakout correction problem, the problem of the mean-free path is a great obstacle. The lowest pressure studied here was about one micron in a 12-liter flask. Even here, where the mean-free path is of the order of centimeters, a large fraction of the collisions occurring are with the walls of the vessel. Consider then the flask size needed to maintain the same fraction of molecular collisions with the walls compared to intermolecular collisions at a pressure a factor of 10 less (0.1 micron). This would require a 12,000-liter flask and a thermostat to heat it in. From these considerations, an extension of this study into lower pressure ranges does not appear feasible.

The Lifetimes of Activated Molecules

It is of some interest to consider the lifetime of an activated molecule. This subject has been reported on before by several authors (Marcus, 1952; Rice and Weininger, 1952; Trotman-Dickenson, 1955, p. 55).

From equation (5) and (6) we see that the equilibrium constant K_1 is

$$K_1 = \frac{k_1}{k_2} . \tag{50}$$

For the case of high pressures where the concentration of A* approaches the equilibrium value $K_1[A]$ that it would have if no A* were lost by reaction, K_1 may be derived from classical statistical mechanics (Hinshelwood, 1949, p. 39).

$$K_1 = \left(\frac{E_o}{R_1 T}\right)^{s-1} \left(\frac{e^{-E_o/R_1 T}}{(s-1)!}\right) \tag{51}$$

Here the substitution $E = E_o$ has been made which according to the KL theory is true at high pressure (see Table XVI, page 72). Now, from equation (21)

$$K_\infty = \frac{k_2 k_1}{k_2} \tag{21}$$

and using equation (50) we obtain

$$K_\infty = k_3 K_1$$

or

$$k_3 = \frac{K_\infty}{K_1} \tag{52}$$

Since the reciprocal of k_3 is the lifetime of an activated molecule and recalling that

$$K_\infty = A\, e^{-E_o/R_1 T}$$

at high pressures, all that remains is to perform the algebra. Therefore, $\overline{t^*}$, the mean lifetime of an activated molecule at high pressure is given by

$$\overline{t^*} = \frac{1}{k_3} \cdot \frac{\left(\frac{E_o}{R_1 T}\right)^{s-1}}{A\,(s-1)\,!} \qquad (53)$$

For the case of azoethane where E_o = 48.5 kcal, at T = 583.16°K; $\overline{t^*}$ is equal to 1.78×10^{-3} sec. and at T = 523.16°K, $\overline{t^*} = 1.14 \times 10^{-2}$ sec. This is an increase by a factor of about 16 for an increase in temperature of only 60°C and 1000 times longer than that calculated for the azomethane case (s = 12; E_o = 50.4 kcal). Under these circumstances the collision rate is at least 10^6 sec^{-1} which means an azoethane activated molecule must undergo at least 1000 collisions before deactivation does occur. Weininger and Rice (1952) in a paper on the photolysis of azoethane gave 4.1×10^{-11} sec (adjusted to 5.5 Å and 1300 mm pressure) for the minimum mean lifetime. Their calculation used simple collision theory and assumed zero activation energy which would account for at least six of the eight powers of ten separating the two numbers. Marcus (1952) in two papers on "Lifetimes of Active Molecules" found 2×10^{-6} sec. for the lifetime of the C_3H_8 molecule. He found, as expected, that the lifetime increases with the size of the active molecule.

At best any calculation of this sort is only an approximation. Direct experimental measurement of these lifetimes is difficult and has not met with much success.

Variation of K with P

The variation of the specific rate constant (K) with initial pressure (P) is shown in Figure 3, page 38. As indicated earlier, the curves are those obtained by the IBM 704 computer evaluation of equation (39), the expression relating K and P given by the KL theory.

That the data agree very well with the calculated curves is evident. The changeover from first to second order kinetics predicted by the HL theory (together with the KL and SL theories) is also borne out.

The lack of good agreement between experiment and theory as pressure and temperature decrease has been discussed and attributed mostly to leak-out correction difficulties. It has been suggested that part of the disagreement could be traced to the relatively small flask (13 liters) used in the low pressure ranges. As the pressure decreases, the mean free path increases and collisions with the walls become more frequent. Under these conditions the rate of activation would appear to fall off, and therefore, K would show a decrease. If this were true, the packing of the reaction flask with Pyrex wool should give the traveling molecule much more opportunity to collide with a surface rather than another molecule. During a series of runs made at 310°C and 270°C with the flask packed with enough Pyrex wool to increase the surface area a factor of twenty, this idea was investigated. The results are shown by the small triangular points on Figure 3, page 38. The values for K obtained with these runs is within experimental error the same as those obtained with the unpacked flask. The only conclusion seems to be that the reaction is homogeneous in the pressure ranges studied. Incidentally, this is also evidence that the free radical chain reaction is not operative. This of course does not mean decreasing the pressure even further would have no effect. As pointed out earlier, it most certainly would be expected to affect the reaction rate greatly. There seems to be

little purpose in extending the pressure range to still lower values where the large majority of the collisions would be with the surface of the reaction vessel.

Toluene Experiments

In the last chapter the experimental results from the toluene experiments were covered. Aside from establishing that no chain reaction existed in the decomposition of azoethane, these experiments can be used in obtaining information on the relative efficiency of activation of the toluene molecule. The relative efficiency of activation (α) is defined by the equation $P_A = P + \alpha P'$ where P is the partial pressure of azoethane, P' the partial pressure of toluene, and P_A, the total pressure of azoethane that will give the same rate constant as the mixture. This efficiency (α) is efficiency per molecule. Rice and Sickman (1936) showed, using collision theory, that

$$\alpha' = \alpha/2 \left(\frac{2M_T}{M_T+M_A}\right)\left(\frac{2\sigma_A}{\sigma_T+\sigma_A}\right)^2 \qquad (54)$$

where α' is the relative activation efficiency per collision, M_T is the molecular weight of tolusne, M_A that of azoethane, σ_A and σ_T the kinetic theory diameter of azoethane and toluene, respectively. From Figure 3, page 38, we see that the K's obtained during the toluene runs are about the same as those obtained without toluene. Therefore from $P_A = P + \alpha P'$ we get $\alpha = 1$. Substituting in equation (54) and using $\sigma_A = 5.5$ A and $\sigma_T = 6.0$ A, we find $\alpha' = 0.52$. From this we can conclude that the toluene molecule is about as efficient as the azoethane molecule in the process of activation. In short, it can transfer about as much of its translational energy to an azoethane molecule as azoethane itself can. To be sure, these

numbers are only an approximation in that the values for the molecular diameters and rate constants are not precise and small errors in these can account for large errors in the efficiencies.

Products and Mechanism

The products of this reaction are given in Tables VII, VIII, and IX; pages 46, 47, 48, respectively. Table X, page 49 is devoted to the material balance obtained by the different methods of analysis.

In general this reaction gives a mixture of products the complexity of which depends on the temperature and initial pressure of the run. At low pressures and temperatures the products are for the most part simple and are given by equation (1),

$$CH_3CH_2N = NCH_2CH_3 \longrightarrow N_2 + CH_3CH_2CH_2CH_3 \qquad (1)$$

with about 9% of a mixture of two and three carbon atom hydrocarbons. However, as the pressure and temperature are increased this 9% mixture increases to 45% and the mixture now contains two to at least eight carbon atom hydrocarbons. The chief hydrocarbon at low P and T is n-butane comprising about 60% (on a weight basis) of the mixture. At high P and T, this decreases to about 28% of the total. An explanation of this might be that free radicals are involved in the decomposition and recombine simply at low P and T but involve further interaction at high P and T. This brings us to the subject of mechanism but, before proceeding, a few words about the formation of nitrogen compounds are desirable.

Insofar as the product analysis goes, no evidence of nitrogen compounds (amines, nitriles, etc.) was ever found. The material balance (Table X, page 49) showed nitrogen to be too low according to gas chro-

matography and about right according to mass spectra analyses. However, the P.H. vs. time curve for mass 17 (NH_3?) shown in Figure 6, page 51 indicates an increasing concentration with time. From Table XI, page 50 we see the total P.H. is only 21 and 31 mm. However, it is difficult to attribute this to anything but NH_3, yet no NH_3 could be found! The possibility that this could be CH_5 seems remote. No real evidence has ever been put forward that the formation of methane proceeds according to

$$CH_3 + H_2 \longrightarrow CH_5 \qquad (2)$$

$$CH_5 + CH_3 \longrightarrow 2CH_4 \qquad (3)$$

Besides, even if this were true, the CH_5 is unstable and would not attain a high steady state concentration.

The comments which follow about mechanism are based largely on speculation and should be recognized as such.

It seems fairly clear that the first step of the thermal decomposition of azoethane involves ethyl radicals (Ausloos and Steacie, 1954).

$$C_2H_5N = NC_2H_5 \longrightarrow N_2 + 2CH_3CH_2 \qquad (4)$$

Ausloos and Steacie (1954) also published a mechanism which they suggest for the photolysis of azoethane. This is given by the equations

$$C_2H_5N = NC_2H_5 + h\nu \longrightarrow 2C_2H_5 + N_2 \qquad (5)$$

$$C_2H_5 + C_2H_5 \longrightarrow C_4H_{10} \qquad (6)$$

$$C_2H_5 + C_2H_5 \longrightarrow C_2H_4 + C_2H_6 \qquad (7)$$

$$C_2H_5 + C_2H_5N = NC_2H_5 \longrightarrow C_2H_6 + C_2H_4N = NC_2H_5 \qquad (8)$$

$$C_2H_4N = NC_2H_5 \longrightarrow C_2H_4 + C_2H_5 + N_2 \qquad (9)$$

Comparing equations (5) through (9) with the curves given in Figures 6, 7, and 8, pages 51, 52, and 53, respectively, the following similarities are noted.

First the $C_2H_5^+$ peak (mass 29) decays at about the same rate independent of pressure while the azoethane parent peak (mass 86) shows the expected decrease with pressure. If the 29 peak were due to free ethyl radicals (which is improbable), then apparently C_2H_5 is produced and used up at the same rate regardless of pressure. According to equation (6) part of the C_2H_5 produced goes to form C_4H_{10} (n-butane, mass 58) but the curve shows mass 58 increasing at the same rate independent of pressure also. This paradox was brought up to illustrate the difficulty involved in using the curves given in Figures 6, 7, and 8 and in general to point out the difficulties of determining mechanism in any reaction. The curves presented here can be used only in the grossest sense. Much more information is needed and a complete simultaneous analysis of all curves is required before an actual mechanism can be obtained. These curves are presented with a twofold purpose: First, to simply present the data as it was obtained so that it may be recorded for future workers; second, is to obtain enough information to allow a plausible mechanism to be presented here.

The explanation of the paradox is that many compounds contribute to the mass 29 peak, including n-butane (58) and azoethane (86). It is perfectly possible to have the same rate of decay and still have different amounts of C_2H_5. It is necessary to distinguish between that part of the total peak height due to a fragment found in the reaction and that part due to the ionizing electron beam in the mass spectrometer source. A

complete analysis of all peaks might remedy this trouble but such an analysis is forbiddingly difficult. It is somewhat safer to consider only the parent peaks of the compounds whose behavior is of interest. For example, for C_2H_6 (mass 30) it is improbable that any molecule contributes to the mass 30 peak other than ethane. Then it is seen that at low pressures the amount of ethane goes through a maximum and then begins to drop off. The fact that at 1200 minutes the concentration is back up to the maximum may be due to competing reactions with different rate constants. For example, while ethane is being formed, there may also be forming another compound that decomposes very slowly giving ethane as one of its products. With regard to equations (5) to (9) the curves in Figures 6, 7, and 8 seem to be in general agreement on the following points. C_2H_5 is certainly formed during the reaction and could react as given in equation (6). C_2H_4 and C_2H_6 (masses 28 and 30) are possible in that Figure 6 shows both of them to be rising. Ethane could also be formed via the reaction given in equation (10)

$$C_2H_5 + C_2H_5N = NC_2H_5 \longrightarrow C_2H_6 + C_2H_4N = NC_2H_5 \qquad (10)$$

and ethylene by

$$C_2H_4N = NC_2H_5 \longrightarrow C_2H_4 + C_2H_5 + N_2 \qquad (11)$$

At low pressures a small amount of methane (mass 16) was found. However, even though Figure 6 shows the high pressure mass 16 to be rising and over three times the low pressure peak height, no methane was found in the products at high pressures.

It is clear that methyl radicals are involved for there is no

other way to explain the presence of hydrocarbons containing an odd number of carbon atoms in the products. Any explanation of this would involve a multiple step reaction or at least a rearrangement reaction. Possibly it could go through a nitrile synthesis and decomposition. This would require a different primary step.

$$C_2H_5N = NC_2H_5 \longrightarrow 2C_2H_5N \qquad (12)$$

The removal of H by ethyl radicals would yield

$$C_2H_5 + C_2H_5N \longrightarrow C_2H_6 + C_2H_4N \qquad (13)$$

$$C_2H_5 + C_2H_4N \longrightarrow C_2H_6 + C_2H_3N \text{ (or } CH_3CN) \qquad (14)$$

$$C_2H_5 + C_2H_3N \longrightarrow C_2H_6 + C_2H_2N \qquad (15)$$

$$C_2H_2N \longrightarrow HCN + CH \qquad (16)$$

$$CH + C_2H_6 \longrightarrow CH_2 + C_2H_5 \qquad (17)$$

So we see that ethyl radicals must perform three H abstractions and from equations (16) and (17), CH abstracting H from the ethane formed. This set of reactions could account for the methane, methyl radicals and the formation of hydrocarbons with odd numbers of carbon atoms. This scheme is in keeping with the curves in Figures 6, 7, and 8. However, no molecules containing single nitrogen atoms were found among the products.

The formation of unsaturates is possible by several different means. Steacie (1954) has shown that diazomethane can be obtained from azomethane via

$$CH_3N = NCH_3 \longrightarrow CH_3NN + CH_3 \qquad (18)$$

$$CH_3 + CH_3NN \longrightarrow CH_4 + CH_2N_2 \qquad (19)$$

which then can go on to give unsaturates,

$$CH_2N_2 \longrightarrow CH_2 + N_2 \qquad (20)$$

$$2CH_2 \longrightarrow C_2H_4 \qquad (21)$$

It seems reasonable to expect azoethane to behave in much the same way. Assuming that it does, it is easy to see how the different unsaturates are obtained. Combining the information given by equations (12) through (17) with that given by equations (18) through (21) the formation of an endless series of hydrocarbons appears possible.

Evidence for the existence of diazoethane is found in Figure 8, page 53 where the mass 56 peak vs. time curve is given.

The only curve in Figures 6, 7, and 8 that is really difficult to understand is that for mass 71. Presumably this is due to the $C_2H_5N = NCH_2$ ion formed in the source by electron bombardment and is therefore not involved in the thermal decomposition itself. This being the case, the ratio of the 71 to 86 peak in pure azoethane (see Table I, page 17) should equal that found in Figure 8 (or see Table XI, page 50). However, this is not the case. The 71 peak does not appear to be related to the behavior of the 86 peak in any way. It does not appear possible that a reaction such as

$$C_2H_5N = NC_2H_5 \longrightarrow C_2H_5N = NCH_2 + CH_3$$

could exist because of the high energy of the C-C bond. There is no way to explain this on the basis of the work done here.

It was interesting and surprising to find that no amines were present in the final products. Ethylamine (mass 45), diethylamine (mass 63), and triethylamine (mass 101) were carefully searched for among the products.

If any of these were present, they amounted to less than 0.05% of the final products. The formation of triethylamine could arise from equation (12) and react with ethyl radicals to give

$$C_2H_5N + C_2H_5 \longrightarrow (C_2H_5)_2N$$

$$C_2H_5 + (C_2H_5)_2N \longrightarrow (C_2H_5)_3N \qquad (24)$$

To be sure, this set of reactions requires three steps which are somewhat uncertain. However, they appear to be no more improbable than some of the other reactions given here that seem to be verified to some extent by experimental evidence. One conclusion is that the -N=N- bond is not easily broken.

The mechanism of a reaction of this sort is an exceedingly difficult problem as are reaction mechanisms in general. A considerable amount of further work is necessary before a complete mechanism can be written for this reaction.

CHAPTER VI

Equipment

A large proportion of the time spent on this work was devoted to instrumentation. Engh (1952) has described the basic instrument. Briefly, the basic parts were a gift from the Los Alamos Scientific Laboratory. These parts included a mass spectrometer tube (60° Nier type), a magnet with coils, a high voltage supply, a magnet supply, an emission regulator and an FP-54 electrometer. In order to obtain a working instrument suitable for our purposes, several alterations and additions were necessary.

The high voltage supply was used essentially as received.

The magnet supply was also used as received with the exception of the addition of a circuit which permitted the spectrum to be scanned magnetically. This circuit consisted of a Heathkit PS-3 power supply with a few changes. These changes involved eliminating the rectifier section of the PS-3 and using in its place the rectifier section in the existing magnet supply. Also in order to handle currents up to 250 ma., an additional 1619 series regulator tube was added. The magnet current was varied by the substitution of a 300 K helipot for the 500 K single turn potentiometer supplied with the PS-3 as a means of varying the output

voltage. The helipot was driven by a 1/3 RPM Haydon motor. An example of the results obtained with this supply are given in Figure 1. Note how the non-linear response of the PS-3 supply helps to compensate for the non-linear mass scale and thereby aids by giving a spectrum with a more nearly constant interval between the different masses.

It was soon discovered that the FP-54 electrometer was not suitable for our purposes and a study was undertaken to find one that would meet our needs. We required an electrometer which had a minimum of zero drift, a low noise level, a high sensitivity, the capability of driving either a galvanometer or a 10 mv. pen recorder, and excellent stability over a period of 24 hours or more. The device finally built met these requirements to a surprising degree. Again from Figure 1 it is seen that the noise is of the order of 5×10^{-15} amps and the sensitivity is about 5×10^{-15} amps/mm. The stability and zero drift were excellent. Over a period of 48 hours, no perceivable zero drift was detected and in a like period no change in stability could be found.

The electrometer was a 100 per cent negative feedback device using a CK 5886 as the input stage, followed with a CK 512 AX and a CK 5678 as first and second stages of amplification respectively. The output stage consisted of a CK 5672 used as a cathode follower. The loop gain without feedback was about 5000. All four tubes used were Raytheon subminiatures and the entire circuit with batteries was contained in a box 8 x 8 x 12 inches. The finished electrometer is shown in Figure 12, lower left. The circuit was designed by John Harrison of the University of Minnesota Electronics Department.

While it is beyond the scope of this report to consider each part of the construction in detail, it seems advisable to go into some detail on those items which are in some sense unique to the problem at hand. These items are the leaks, the thermostat, phase-shift thermoregulator, and emission regulator. In the text that follows, a section will be devoted to each of these.

The Leaks

One of the most difficult and time consuming parts of this work was the fabrication of leaks for use in sampling the reaction vessel. The problem itself is simple and has been described in the literature (Dibeler, 1948; Munson, 1955, Marks, 1957). The technique, however, is difficult and can be mastered only by much practice.

In order to admit a sample into the ionization chamber of the mass spectrometer, a leak must be provided. It is desireble that the peak heights be linear function of the pressure behind the leak and that the leak does not change the composition of the gas mixture being analyzed, i.e. it does not fractionate. A leak which does not fractionate is known as a viscous leak and usually consists of a long thin tube with an internal diameter of about 20 microns. The peak height is proportional to the square of the pressure behind the leak when using a viscous leak, but it is proportional to the pressure when using a molecular leak.

The most important property of a leak in the present work is that the peak height be proportional to the pressure behind the leak, i.e. that the leak be a molecular leak. Such a leak is a small hole in a thin membrane. If T is the thickness and D the diameter of the leak,

the ratio T/D should be as small as possible. With the smallest leaks values of T/D could not be reduced much below 10. However, direct measurement showed good linearity of peak height with pressure within the experimental error. Direct tests showed no measurable fractionation within the experimental error either, presumably because such fractionation would be expected to be small anyway when a small fraction of the total sample is lost by leakout.

The technique used in making the leaks involved the heating of a short length of Pyrex capillary (1 mm I.D.) until it collapsed down to a fine hole. By careful heating, one can get holes as small as one micron in diameter. The next step requires careful grinding of the end of the tube from the inside and outside until a thin membrane of glass remains. Obviously the danger of breaking the membrane is very great. Out of the first batch of 50 leaks all but 3 were broken through. After gaining experience only 10 - 15 per cent of the leaks were lost.

Another technique which shows great promise is the use of Taylor Process wire (available from Baker and Company, 113 Astor Street, Newark, New Jersey). Taylor Process wire is supplied in most metals (platinum, gold, iron, nickel, zinc, tin, etc.) in sizes down to 0.5 micron in diameter. It is enclosed in a Pyrex coat giving the wire plus glass a total outside diameter of about 80 microns. By collapsing the glass capillary down around a short length of Taylor wire and grinding the end down just as before, a thin glass membrane with a short length (equal to the thickness of the membrane) of wire was obtained. The wire was then dissolved out electrolytically. The best metal was found to be gold

because it is relatively insoluble in molten Pyrex glass. The leak was placed in a 10% solution of KCN and a small amount of the same solution was added to the inside of the tube. Platinum electrodes were placed very close to both sides of the membrane and a potential of 60 volts applied. By observing the current flow as a function of time, one can detect when the gold has been removed. It is important to remove the potential as quickly as possible because the high current flow might fracture the leak due to water vaporizing in the small hole. A finished leak is shown in Figure 18 at the end of the top tube.

The Mass Spectrometer Chassis

Included here are three figures showing general views of the mass spectrometer. The main console of the instrument is shown in Figure 11. On the left, top to bottom, are shown the ionization guage supply (Alpert Guage, Alpert (1953)), emission regulator, and the main control panel which was used to set the different potentials needed for the plates in the source. Also the main control panel allowed one to select the accelerating voltage applied to the ions. On the right, top to bottom, are shown the magnet supply, the magnet scanning supply, and the electrometer shunt panel. Extending across the entire panel one third the way up is the galvanometer scale which was used for visually observing a spectrum. The Leeds and Northrup Speedomax 0 - 10 mv. recorder was used for recording spectra and following peak heights for long periods of time. The spectrum shown in Figure 1 was obtained with it.

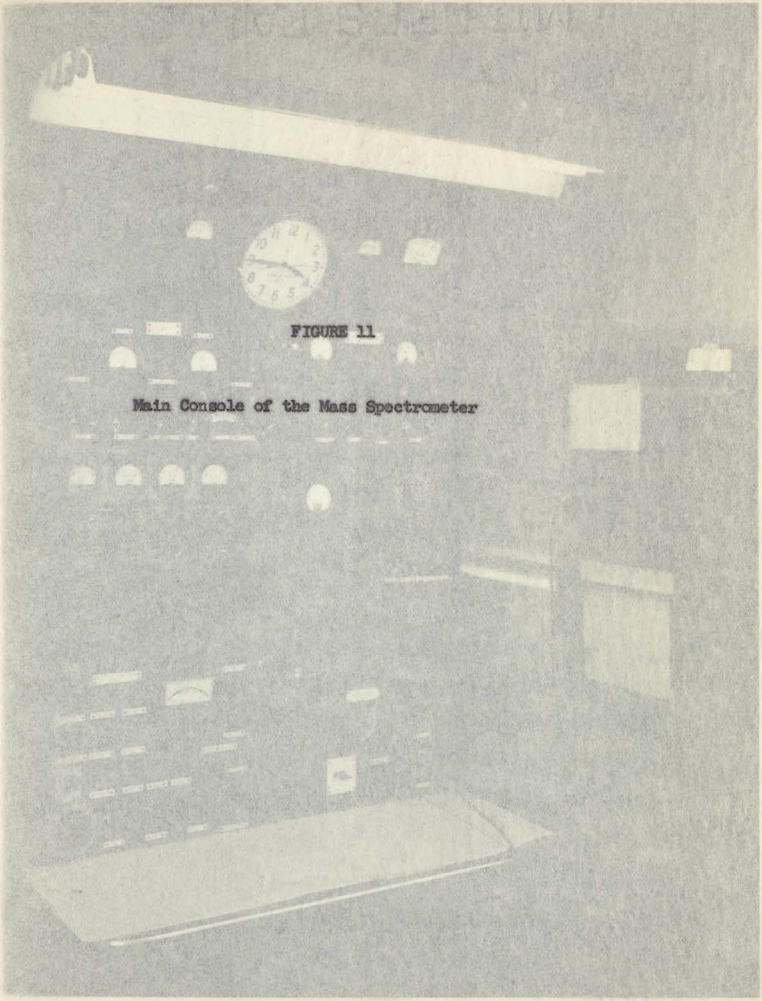

FIGURE 11

Main Console of the Mass Spectrometer


EMISSION REGULATOR

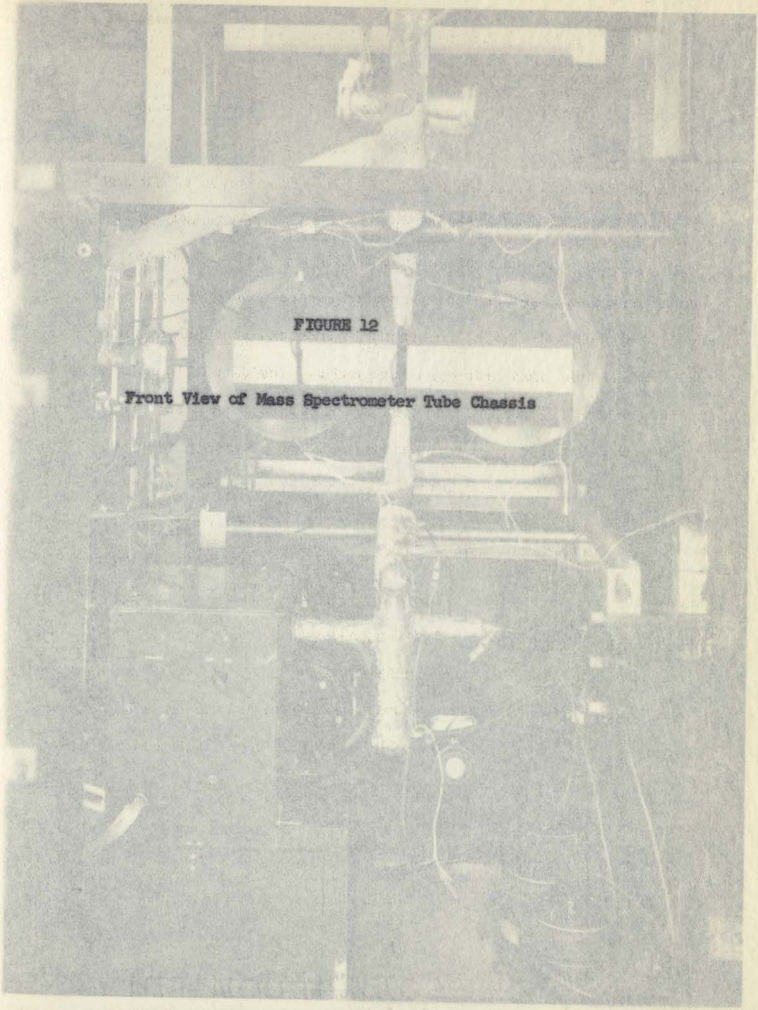

FIGURE 12

Front View of Mass Spectrometer Tube Chassis

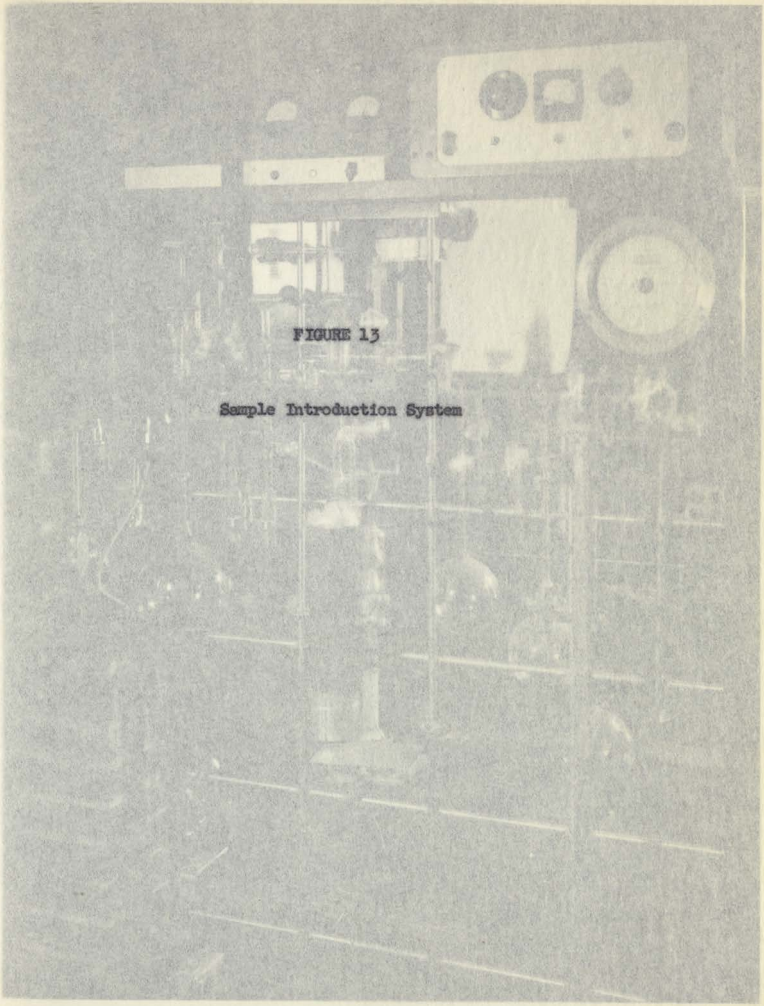

FIGURE 13

Sample Introduction System

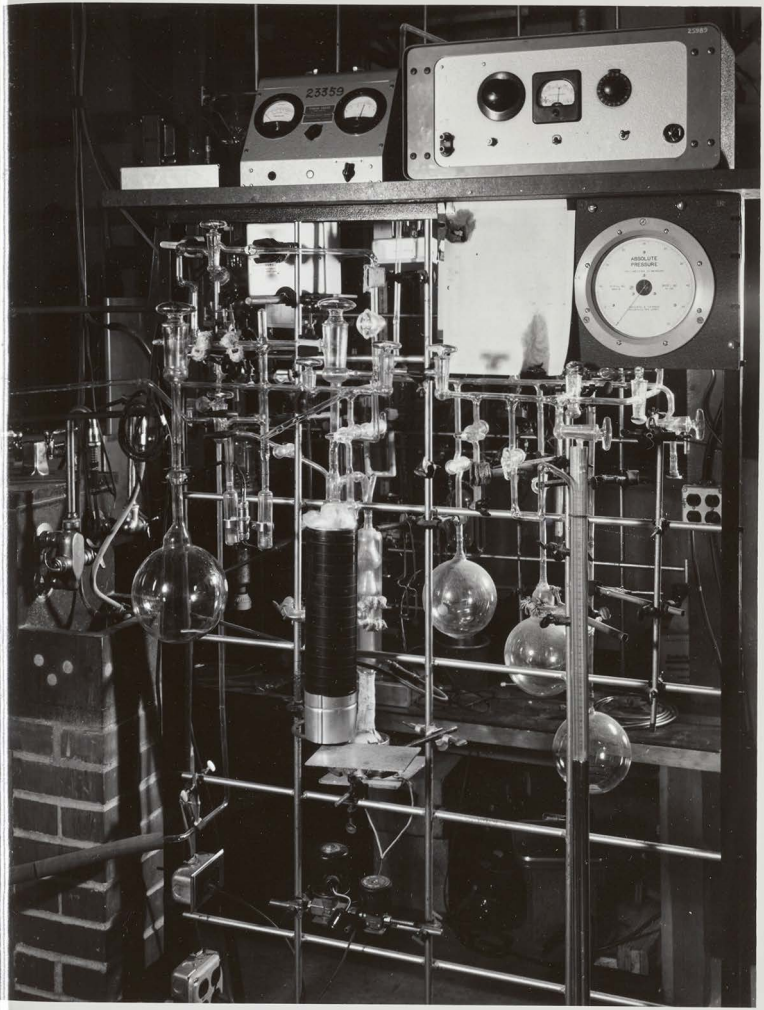
23359
ABSOLUTE
PRESSURE

A front view of the mass spectrometer tube chassis is given by Figure 12. On the extreme left is seen the vacuum system and the electrometer is shown at the lower left. The spectrometer is inverted from the position in which it usually is found in that the source is on top. This was done to allow as short a path as possible from the reaction vessel to the source. Note that with the exception of that part of the tube between the poles of the magnet and the upper part of the source, the entire tube is wrapped with heaters. These heaters were run at 300°C continuously.

In Figure 13, a general view of the sample introduction system is given showing the three pressure measuring devices used. The mercury manometer was used over the pressure range of 50 to 700 mm, the Wallace Tiernan guage (upper right) over the range of 10 to 50 mm and the Consolidating Engineering Company micromanometer (top) over the range of 1 to 200 microns. Intermediate pressures were obtained by expanding a known small volume of gas at a known pressure into a known large volume (the reaction flask) and assuming the ideal gas law to be valid. Experiments showed azoethane to obey the ideal gas law to pressures of one atmosphere or less to better than 1%, (the accuracy of the pressure measuring device).

The Thermostat

One of the major problems in the construction of instrumentation was that of the thermostat. Because of the high temperature ranges that were necessary, a material from which a bath could be fabricated was difficult to obtain. After investigating many materials ranging from

mercury to mixtures of different inorganic salts, it was discovered that the objections to liquid baths were so great as to preclude their use. After careful consideration, the decision to use an air bath was reached.

We required that the thermostat have temperature gradients of no greater than 0.1°C. It was also necessary that a temperature regulation of ±0.05°C. be obtained. Also, a reaction flask having a volume ranging from 250 ml. for the high pressure runs to 13,000 ml. for the low pressure runs was necessary. The large volume on the low pressure runs was necessary in order to minimize the fraction of the material lost due to leak-out during the time the reaction was being studied.

A device having these characteristics was constructed and is shown in the break-away drawing in Figure 14. In Figures 15 through 18 different views of the finished device are given.

The thermostat consisted of a transite box having a double wall five inches thick. The space between the inner and outer wall was filled with five inches of Vermiculite. A 1/3 h.p. electric motor mounted in the bottom of the box provided power to drive a fan seen in the bottom of the transite box. A lid with a removable center section providing easy access to the glass work contained in the box was constructed. Contained in the transite box was a smaller cube constructed to allow a 2 inch space all around between it and the inner box of the thermostat. This inner cube is shown in Figure 16. The cube served the dual role of defining a path (see arrows in Figure 14) through which the air was circulated by the fan and also providing a support for the heaters. These heaters are indicated by "C" and "D" in Figure 14. Heaters "C" were eight chromalox heaters each providing 250 watts at 110 volts and were used to provide the bulk

of the necessary power. Heaters "D" were nichrome coils wound on glass tubes which were directly exposed to the air stream. They were parallel connected to present a total resistance of 45 ohms and were used to supply the small additional power needed for temperature regulation and are shown by R_H in Figure 19.

The air was circulated over all these heaters by the fan. From the arrows shown in Figure 14 the path taken by the air is obvious. The maximum theoretical air velocity around this path is 2,500 ft/min. The measured velocity gave 1,100 ft/min as measured with a velometer.

The temperature sensing element was an AW-5525-2 resistance thermometer manufactured by the Edison-Spitdorf Company and is shown as E in Figure 14 and R_T in Figure 19. It was a coil of 0.004 in. OD nickel wire and had a resistance at room temperature of about 90 ohms. This element determined the temperature of the thermostat and fed a signal to the phase-shift thermoregulator. Considering the length of path the air took in one cycle to be about 2.5 feet, the resistance thermometer was to sense the temperature of a given volume element of air about 7 times a second. While this seemed to be adequate it must be pointed out that had the inner box and its contents been designed more in keeping with aerodynamic principles and the speed of the fan increased, 28 to 30 times a second would not be an unreasonable number. After all, this device is nothing more than a recirculating wind tunnel with heaters.

In Figure 14, "B" shows the ice junction used as a reference junction for a calibrated thermocouple contained in the reaction flask itself. This thermocouple was used in determining the temperature at which the decomposition was being run.

The reaction flask is shown in Figure 17. The tube on the lower right was connected to the mass spectrometer, and was used to sample the reaction through the leak "A." Just above the leak lead is the thermocouple well. The tube on the lower left was connected to the sample system and was used in admitting the sample to the flask. The reaction flask itself is shown in more detail on Figure 18. Here the sample introduction sidearm has been sealed off in the interests of keeping dust and dirt from entering the reaction flask when it is not in use. Ordinarily, this tube is connected to the sample inlet system.

The completed thermostat with its associated electronic regulating equipment is shown in Figure 15. Figure 17 shows a top view of the thermostat with the lid removed. In the lower right hand corner the temperature sensing element is visible. The flask with its two tubes is in place as it ordinarily is during a decomposition run. The inner cube containing the heaters is shown in Figure 16. This is a bottom view showing the hole for the circulating fan.

Upon completion of the thermostat, an extensive series of tests were carried out. The purpose of these tests was to determine the temperature gradients present and the degree of temperature regulation possible. Also, it was not known whether the air travelling upward or downward in the center of the thermostat would produce the best results. It must be remembered that at the time of this testing the phase shift thermoregulator was not yet constructed and a mercury-in-glass regulator was used together with the thyratron circuit as described by Swinehart (1949). As will be seen in the next section the phase shift thermoregulator improved performance of the thermostat at least an order of magnitude. It is reasonable to expect that had the phase shift thermoregulator

been used during these tests the results would have correspondingly improved.

The results of the tests were as follows. Temperature regulation improved from ±0.8°C to ±0.3°C when the air flow was changed from a downward to an upward direction in the center of the thermostat. As a consequence, the motor was wired so as to cause an upward flow of air.

All subsequent tests were made under these conditions. The volume of the thermostat available for a reaction flask was a cube 12 inches on an edge. In order to conduct the temperature gradient tests, a series of five thermocouples were prepared and carefully calibrated against a platinum resistance thermometer. These thermocouples were then mounted in long glass tubes which entered the thermostat through the cover. One of the tubes was placed in the geometric center of the thermostat allowing it to be moved from the bottom to the top of the cube from outside of the thermostat. The remaining four thermocouples were also mounted in tubes which were located at the corners of a square having its center coinciding with the center of the cube bracket (center line of the fan shaft) and measuring 8 inches on a side. These tubes were moveable to allow measurement of the temperature anywhere along their path into the thermostat. By this means the temperature through the center of the cube could be determined as a function of vertical position of the thermocouples. The greatest temperature difference measured from the bottom to the top of the cube on any of the five thermocouples was 0.8°C. Further, the greatest temperature difference measured between any two thermocouples in any two positions regardless of distance apart (under the restrictions of the thermocouple movements pointed out above) was 1.0°C. The conditions under

which these tests were conducted ranged from a temperature of 260° to 320°C. When one of the thermocouples was placed adjacent to the mercury bulb of the thermoregulator, a regulation of 0.5 to 0.9° was observed. Therefore, it is reasonable to expect that a considerable amount of the temperature gradient observed was due to the inadequate regulation being obtained from the mercury-in-glass thermoregulator. In most of the kinetic runs, a thermocouple was placed in the well in the reaction flask provided for that purpose. Also, a platinum resistance thermometer was placed through the lid so that it measured the temperature in one corner of the center cube during the kinetic run. The temperature indicated by these two devices was recorded all during the kinetic runs. In no case did the temperature difference exceed 0.08°C after the phase-shift thermoregulator was built, tested and installed. Time did not permit the reinstallation of the five thermocouples after the installation of the phase-shift thermoregulator. However, from experience gained during the course of 151 runs, comparisons between the temperature of the platinum resistance thermometer in one corner of the center thermostat cube lead us to the conclusion that a reasonable number for the greatest temperature gradient is about 0.2°C. This gradient would exist between the center of the cube (also center of reaction flask) and the farthest corner of the cube. The temperature gradient through the reaction flask itself was probably no greater than 0.1°C.

After completion of the phase-shift thermoregulator a series of experiments were performed in an effort to determine the optimum amount of power to be dissipated in the main heaters (see C, Figure 14) and in the auxiliary control heaters (see D, Figure 14). These two sets of

heaters were installed because it was felt that a regulating device regulating the entire input power would be required to handle too much current. Therefore, it was felt that the bulk of the power necessary to maintain the thermostat at a given temperature could be supplied by a set of rather rugged heaters powered directly from the 120 volt lines through a variac. The small additional power necessary to bring the thermostat to the desired temperature could then be supplied by small wire-wound heaters having their windings exposed directly to the air flow, thereby effecting a better transfer of energy. These small auxiliary heaters would then be used to control the temperature. They would also offer the additional advantage of a small thermal inertia. In practice this worked out very well. The variac provided to control the input power to the main heaters is seen in the lower right hand panel of Figure 15. By means of this variac the power to the main heaters was increased to the point where the phase-shift thermoregulator could supply the additional small increment of power needed for temperature control. Optimum values for the variac setting as a function of desired regulation temperature are given in Table

Table XVIII

Variac Settings for Thermostat

Temperature (°C)	Variac Setting (Volts)
250	50
260	55
270	60
280	65
290	65
300	70
310	70

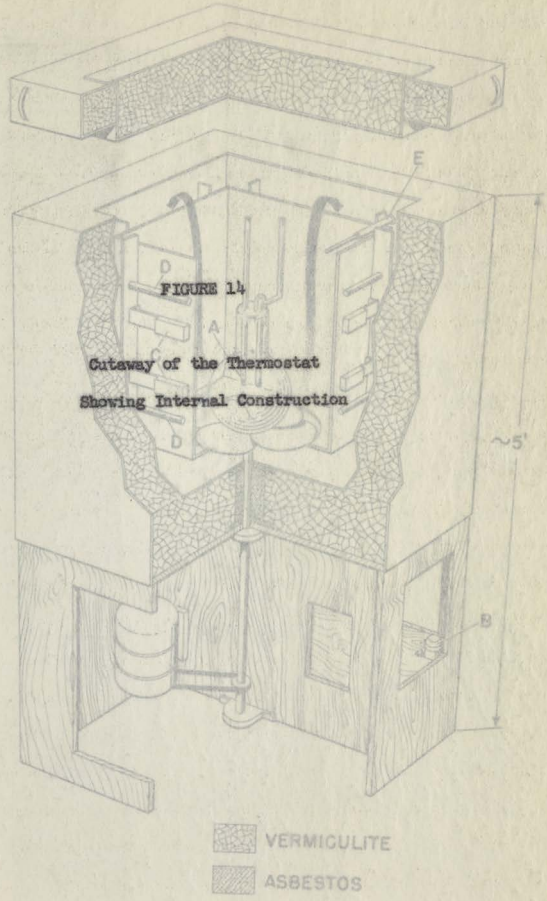

FIGURE 14

Cuteway of the Thermostat

Showing Internal Construction

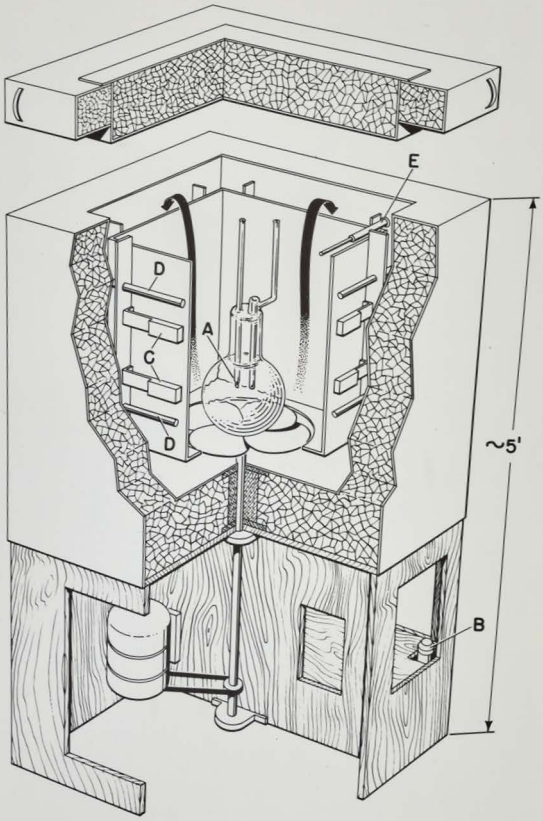
E
D
A
C
D
~5'
B
VERMICULITE
ASBESTOS

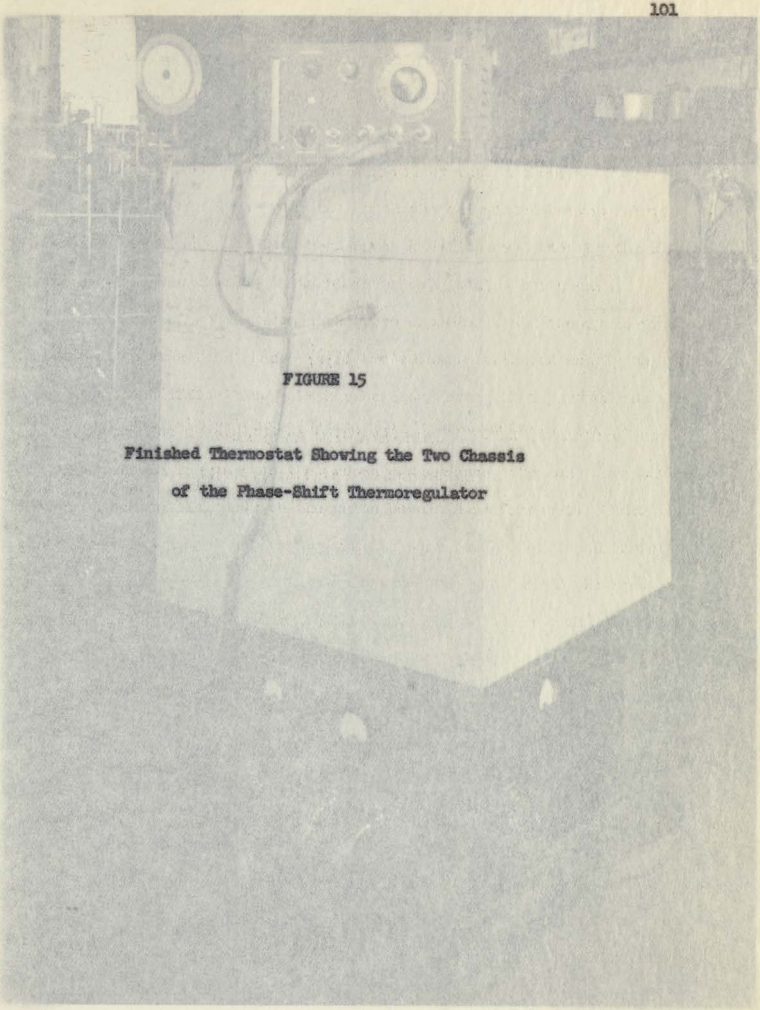

FIGURE 15

Finished Thermostat Showing the Two Chassis of the Phase-Shift Thermoregulator

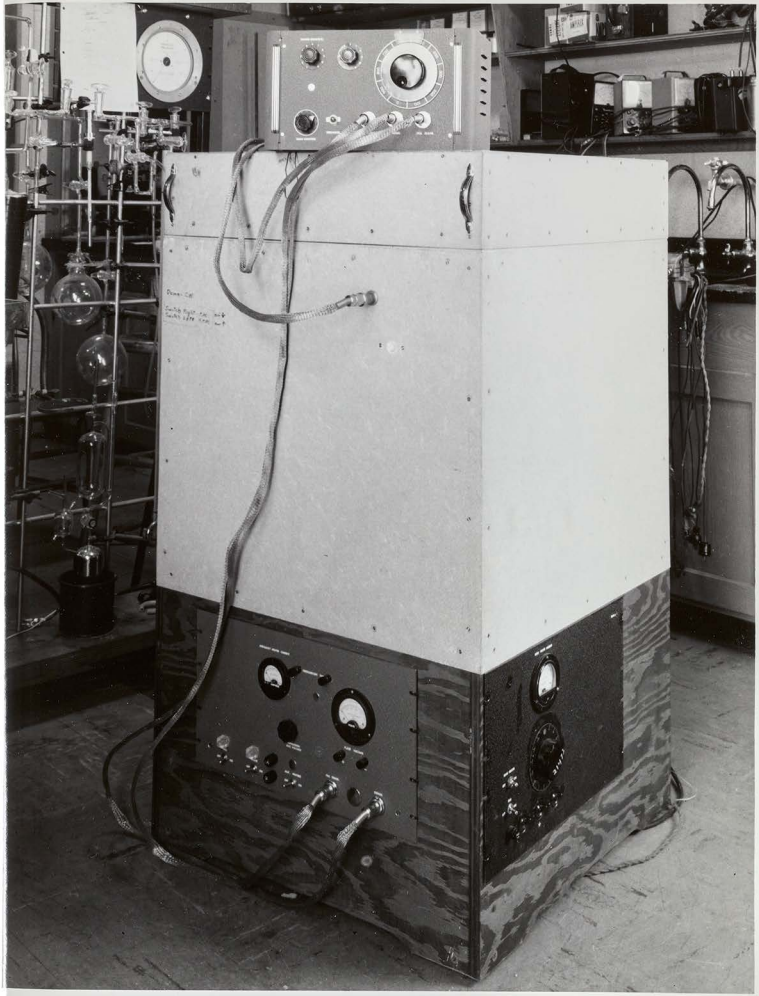

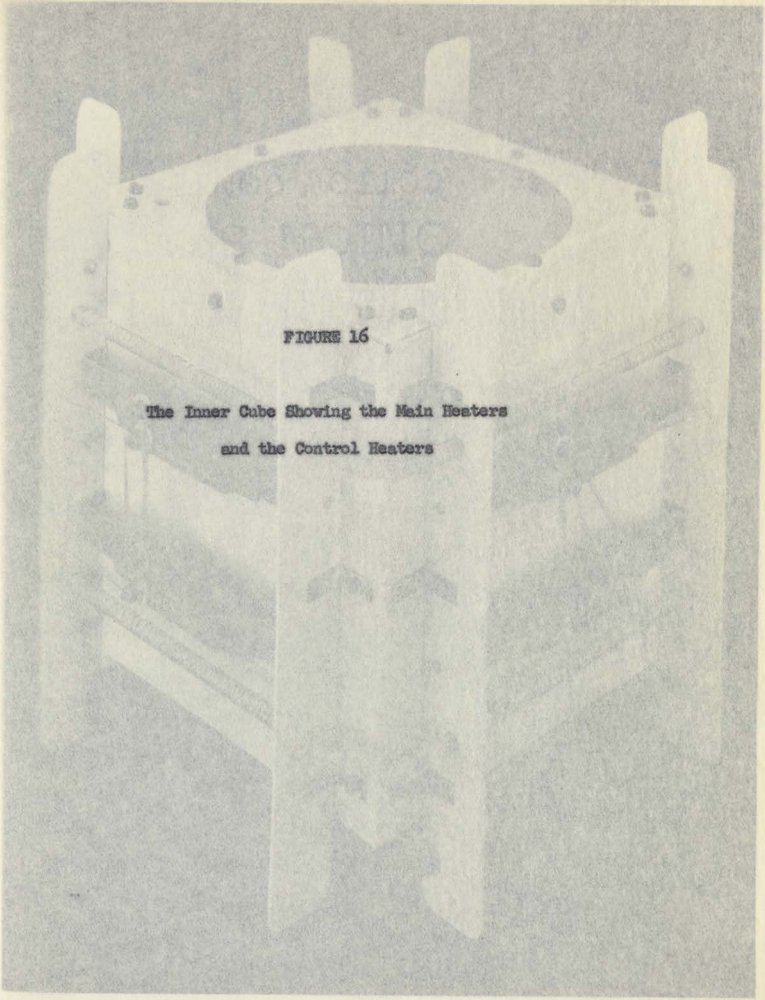

FIGURE 16

The Inner Cube Showing the Main Heaters
and the Control Heaters

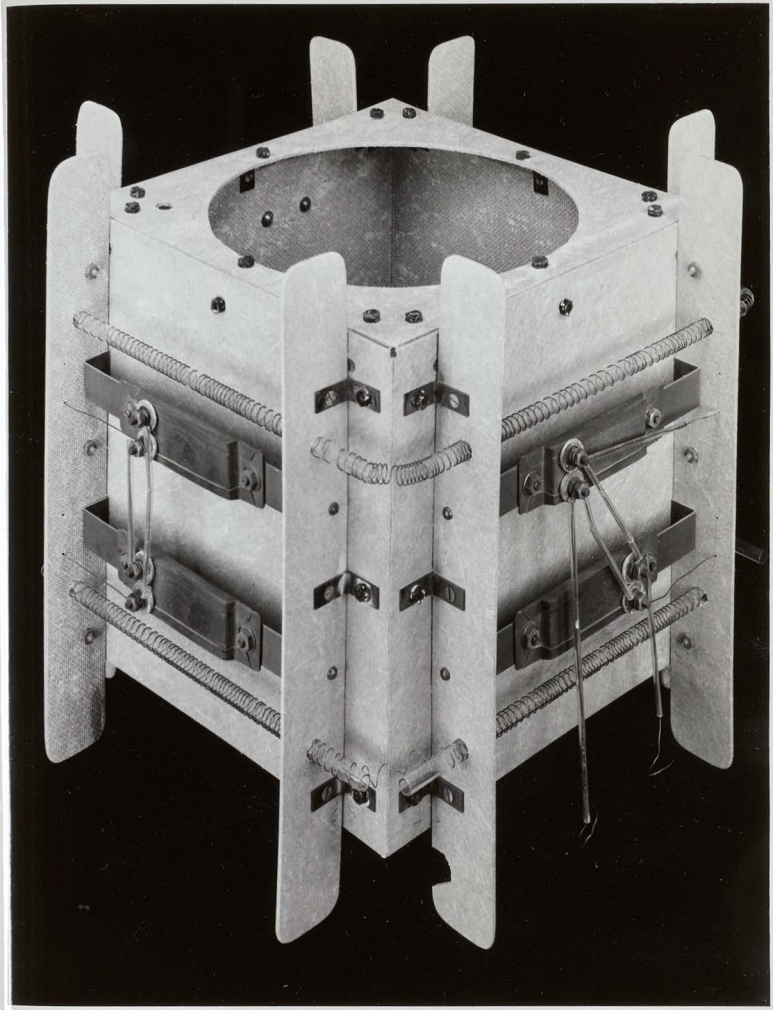

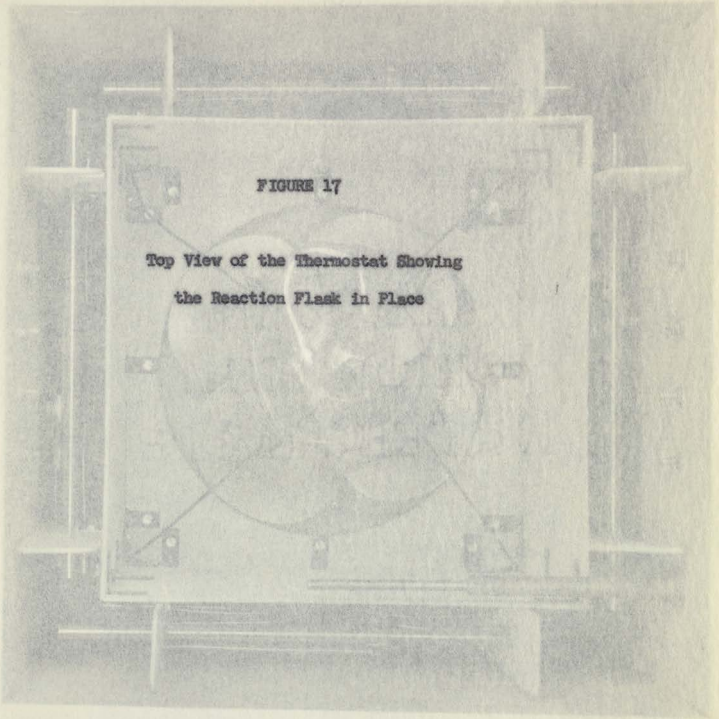

FIGURE 17

Top View of the Thermostat Showing the Reaction Flask in Place

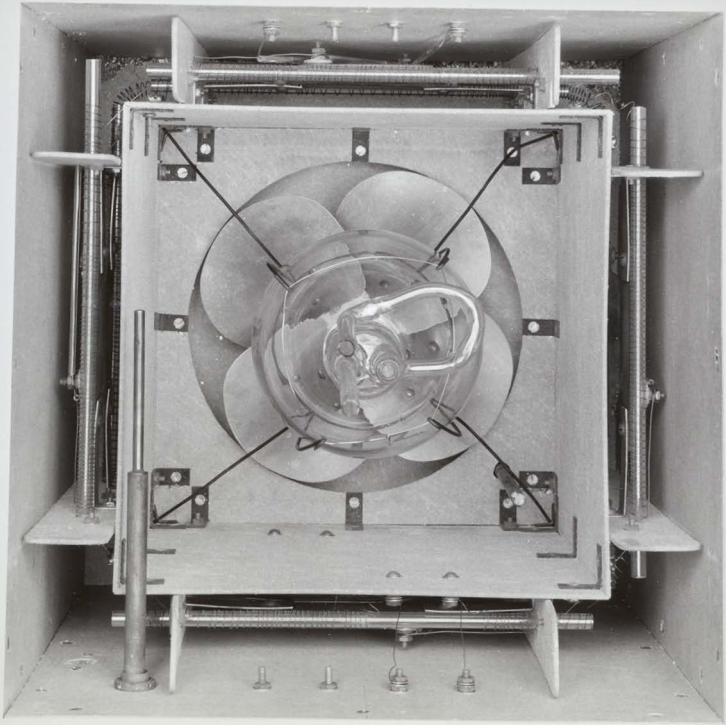

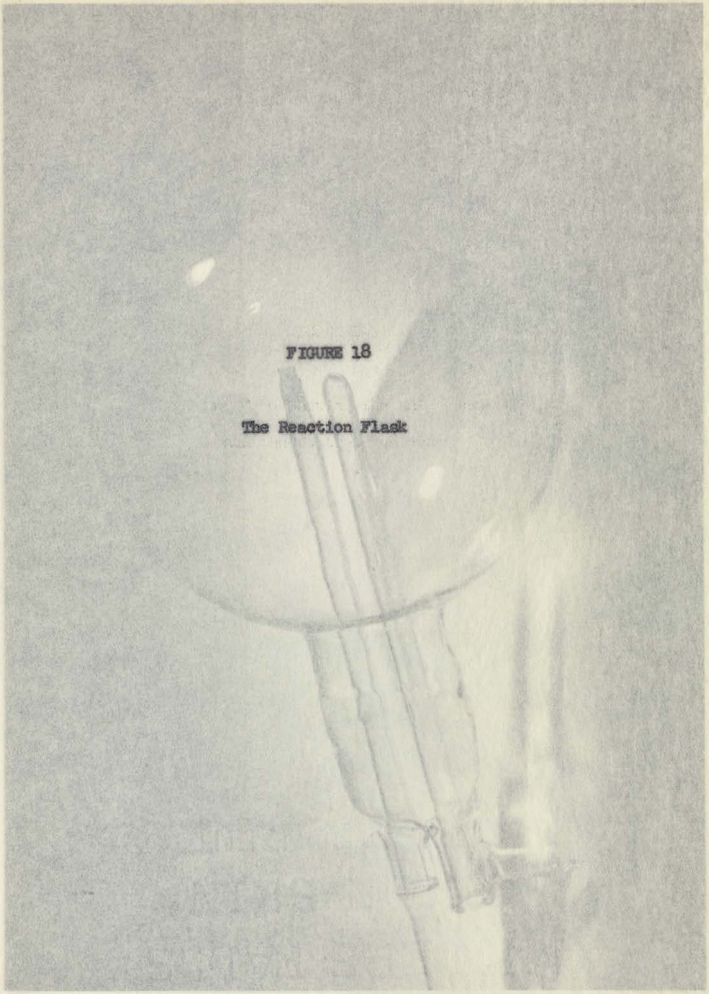

FIGURE 18

The Reaction Flask

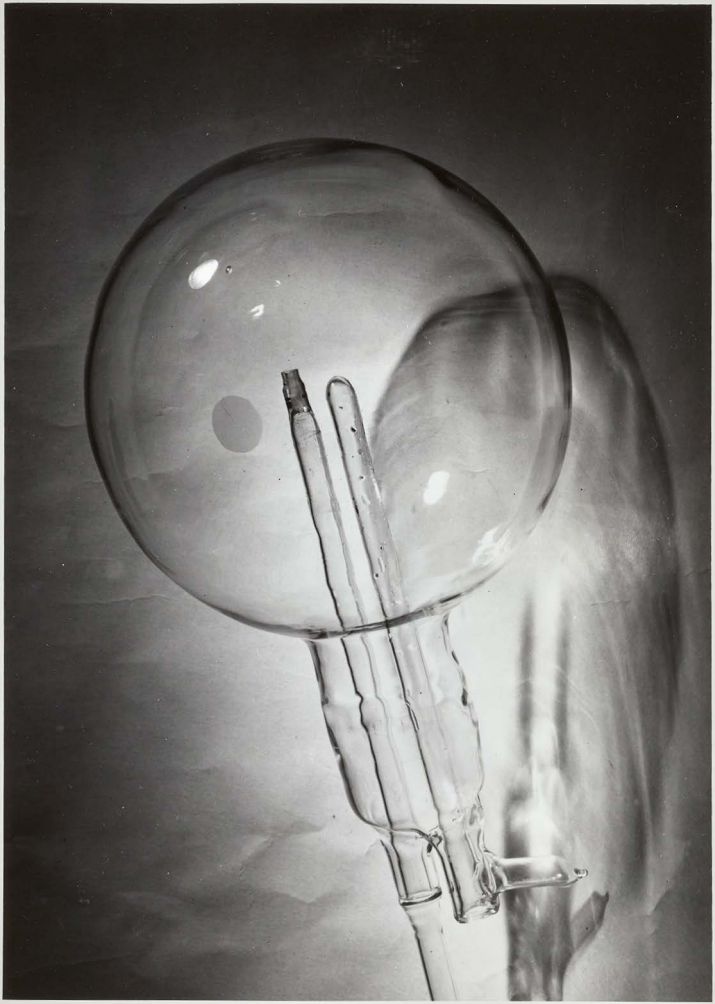

At the time this report was written, the thermostat had seen about three years of use and had proved itself quite dependable and entirely equal to the task for which it was constructed.

The Phase Shift Thermoregulator

Upon completion of the thermostat, the problem of temperature regulation was attacked. At the outset, a mercury-in-glass regulator was used. It was soon apparent that other means of regulation were necessary. The mercury-in-glass thermoregulator was difficult to set for a specific operating temperature and would only regulate to ±0.5°C. Very often this value varied as much as 0.8°C on both sides of the set temperature. This, together with the fact that the temperature drifted upward over a period of time to the extent of 0.2°C per hour, necessitated the construction of some other device for regulation. Considerable thought was given to this problem and the device shown in Figure 19, page 108 was the result.

The sensing element was a resistance thermometer made of nickel wire which was placed in the thermostat shown in Figure 14, page 100 in position E. This sensing resistor formed one arm of a Wheatstone bridge, R_T, Figure 19, page 108. At balance there would be no signal applied to the grid of V_1. When the temperature of the thermostat dropped R_T would decrease and a proportional signal would be applied to V_1; on the other hand, when the temperature increased, the value of R_T would likewise increase, placing a signal again on the grid of V_1. The only difference between these two signals was a shift in phase of 180°. As we shall see, the circuitry was so arranged to recognize this change in phase. The signal, due to a temperature change in the thermostat, is applied to V_1 where it experiences one stage of amplification and is applied to the first half

of V_2 for another stage of amplification. The output of the first half of V_2 is fed through V_3 back into a twin T network which is so arranged so as to feed back all harmonics but the fundamental 60 cycle signal. The output of V_2 is placed on the first half of V_3 where another stage of amplification is experienced and subsequently into the second half of V_3 which is a cathode follower stage. In order to minimize hash feedback from the phase sensitive detector V_5, another stage of amplification and cathode follower was added in V_4. The output of the cathode follower stage of V_4 was fed into a phase sensitive detector, V_5, which performed the following function. By sensing the phase of the E.M.F. applied to the bridge and comparing it with the phase obtained from the output of the amplification network, V_5 is capable of supplying a signal which is larger or smaller than the IR drop across R_{40}. This signal, which at the chosen operating temperature of the thermostat is equal to the potential across R_{40}, is the controlling signal to V_6. V_6 is a mercury thyraton capable of handling continuously a current of 2.5 amperes. C_6 in the grid circuit of V_6 is chosen so as to shift the phase of the A.C. potential on the grid 90° ahead of that on the plate. R_{45} is adjusted so that V_6 is cut off when the bridge is balanced. When R_T experiences a rise in resistance corresponding to a rise in temperature the DC signal from V_5 becomes more negative, therefore biasing V_6 further toward cut-off. When R_T experiences a drop in resistance due to a decreasing temperature the DC signal from V_5 is increased a proportionate amount which changes the bias of V_6 away from cut-off. The point on the sinusoidal wave where V_6 fires, is determined by the magnitude of the DC signal received from V_5.

The signal from V_5 can become more and more positive which results in an earlier firing of V_6 up until the point where the entire half-wave of the applied sinusoidal voltage is being obtained. In consideration of the fact that the power supplied to a circuit from an AC source is proportional to the area under the E. M. F. vs. time curve, it is apparent that this is a proportional device. It is proportional in the sense that the amount of power fed into the thermostat is roughly proportional to the error temperature.

In practice, power from the auxiliary heaters is so adjusted that the thyratron fires during just half of each half-cycle when the thermostat is at the desired temperature. Then the bridge is slightly off balance. The further the thermostat drifts from the desired temperature, the more, or less power is applied to the regulating heaters, depending on whether the drift is down or up, respectively, in temperature which, in either case, tends to restore thermal equilibrium at the desired temperature.

R_H in series with the plate of V_6 is the regulating heater. It is sometimes desirable to monitor the wave shape of the potential applied across R_H. For this purpose the leads "Oscilloscope test" have been provided. The part of the circuit composed of V_7, V_8, V_9, V_{10}, and V_{11} is a regulated B+ supply. It is standard in every way and its only function is to provide a regulated plate supply for the amplification part of the circuit.

It is seen that by setting resistors R_1 - R_4, R_5, R_6 - R_{16}, a large range of temperatures is easily obtained. Furthermore, the temperatures so obtained are easily reproducible by simply reproducing the settings

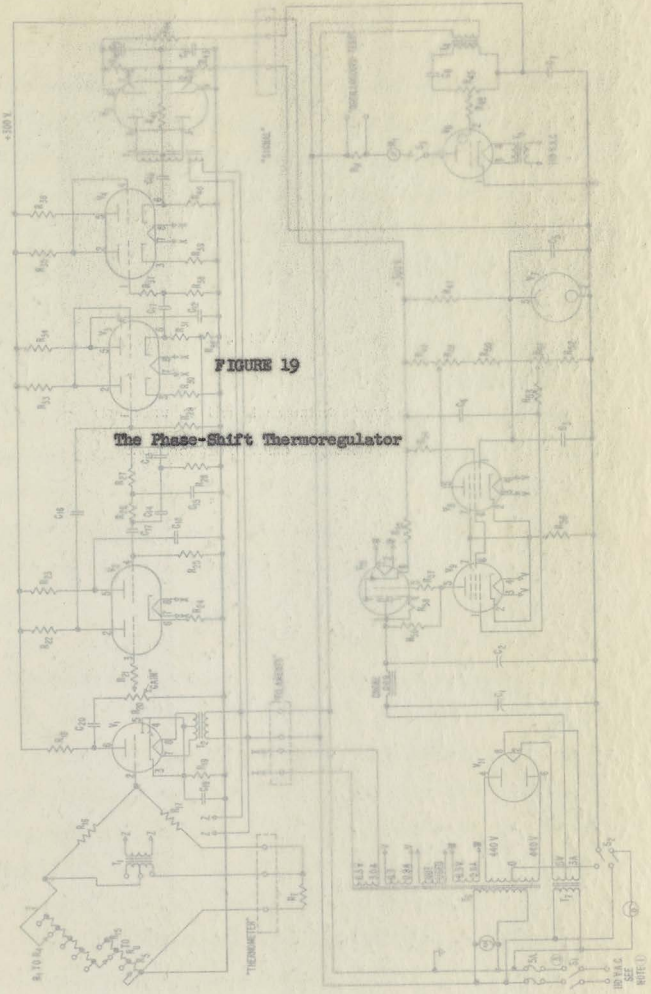

FIGURE 19

The Phase-Shift Thermoregulator

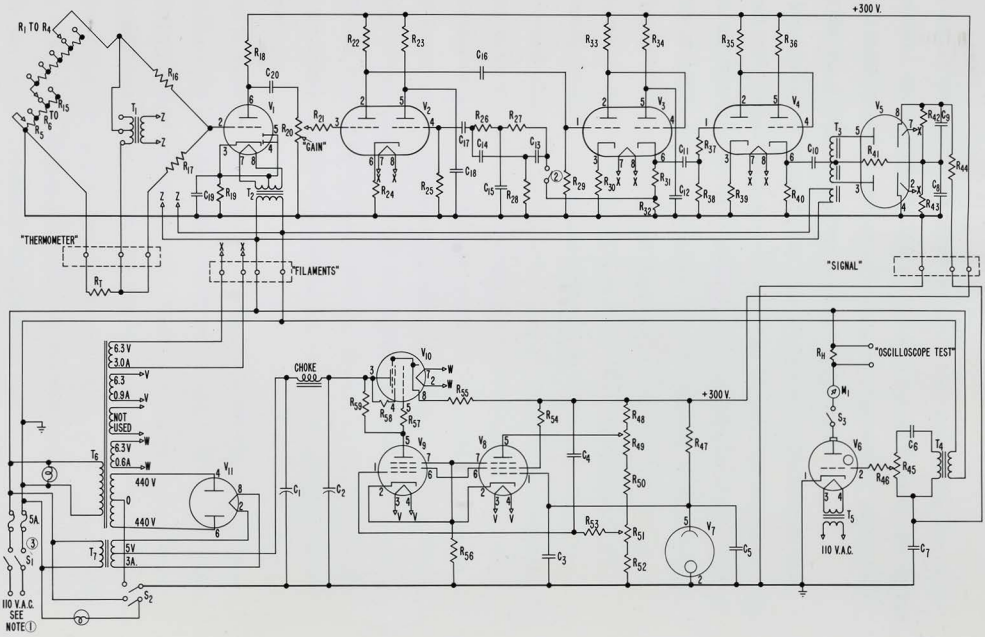
+300 V.
"GAIN"
"THERMOMETER"
"FILAMENTS"
"SIGNAL"
"OSCILLOSCOPE TEST"
CHOKE
6.3 V 3.0 A
6.3 V 0.9 A
NOT USED
6.3 V 0.6 A
440 V
0
440 V
5V 3A.
5A
110 V.A.C. SEE NOTE (1)
110 V.A.C.

of this arm of the bridge and resetting the variac controlling the auxiliary heaters. The circuit will react in such a way as to bring the bridge to a null point by either heating or cooling the thermostat, thereby adjusting the value of R_T to produce thermal equilibrium.

The regulation obtained with this circuit was quite satisfactory. Long term drifts experienced were of the order of 0.01° in 24 hours. Runs in which the largest temperature excursion for a period of a week were of the order of $0.05^\circ C$ were not uncommon. This is at least an order of magnitude better than that previously reported from circuits of this sort. A large part of this improvement is attributed to the arrangement of R_T in the bridge itself. In previous circuits, R_T and its two leads were connected exclusively in one arm of the bridge; therefore, any temperature gradients along the leads from the bridge to the thermostat were "seen" by the bridge as a change in temperature of the thermostat. This was remedied in our case by using a three-lead thermometer. This meant that any change in the resistance of the lead wires was added half to one leg of the bridge and half to the opposite leg. Therefore, the overall balance of the bridge was not disturbed by the temperature gradients along the lead-in wires.

As in cases involving the development of electronic gear to perform a task, it is felt that this circuit is perhaps a little more elaborate than need be to perform the job. Experience has shown the twin T to be largely unnecessary. Also, the highly regulated B+ supply is probably superfluous. It is felt that if the value of R_T at room temperature could be increased to perhaps 2000 ohms and the frequency of the input signal to the bridge increased to 20 kilocycles that an ordinary RF amplification setup to power the phase sensitive detector would be adequate.

TABLE XIX

Parts for the Phase-Shift Thermoregulator

R_1-R_4	100 Ω	WW-4
R_5	10 Ω	10 turn Helipot
R_6-R_{15}	10 Ω	WW-4
R_{16}-R_{17}	100 Ω	WW-4
R_{18}	100 K	1 W
R_{19}	2.3 K	2 W
R_{20}	1 meg	1 W Pot.
R_{21}	500 K	1 W
R_{22}	220 K	1 W
R_{23}	46 K	1 W
R_{24}	500	1 W
R_{25}	1 Meg	1/2 W
R_{26}, R_{27}	270 K	WW-4
R_{28}	135 K	WW-4
R_{29}	15 K	1/2 W
R_{30}	470 K	1 W
R_{31}	33 K	1/2 W
R_{32}	15 K	1/2 W
R_{33}	100 K	1 W
R_{34}	50 K	1 W
R_{35}	50 K	1 W
R_{36}	10 K	1 W

TABLE XIX (continued)

R_{37}	1 Meg	1/2 W
R_{38}	1 Meg	1 W
R_{39}	2 K	1 W
R_{40}	50 K	1 W
R_{41}	220 K	1/2 W
R_{42}, R_{43}	1 Meg	1/2 W
R_{44}	50 K	1/2 W
R_{45}	10 K	WW Pot.
R_{46}	50 K	1/2 W
R_{47}	270 K	2 W
R_{48}	1 K	WW-4
R_{49}	10 K	WW Pot.
R_{50}	40 K	WW-4
R_{51}	10 K	WW Pot.
R_{52}	20 K	WW-4
R_{53}	370 K	1 W
R_{54}	220 K	2 W
R_{55}	10 Ω	1 W
R_{56}	56 K	2 W
R_{57}	1 K	1 W
R_{58}	47 Ω	1/2 W
R_{59}	470 K	1/2 W

TABLE XIX (continued)

R_H	Nichrome heater about 45 ohms total
R_T	An 5525-2 Thermo-resistance bulb Edison-Spitdorf Corp. R = 90 Ω at 30°C.
C_1, C_2	10 mfd. 600V
C_3	0.5 mfd. 200V
C_4	0.01 mfd. 400V
C_5	0.1 mfd. 200V
C_6	Choose to give a phase shift of 90° (value here was 0.1 mfd. 400V)
C_7	1.0 mfd. 400V
C_8, C_9, C_{10}	0.1 mfd. 400V
C_{11}	0.05 mfd. 400V
C_{12}	750 mmfd. 400V
C_{13}, C_{14}	0.01 mfd. 400V mica (choose as close as possible)
C_{15}	0.02 mfd. 400V mica (choose as close as possible)
C_{16}	0.1 mfd 400V
C_{17}	5000 mmfd. 200V
C_{18}	750 mmfd. 400V
C_{19}	100 mfd. 10V
C_{20}	0.02 mfd. 400V
V_1	6SQ7 T_1 Triad F-14X

TABLE XIX (continued)

V_2	6SC7	(use 1/2 of secondary)
V_3	6SL7	T_2 Triad F-14X
V_4	6SN7	T_3 Thor. T20A19
V_5	6H6	T_4 Merit P2962
V_6	FG-57	T_5 Triad F-8X
V_7	5651	T_6 Triad R-70A
V_8, V_9	6AG5	T_7 Triad F-7X
V_{10}	6L6	Choke Triad C-7X
V_{11}	5U4 or 5R4	M_1 0-5 AMP. D.C.

NOTES:

(1) ONE SIDE OF PLUG IS GROUNDED. USE CARE IN PLUGGING IN CIRCUIT TO LINE.

(2) FEEDBACK SWITCH.

(3) ALLOW 1 MIN. BETWEEN TURNING ON S_1 AND S_2 AND FIVE MINUTES BETWEEN S_2 AND S_3.

A full wave rectifier with perhaps a couple of L sections should provide a sufficiently smooth B+ voltage. Also, two low current thyratrons wired to give full wave into R_H would allow the use of less expensive tubes with the advantage of still being able to dissipate a like amount of power in R_H. If 440 volts AC or 660 volts AC were available, this would offer the obvious advantage of allowing an even smaller thyratron to be used. It must be remembered that the fundamental parameter of this circuit is the bridge, and that the circuit need only to operate in such a way as to feed power into the heaters when the bridge is out of balance. Therefore, factors such as frequency shift, B+ ripple, varying tube parameters, varying line voltage, etc., are not of consequence here. If the values of the resistors making up the bridge stay constant, and the temperature of the thermostat is such that R_T is equal to $(R_1 - R_4) + R_5 + (R_6 - R_{17})$, then no signal will be obtained from the bridge and no power will be fed into the thermostat.

The Emission Regulator

Some means must be provided for the control of the ionizing electron beam. This control must extend to both the number of ionizing electrons and their energy. In most mass spectrometers, the ionization of the sample occurs in a nearly equipotential region called the case or shield. The ionizing beam itself is so arranged that it obtains its energy before it enters the equipotential region. A heated tungsten filament is placed outside the case. Slits are provided at both ends of the case in line with the tungsten filament. A portion of the current emitted by the filament enters the equipotential region through one of the slits. Its energy is acquired from a potential difference that is maintained between the filament and the case. The bombarding current then travels through

the equipotential region. It is here that the ionization of the sample gas occurs. The bombarding electrons then leave the equipotential region through the slit on the far side of the case. This electron current is collected by an anode called the trap which lies outside the equipotential region. The electron current leaving the filament and travelling through this region is called the trap current. Also, that electron current leaving the filament and being collected by the case is called the case current. The electronic device which regulates these currents and potentials is known as an emission regulator. There are only two types of emission regulators that have been used. Both types have means of providing a relatively monoenergetic bombarding electron stream. In one type the total current emitted by the filament is controlled. This is the sum of the case and the trap current. In the second type only the trap current (actual bombarding current) is controlled. During the course of this project three emission regulators were constructed. Two of the first type and one of the second. The work done on azomethane (McCoy, 1956) used the emission regulator of the first type. When the present work was begun, it was noted that several instabilities were present in the emission regulator. This amounted to an instability in both the case and the trap current (however, the sum of these two stayed constant to about a part in 300), and a fluctuation in the electron accelerating voltage. After considerable discussion and literature investigation, an emission regulator of the second type was built. The basic circuit chosen was that of Greenhalgh and Jeffrey, (1955). Although much more sophisticated circuits are available (Solomon and Caton, 1952), it was decided that the circuit

of Greenhalgh and Jeffrey would be satisfactory for our needs. We asked that this emission regulator meet the following demands. First, that it hold the trap current constant to 1 part in a thousand for a period of at least 12 hours. Second, that it maintain the electron accelerating voltage constant to 1 part in 500 for a similar period. Third, that the circuit be as simple as possible. Greenhalgh's circuit did not meet these specifications and certain changes became necessary. A schematic of the final emission regulator is shown in Figure 20, page 125.

Both of the above described emission regulators depend on the variable loading of a transformer for control. (Ridenour and Lampson, 1937) The circuit reacts as follows. Suppose the filament, whose emission is temperature limited, experiences an increase in temperature. The immediate result of this is an increase in the trap and case current. The increase in trap current results in a greater IR drop across R_3 and R_4. This causes the grid of V_4 to become more negative, which in turn results in a lowered voltage across R_2. This voltage is placed between grid and cathode of V_6 and V_7, and results in an increase in the conductivity of these tubes. This draws more current through the primary of T_4 and consequently through R_{10} and R_{11}. Therefore, the potential presented to the primary of T_5 is decreased by an amount equal to the IR drop across R_{10} and R_{11}, plus, of course, the IR drop of the reflected resistances of the secondary of T_4 and the plate resistances of V_6 and V_7. The decrease in potential in the primary of T_5 results in a lower voltage presented to the filament which, of course, decreases the emission of the filament, thereby restoring the trap current to some preassigned value.

A considerable amount of difficulty was experienced in the selection of T_5. The current necessary to produce a desired filament emission is determined by the size of the filament. This, in turn, determines the optimum voltage of the secondary of T_5. Once these values are chosen, it is not easy to obtain a transformer of the proper voltage. Therefore, it was necessary to rewind T_5. After much experimentation, the following rule of thumb was obtained:

> The secondary winding of T_5 should contain a sufficient number of turns to produce a voltage equal to at least twice and no greater than three times the voltage necessary to produce the desired amount of emission from the chosen filament with an input voltage to the primary of 120 volts.

In our case the filament chosen was 0.008 inch tungsten wire (unthoriated) about 11 mm long. One and one-half volts at the secondary were necessary to produce the desired emission where the primary was at 120 volts. According to the above rule, a secondary voltage of between 3.0 and 4.5 volts would be necessary. Consequently, an average of these two numbers, or 3.75 volts, was chosen. A Triad F8X filament transformer, rated at 5 volts at 6 amps, was selected and the secondary unwound. It was found to consist of 38 turns of wire. A new secondary of No. 15 (heavier than the old secondary) was wound, 28 turns being required to give the necessary voltage. The diameter of the wire was so chosen as to accommodate the necessary filament current which in our case was 5.5 amperes at its maximum.

The difficulties involved in the selection of a filament transformer are usually overcome by the expedient of installing a low resistance, high power rheostat in series with the filament. By adjusting the rheostat, more or less of the output of the filament transformer is dissipated across it rather than the filament. This would be a simple solution of the transformer matching problem were it not for the fact that the resistance value of the rheostat needed is small and the changes in the contact resistance are large in comparison to the value of the resistance placed in the circuit. Therefore, these small contact resistance changes manifest themselves identically as a signal from an overheated or underheated filament. The circuit in reacting to compensate for this, produces considerable instability, especially if the loop gain is small. The first model built used a series rheostat in the filament circuit. We obtained instability ranging from 0.1% to 5% per hour. This instability was measured by placing a 15 K series resistor in the trap current circuit, using a Rubicon type B potentiometer to "buck out" all but 5 millivolts. This 5 millivolts was recorded on a Leeds and Northrup Speedomax recorder. After the removal of the series rheostat and the fabrication and installation of the above described transformer, the instability decreased considerably. The total excursion of the trap current, now, was from 0.05% to 0.1%. After the regulator was allowed to run for 36 to 48 hours, total excursions for the next 48 to 72 hours were not greater than 0.08%. Thus the regulation of the trap current exceeded expectations. It is believed that the removal of the rheostat and the rewinding of the filament transformer are largely responsible for its success.

As in all construction work of this sort, considerable experience is gained that is not practical to apply inasmuch as another complete circuit would have had to be fabricated and tested. In consideration of the fact that this circuit was more than adequate for the task, no further changes were made even though the course of the work showed the advantage in making these changes. Clearly, the stability of this circuit, to a large extent, is dependent on the physical characteristics of V_4 remaining constant. This tube has a remarkable ability to do just that. Also, the voltage regulating properties of V_1, V_2, and V_3 leave much to be desired. A 6627 tube could be substituted for V_2 and V_3 and the 6626 tube would make an excellent substitution for the V_1. In place of V_4, a difference amplifier which would feed one or two stages of direct coupled amplification would also improve the characteristics to a large extent. The limiting stability controlling factor of this circuit is the speed with which it can react to a change in filament emission. As far as long-term variation is concerned, the author knows of no reason why stabilities of the order of 0.01% per 24 hours are not possible, assuming a reasonable loop stability. The only limitation is that imposed by the electronic components themselves.

When turning the filament on after a period of idleness, certain precautions are necessary. With R_4 and R_{11} set at their maximum resistance, switch 1 is turned on. After a period of not less than 2 minutes, switch 2 is turned on. With "B" of switch S_3 in position 1, R_{11} is slowly decreased until meter M_4 reads 6 milliamperes. At this point R_4 is adjusted to give the desired trap current. In our case this was 15.5

microamperes. After these initial adjustments, "B" of S_3 can be returned to position 3 where it will read case current. The function of S_3 is to provide a means of checking the amount of regulation current in the secondary of T_4.

It is obvious that this circuit will also regulate to minimize fluctuations in line current. However, the range of fluctuation of line current experienced in our laboratory was outside of the range of regulating current in the secondary of T_4. Therefore, it was often necessary to re-set R_{11} to give 6 milliamperes through T_4 secondary in order to compensate for either a lower or higher line voltage. Switch S_3 is arranged so that this switching can be made without disturbing the circuit or affecting any momentary discontinuities in any of these paths. Of course, a milliammeter could be installed permanently between positions AA and a microammeter between positions BB. This, however, would necessitate an extra meter and since current in AA need only be checked periodically, the additional component was not considered to be warranted.

One of the great advantages of a trap current controlled emission regulator is the ability of it to reproduce sensitivities and voltage discrimination curves after the installation of a new filament. The "lining-up" of a new filament, insofar as sensitivity and voltage discrimination are concerned, proceeds as follows.

A sample of butane is admitted to the mass spectrometer. The 43 peak is located and the instrument is adjusted to observe it. By carefully adjusting the source magnet and noting the values of the case current, the trap current, and the peak height, a point where the case current is a

minimum and peak height is a maximum can be obtained. While making the source magnet adjustments, the trap current must be kept under constant observation even though the emission regulator will react to maintain it constant. The reason for this is that by a suitable positioning of the source magnet, the trap current beam can be reflected from the trap entirely, reducing the trap current to zero. The reaction of the circuit is the same as if the filament cooled very rapidly. This results in the emission regulator attempting to heat up the filament to restore the trap current to its pre-assigned value. If this current does not find its way to the trap and consequently into the regulating circuitry of the emission regulator, the temperature of the filament will rise to such a point as to burn it out. Therefore, considerable care must be taken to move the source magnet in very small increments and be alert to return it to the previous setting if the new setting resulted in a decrease in trap current.

A short discussion of the behavior of a newly installed filament is desirable. During the initial heating of a newly installed pure tungsten filament, it was noted that larger currents were necessary to produce a given emission than after the filament was in use for some period. This decrease in heating current was especially apparent if hydrocarbons were being worked in the mass spectrometer. Also, during this process, the sensitivity of the instrument varies over a wide range and it is difficult to obtain consistent results. These effects can be reduced to a minimum by a process known as carbonization or carbiding. This process involves the temporary installation of a new filament in a system where it can be exposed to a few hundred microns of a hydrocarbon while being

heated to a temperature of about 1800°C. Long experience has shown that 4 hours in 200 microns of n-butane and an additional 4 hours in 200 microns of either trans, or cis butene is sufficient. In this particular instrument, if a new uncarbided filament had been installed, the filament current necessary to produce a trap current of 15.5 microamperes at the outset was about 6.5 amperes. After a period of from 2 to 6 weeks of continued use, especially with hydrocarbon samples, the filament current would drop to 4.5 or even as low as 3.9 amperes. Apparently a thin layer of tungsten carbide formed on the filament reduces the work function of tungsten to a point where it is no longer necessary to heat the filament to as high a temperature as previously. Therefore, it is strongly recommended that the above carbiding procedure be used on all new filaments prior to their installation into the mass spectrometer ion source. Even after carbiding, it is not unusual to have a filament start out requiring 5 amperes and after a period of 2-3 weeks, drop down to 3.9 to 4.1 amperes. Carbided filaments also improve stability of the ion beam to a considerable extent.

TABLE XX

Parts List for the Emission Regulator

R_1	15 K	25 W
R_2	500 K	1 W wire wound
R_3	50 K	1 W wire wound
R_4	100 K	1 W poten
R_5	94 K	WW-4
R_6	50 K	1 W wire wound
R_7	40 K	WW-4 wire wound
R_8	100 Ω	1 W
R_9	100 Ω	1 W
R_{10}	150 Ω	50 W
R_{11}	300 Ω	50 W
R_{12}	Shunt to make M_4 read 0-20 ma.	
R_{13}	100 K	1 W
R_{14}	470 K	2 W

V_1	0D3	M_1	0-10 amp. A.C.
V_2, V_3	0C3	M_2	0-100 volts D.C. 10,000 Ω/V
V_4	6SJ7	M_3	0-20 microamp. D.C.
V_5	5U4GB	M_4	0-100 microamp. D.C. also when shunted with R_{12} 0-20 ma.
V_6, V_7	6Y6		

TABLE XX (continued)

C_1, C_2	16 mfd 600V	T_1	1:1 Isolation transformer
C_3	0.1 mfd 200 V		3,500 V insulation
C_4	0.5 mfd 200 V		4 amps. A.C.
C_5	1.0 mfd 200 V	T_2	Triad R68A
C_6	0.06 mfd 600 V		800 C.T. 30 ma 5V. 2A. 6.3V 1.2A 6.3V 1.2A
C_7	0.05 mfd 600 V	T_3	6.3 V 1 amp. 325-0-325 70 ma.
C_8	0.04 mfd 600 V	T_4	Merit P3151 5V-3A 6.3V 3.5A
CH	Triad C-7X		use 325-0-325 winding only
	10 kerri 90 ma	T_5	Triad F8X
	270 ohms		The secondary was replaced
Relay	Advance AH/2C/115 A.C.		with 28 turns of No. 15 wire.
S_1	DPDT		With an input of 117 V A.C.
S_2	SPST		it gave an output of 3.7 volts.
S_3	6 circuits 3 pos. shorting		

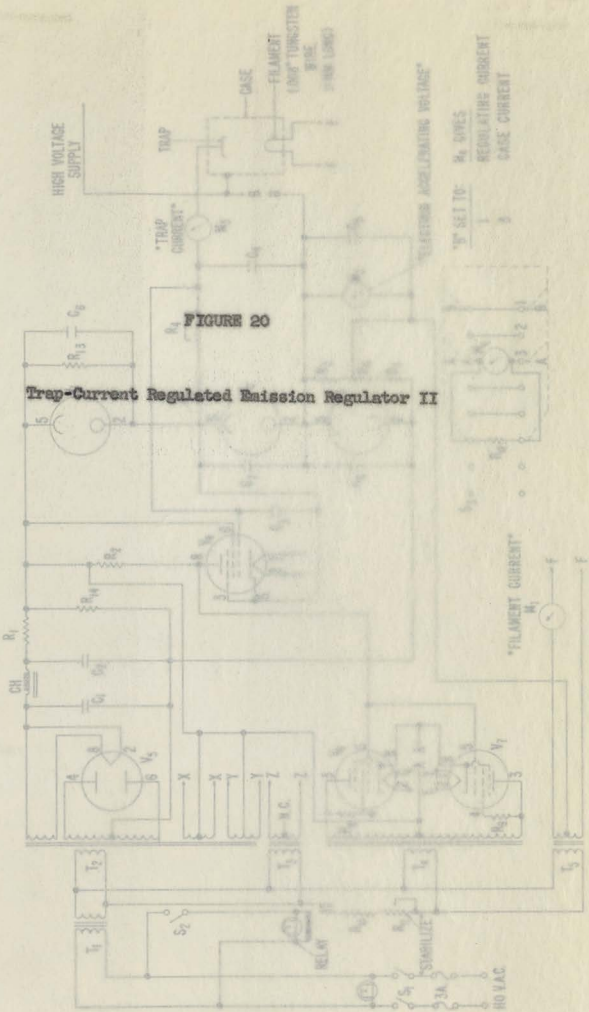

FIGURE 20

Trap-Current Regulated Emission Regulator II

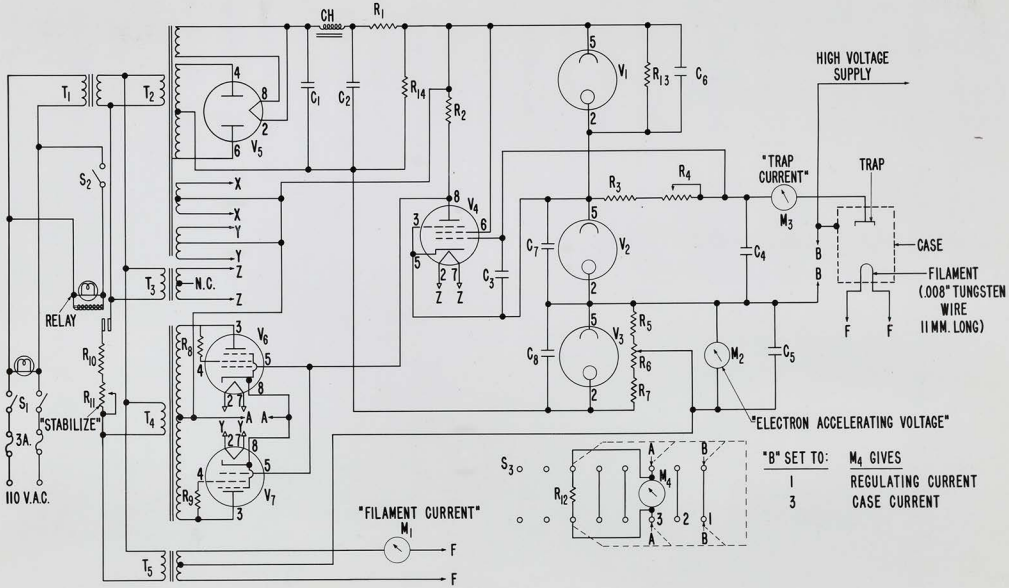
CH
R1
T1
T2
S2
RELAY
T3
N.C.
R10
R11
S1
3A.
110 V.A.C.
"STABILIZE"
T4
T5
V5
X
X
Y
Y
Z
Z
R8
R9
V6
V7
R14
R2
V4
C1
C2
C3
V1
R13
C6
HIGH VOLTAGE SUPPLY
"TRAP CURRENT"
M3
TRAP
R3
R4
C7
V2
C4
CASE
FILAMENT (.008" TUNGSTEN WIRE 11 MM. LONG)
C8
V3
R5
R6
R7
M2
C5
"ELECTRON ACCELERATING VOLTAGE"
S3
R12
M4
"B" SET TO:
M4 GIVES
1
REGULATING CURRENT
3
CASE CURRENT
"FILAMENT CURRENT"
M1

CHAPTER VII

Conclusions and Suggestions for Further Work

We may conclude from this work that the thermal decomposition of azoethane is unimolecular, homogeneous, and first order over the pressure and temperature ranges studied. The mechanism of the reactions appears to be complex and a function of both initial pressure and the temperature. Several runs, recording all peaks, at different pressures and temperatures would have to be made in order to establish a mechanism. Each run would be an analytical run and corrections would have to be made for change of composition during the run. The volume of data obtained would be considerable and access to a computer would be necessary in order that the data be reduced within a reasonable period.

The effect the surface area exposed to the reaction has on the final composition of the products would be of considerable interest. This would require running a series of decompositions at different initial pressures and temperatures in a flask packed with Pyrex wool. During these runs, all peaks would be recorded and the data treated just as that obtained from the mechanism runs.

In this work, decompositions having a half life of greater than 2.5 minutes were studied. The limitations on studying shorter half lives is in the instrumentation and much work could be done to extend the range down to perhaps 100 milliseconds. Some of the difficulties are the detection system, the pumping system, the recording system, and the thermostat. The detection system would have to be capable of a time response of at least 10 milliseconds. This is difficult to achieve with vacuum tube or vibrating reed electrometers, but could probably be done with an electron multiplier or a scintillation crystal and a photomultiplier. One of the most difficult problems would be obtaining a pumping system capable of evacuating the tube at such a rate to prevent the partial pressure of the sample rising to a level not indicative of the pressure in the reaction flask. The installation of high capacity pumps and short, large diameter pumping leads should do much toward the solution of this problem. A recording system suitable for use in these ranges has been described (Leger and Ouellet, 1953). It consists of an oscilloscope on which is displayed the output of the detector. A range of as many as 15 mass units can be displayed at a given time. A major change in the thermostat setup would also be necessary. The construction of a thermostat-mass spectrometer combination in which the source of the mass spectrometer were placed directly in the reaction vessel itself, would seem to be desirable. Under these conditions, the leak could be placed in the ionization chamber of the mass spectrometer source directly. This setup would have the additional advantage of heating the source and thereby helping to keep it outgassed. Perhaps the most significant advantage would be the short distance between reaction vessel and ion

detector. With half lives of 100 milliseconds, the time of flight of the ion from its point of formation to its final collection would be insignificant.

As pointed out earlier, the problem of the leak-out correction was troublesome. It does not appear possible to calculate a theoretical leak-out rate which is compatible with experimental data. Further work to determine the parameters involved in the rate at which the gas will leak out of a small hole appear to be highly desirable. Certainly much data of this sort must be obtained before kinetic studies can be carried much further into the low pressure ranges.

BIBLIOGRAPHY

Alpert, D., J. Appl. Phys. 24, 860 (1953).

American Petroleum Institute (A.P.I.), Mass Spectral Data.

Arrhenius, Z. Physik Chem. 4, 226 (1889).

Ausloos, P., and Steacie, E. W. R., Bull. Soc. Chim. Belges, 63, 87 (1954).

Blades, H., Blades, A. T., and Steacie, E. W. R., Can. J. Chem. 32, 298 (1954).

Christiansen, J. A., Reactionkinetiske Studies, Thesis, Copenhagen, 1921, p. 50-51.

Daniels, F., and Johnston, E. H., J. Am. Chem. Soc. 43, 53 (1921).

Daniels, F., J. Am. Chem. Soc. 48, 607 (1926).

Dibeler, V. H., and Taylor, T. I., Science 108, 686 (1948).

Engh, R. O., Master's thesis, University of Oregon, 1952.

Frost, A. A., and Pearson, R. C., Kinetics and Mechanism, John Wiley and Sons, Inc., New York, 1953.

Glasstone, S., Laidler, K. J., and Eyring, H., The Theory of Rate Processes, McGraw-Hill Book Company, Inc., New York, 1941.

Greenhalgh, D., and Jeffery, P. M., J. Sci. Instr. 32, 36 (1955).

Hatt, H. H., Organic Syntheses, Vol. II, John Wiley and Sons, Inc., New York, 1943.

Hinshelwood, C. N., and Topley, B., J. Chem. Soc. 125, 393 (1924).

Hinshelwood, C. N., Proc. Roy. Soc. (London) A113, 320 (1927).

Hinshelwood, C. N., The Kinetics of Chemical Change, Oxford University Press, London, 1949.

Jahn, F. P., J. Am. Chem. Soc. 59, 1761 (1937).

Kassel, L. S., J. Phys. Chem. 32, 225 (1928).

Kassel, L. S., The Kinetics of Homogeneous Gas Reactions, American Chemical Society Monograph No. 57, Chemical Catalog Co., 1932.

Laidler, K. J., Chemical Kinetics, McGraw-Hill Book Company, Inc., New York, 1950.

Langmuir, I., J. Am. Chem. Soc. 42, 2190 (1920).

Leger, E. G., and Ouellet, C., J. Chem. Phys. 21, 1310 (1953).

LeRoy, D. J., Can. J. Chem. 28, 492 (1950).

Lewis, G. N., and Mayer, J. E., Proc. Natl. Acad. Sci. U.S. 13, 623 (1927).

Lewis, W. C. McC., J. Chem. Soc. 113, 471 (1918).

Lindemann, F. A., Trans. Faraday Soc. 17, 598 (1922).

Marcus, R. A., J. Chem. Phys. 20, 352 (1952) and J. Chem. Phys. 20, 355 (1952).

Marks, Robert, Rev. Sci. Instr. 28, 381 (1957).

McCoy, R. D., A Mass Spectrometric Study of the Thermal Decomposition of Azomethane at Low Pressures, Ph.D. Thesis, University of Oregon, 1956.

Munson, R. J., Rev. Sci. Instr. 26, 236 (1955).

Ogg, R. A., J. Chem. Phys. 15, 337 (1947) and J. Chem. Phys. 18, 572 (1950).

Perrin, J., Les Atomes. (1913)

Perrin, J., Ann. Phys. 11, 5 (1919).

Renaud, R., and Leitch, L. C., Can. J. Chem. 32, 545 (1954).

Rice, F. O., and Herzfeld, K. F., J. Am. Chem. Soc. 56, 284 (1934)

Rice, O. K., and Ramsperger, H. O., J. Am. Chem. Soc. 49, 1617 (1927).

Rice, O. K., and Ramsperger, H. O., J. Am. Chem. Soc. 50, 617 (1928).

Rice, O. K., and Sickman, D. V., J. Chem. Phys. 4, 608 (1936).

Rice, O. K., and Weininger, J. L., J. Am. Chem. Soc. 74, 6216 (1952).

Ridenour, L. N., and Lampson, C. W., Rev. Sci. Instr. 8, 162 (1937).

Slater, N. B., Proc. Cambridge Phil. Soc. 35, 56 (1939).

Slater, N. B., Proc. Roy. Soc. (London) 194A, 112 (1948).

Slater, N. B., Proc. Roy. Soc. (London) 218A, 224 (1953).

Slater, N. B., Phil. Trans. Roy. Soc. London. Ser. A. 246, 57 (1954).

Solomon, A. K., and Caton, D. C., Rev. Sci. Instr. 23, 757 (1952).

Steacie, E. W. R., Atomic and Free Radical Reactions, American Chemical Society Monograph No. 125, 2nd ed., 2 vols., New York, Reinhold Publishing Corporation, 1954.

Swinehart, D. F., Anal. Chem. 21, 1577 (1949).

Szwarc, M., Chem. Revs. 47, 75 (1950).

Taylor, H. A., J. Am. Chem. Soc. 48, 577 (1926).

Thiele, Ber., 42, 2575 (1909).

Trautz, M., A. Anorg. Chem. 102, 81 (1918).

Trautz, M., and Bhandarkar, D. S., Z. Anorg. Chem. 106, 95 (1919).

Trotman-Dickenson, A. F., Gas Kinetics, Butterworths Scientific Publications, London, 1955.

Willbanks, E. M., The Evaluation of the Kassel Integral via IBM-704, Los Alamos Scientific Laboratory Report LA 2178, 1958.

BIOGRAPHICAL SKETCH OF THE AUTHOR

William Dempsey Clark was born in Buffalo, New York on July 15, 1921. He attended public schools in Buffalo, New York. While he attended Buffalo Technical High School for two years and Cass Technical High School for one year, he never obtained a diploma, but went directly on to the university. From 1940 to 1944 he worked as an instrument engineer at Lockheed Aircraft Corporation in Burbank, California. He then served one year in the U. S. Navy as a photographer.

From 1946 to 1950 he attended the University of Miami, receiving the Bachelor of Science degree cum laude in June 1950. At the University of Miami he received an Office of Naval Research Fellowship in his sophomore year which he held until one year after graduation. The work done covered the synthesis of unsaturated amines and is covered by the final report covering contract N7-ONR-357 entitled, "The Preparation of Unsaturated Amines."

From December 1951 to December 1956 he was a research assistant under a contract sponsored by the Atomic Energy Commission at the University of Oregon, Eugene, Oregon. It was while working on the kinetics of gas reactions on this contract that he received his Masters of Science Degree in June 1954 and became a candidate for the Doctor of Philosophy Degree in June of 1955.